STUDIES ON THE DYNAMICS OF THE ROTATING EARTH

GARY PETER HAARDENG-PEDERSEN

PREVIOUSLY COPYRIGHTED MATERIAL,

IN PART II,

NOT MICROFILMED.

(Reprint of Symposium No. 48,
"Rotation of the Earth".
International Astronomical
Union.)

STUDIES ON THE DYNAMICS OF THE ROTATING EARTH

by

Gary Peter Haardeng-Pedersen, M.Sc.

A Thesis submitted in partial fulfillment
of the requirements for the degree of
Doctor of Philosophy

Department of Physics
Memorial University of Newfoundland

June 1975

St. John's Newfoundland

ABSTRACT

The spectrum of the geographic motion of the Earth's rotation pole and confidence limits on this estimation of the spectrum are obtained in the first part of this thesis. These statistical tests negate the evidence for multiple peaks in the Chandler region and conclude that the Chandler excitation may be a non-stationary process.

The response of the Earth to an external harmonic potential of second or third degree is presented in the second part of this thesis. An Earth model with a sub-adiabatic fluid core is considered for the second degree excitation and Love numbers are calculated; these give evidence of free oscillations called undertones. As the direct effects of rotation have been fully retained in this study, it is shown that the rotational couplings excite torsional modes and other spheroidal modes of oscillation. Love numbers for the terdiurnal tide (M_3) are calculated for Earth models with both adiabatic and sub-adiabatic fluid cores.

ACKNOWLEDGEMENTS

I wish to thank the following:

My supervisor, Dr. M. G. Rochester of the Physics Department, Memorial University of Newfoundland, for supervision of this work;

Dr. S. W. Breckon and other faculty members of the Physics Department for making available research facilities and financial assistance;

Dr. A. P. Annan, Dr. D. J. Crossley, Mr. P. G. Gillard, Dr. R. D. Murphy, Prof. P. D. P. Smith and Dr. J. A. Wright for valuable discussions;

Miss D. Janes, Mr. R. Tucker, Mr. R. Alexander and Mr. P. Stone for helping in the preparation of this thesis;

Dr. F. A. Aldrich and Dr. A. M. Sullivan for financial assistance.

Finally I wish to thank my wife and daughters for their patience and their encouragement throughout the course of this work.

TABLE OF CONTENTS

LIST OF TABLES

LIST OF FIGURES

GENERAL INTRODUCTION

This thesis describes two separate investigations on the dynamics of the rotating Earth.

The first is a spectral analysis of the ILS-IPMS data on the variation of latitude (1899-1970), carried out to show the statistical uncertainty in the spectra and the consequent unreliability of interpretations involving splitting of the Chandler peak.

The second investigation is a theoretical study of the response of the rotating Earth to a harmonic potential of external origin (tides of the solid Earth) and of the free oscillations with periods longer than those of the gravest elastic mode; in the case when the temperature gradient in the liquid core is sub-adiabatic.

PART I

SPECTRAL ANALYSES OF THE CHANDLER WOBBLE

INTRODUCTION

The changes in the geographic position of the Earth's rotation pole have been the cause of much theoretical and observational research. The motion is now known to have three principal components: the annual wobble, the Chandler wobble and the secular drift. Of these the secular drift appears to be a random walk process, the annual wobble is well understood as a forced vibration and the Chandler motion is a free vibration of the Earth.

In the latter part of the 18th century Euler's studies of the motion of a rotating uniaxial rigid body indicated that the body has a free wobble observable as the motion of the rotation pole about the pole of figure. For the Earth, the predicted wobble period is 305 days. During the 1840's observatories began to search for evidence of this free wobble.

In 1870 Kelvin showed that the annual rearrangements of atmospheric mass would excite an annual wobble with an amplitude $\sim 0''.1$ (arc sec). In 1891 observatories in Berlin (near 0^{o} longitude) and in Honolulu (near 180^{o} longitude) followed a program of observations to test Kelvin's theoretical results. The correlation between their latitude data supported Kelvin's prediction and inspired Chandler to re-evaluate existing latitude data. Chandler found that the pole path could be described as a beat phenomenon between two periodic components, the forced annual motion and another motion with a period of approximately 14 months.

Newcomb (1892) argued that the latter component was the free wobble predicted by Euler but that the Earth's departure from rigidity (due to the elasticity of the solid Earth and the fluidity of the oceans) lengthened this period. Love (1909) and Larmor (1909) investigated this hypothesis by taking into account the bulk elasticity of the Earth as determined from the analysis of Earth tides. The agreement between their results and the observationally determined period substantiated Newcomb's suggestion that the Chandler motion was the free wobble of the Earth.

The effect of the liquid core, which shortens the wobble period by approximately 30 days, had been investigated by Hough (1895), and the oceans lengthen the period by about 40 days (Larmor, 1915).

CHAPTER 1

THE PHYSICAL PARAMETERS OF THE CHANDLER WOBBLE

For a rigid uniaxial Earth, the free wobble mode occurs at the Eulerian frequency

$$\omega_r = \frac{HC\Omega}{A} \tag{1.1}$$

which is determined by the bulk properties of the Earth: its polar and equatorial moments of inertia (C and A, respectively), angular velocity Ω and dynamic ellipticity H ($\equiv \frac{C-A}{C}$). A power spectrum of the polar motion should be able to determine the frequency of the free wobble of the real Earth since an ideal record of an undamped cyclic system with circular frequency ω_o produces a power spectrum symmetric about the circular frequency and of the form

$$\frac{1}{(\omega-\omega_o)^2}$$

Furthermore the power spectrum of a damped cyclic motion has the form

$$\frac{1}{(\omega-\omega_o)^2+1/\tau^2}$$

where τ is the damping time. The width of the spectral peak is then an estimator of the damping time, where a shorter damping time is represented by a broader spectral peak. The quality factor Q of any damped periodic system is an estimator of the rate at which energy is dissipated in that system and its reciprocal, the specific dissipation function, is defined by

$$Q^{-1} = \frac{1}{2\pi}\frac{\Delta E}{E} \tag{1.2}$$

where E is the maximum energy stored in any cycle and ΔE is the energy dissipated in that cycle. In a damped periodic system the quality factor is directly proportional to the product of the frequency $f_o = \frac{\omega_o}{2\pi}$ and the damping time τ:

$$Q = \pi f_o \tau = \omega_o \tau / 2 \quad . \tag{1.3}$$

The effective Q for a periodic phenomenon will depend on the distribution of the wobble energy within the Earth, that is the Q will reflect on the extent to which this phenomenon samples the internal regions of the Earth (Lagus & Anderson, 1968). For a layered system, the effective or bulk quality factor is defined as

$$\frac{1}{Q} = \sum_k \left(\frac{V_k}{V}\right) \frac{1}{Q_k} \quad ,$$

where V_k is the elastic potential energy stored within the k'th layer and V is the total elastic potential energy of the Earth. Thus knowledge of the Q of the wobble would suggest the region of the Earth within which most of the wobble energy is dissipated. Within the mantle the departure from elasticity is primarily due to frictional losses in shear. The difference between the actual temperature distribution and the melting point distribution can be relatively small as evidenced by the low velocity zone and the anelasticity provided by a region of partial melting will contribute to high damping in the mantle.

Kaula (1968) states that surface waves, body waves and free oscillations indicate a Q of at least 100 but that the Earth tides indicate a Q of only 11. The first Q is determined from the non-geometric attenuation

of seismic waves and from the decay of free oscillations. The Earth tide Q is estimated from the phase lag between the Moon's position and the tidal response and is poorly determined due to the uncertainty in the phase lag. ($Q = \cot \delta$ where the lag δ is $0.^{\circ}8 \pm 3.^{\circ}5$ (Lagus & Anderson, 1968)). Anderson (1967) models the Q distribution within the Earth's mantle with regions having quality factors between 100 and 2200 and a bulk Q of 500. Lagus & Anderson (1968) model the mantle as a simpler two-layer structure with a region of strong attenuation overlying a more elastic lower mantle to give an observed Q of 380 for the ${}_0S_2$ free oscillation in agreement with the Q (350 ± 70) calculated by Smith & Anderson (1967). Bodri (1974) has incorporated attenuation in the mantle into an Earth model to predict Earth tides and also the phase lag, he obtains a lag of practically zero (1-2 minutes of arc).

Modelling the attenuation in the fluid and inner core has been done by observations of the ratios of the amplitudes of seismic waves which have made multiple passes through these regions. Buchbinder (1971) has assigned a Q of 4000 to the fluid outer core of the Earth, and Doornbos (1974) has modelled the Q of the inner core finding a variation from Q = 200 near the inner core boundary to Q = 600 at a depth of 400 km into the inner core with a maximum value for Q of less than 2000 at the geocenter. Qamar & Eisenberg (1974) obtained a Q for the outer core between 5000 and 10,000 and a Q between 120 and 400 in the inner core.

On the Earth's surface tidal energy dissipation has been understood as due to turbulent bottom friction in the shallow seas and in narrow estuaries. Recent estimates of the Q of the oceans (Hendershott, 1973) are between 5 and 34.

Among the mechanisms suggested for the wobble's excitation have been non-seasonal movement of atmospheric masses, earthquakes and electromagnetic core-mantle coupling. Munk & Hassan (1961) investigated the first of these proposals and found it insufficient by an order of magnitude; Rochester & Smylie (1965) did a detailed study of the electromagnetic torques between the core and the mantle and rejected this mechanism as a source (or sink) of the Chandler energy. Although Munk & MacDonald (1960, p. 163) had rejected earthquakes as a plausible source of the Chandler motion (because of the supposedly limited extent of the accompanying displacement field), permanent displacements of the crust were measured at thousands of kilometers from the epicentre of the Alaskan earthquake. This constituted evidence of a much more extensive displacement field than than previously considered leading Mansinha & Smylie (1967, 1968) to reassess this possibility. They found correlations between the occurrence of large earthquakes and breaks in the pole path. A later theoretical study by Smylie & Mansinha (1971) of the changes in the inertia tensor which result from the mass redistribution due to earthquakes then predicted that a major earthquake could be responsible for wobble, exciting wobble with an amplitude of 0".1. However similar calculations by Dahlen (1971) and by Israel, Ben-Menahem & Singh (1973) question the effectiveness of this excitation process as they calculate a much smaller wobble amplitude.

For the deformable Earth the dynamics of the polar motion can be summarized by a set of linearized equations (Munk & MacDonald, 1960, p. 38). The instantaneous rotation vector can be referred to the average rotation vector by using the direction cosines

$$\vec{\Omega} = \Omega\left(m_1, m_2, \sqrt{1-m_1^2-m_2^2}\right).$$

The equatorial components can then be combined in complex form

$$\tilde{m} = m_1 + i m_2$$

which gives the geographic position of the instantaneous rotation pole.

Changes in the position of the rotation pole can be produced by the application of an external torque on the Earth ($\vec{L}$), by a redistribution of the angular momentum within the Earth ($\vec{h}$) or by changes in the Earth's inertia tensor c_{ij}. The equatorial components of these quantities can be combined in a complex form

$$\tilde{h} = h_1 + i h_2$$

$$\tilde{L} = L_1 + i L_2$$

$$\tilde{c} = c_{13} + i c_{23}.$$

The linearized equation of motion of the rotation pole is then

$$\dot{\tilde{m}} = i\omega_r(\tilde{m} - \tilde{\phi})$$

where the excitation function $\tilde{\phi}$ is defined in terms of the above sources by

$$\Omega^2(C-A)\tilde{\phi} = \Omega^2\tilde{c} - i\Omega\dot{\tilde{c}} + \Omega\tilde{h} - i\dot{\tilde{h}} + i\dot{\tilde{L}}.$$

In the case of a torque-free, uniaxial rigid body this excitation function vanishes and the Eulerian solution (1.1) results. Departure from rigidity allows the equatorial bulge to adjust to the instantaneous equator

($\tilde{c} \propto \tilde{m}$) and hence lengthens the wobble period. Alternatively abrupt changes in the mass distribution within the Earth (for example, that due to large earthquakes) can excite polar motion.

The gross features of the Chandler wobble and the physical parameters of the Earth which determine this phenomenon can in principle be estimated from spectral analyses and autoregressions. An ideal record for the purposes of spectral analysis would not only be free of noise but would also be continuous, stationary and of infinite length. Only then will the spectral analysis uniquely determine the distribution of power with respect to frequency. A noiseless stationary record sampled at a finite number N of equally spaced time intervals can only determine the power in each of N harmonics of the fundamental frequency

$$f = \frac{1}{N\Delta t}$$

($\frac{N}{2}$ prograde and $\frac{N}{2}$ retrograde harmonic components) which best approximates the continuous distribution. The shape of the resulting spectral peak is modified by the sampling process and this leads to errors in the estimations of the physical parameters of the motion. Therefore it is mandatory that the best available record by used for the analysis.

Observational data on the polar motion have been systematically collected (by measuring the variation of latitude) since the 1880's when a set of 5 observatories (operated under the aegis of the International Latitude Service, now the International Polar Motion Service) was established at regular spacings on latitude $39^{\circ}08'$ N. These stations have recorded pole positions and published monthly means of these since December 1899. Since 1958 they have collected data from an additional 26

stations and have been publishing the mean pole positions at 0.05 year intervals as well as the monthly means.

A second organization, the Bureau International de l'Heure (BIH) has also been publishing the pole positions calculated for 5- and 10-day means since 1955. This organization has more stations contributing (some 50 as of 1970) with better instrumentation than the IPMS observatories (most BIH stations have a PZT); however, they have neither the length of record nor the advantage of a latitude chain which can employ common star catalogues. Both the IPMS and the BIH give the pole position relative to the Conventional International Origin (CIO) which was the mean position determined for the rotational pole over the interval 1900-1905; both currently quote error levels on their published means as approximately 0".01 although the derived pole positions may differ by as much as 0".1.

Rudnick (1956) used 54.4 years of ILS data which he interpolated from the monthly means to a spacing of 0.1 years to obtain the Fourier line spectrum or periodogram shown in Figure 1. The spectrum shows a narrow peak at about 1.0 cycles per year (cpy) and a much broader peak at 0.84 cpy. As the forced annual motion is approximately in equilibrium, with the forcing and the dissipation in balance, the wider Chandler peak indicated the presence of dissipation. The relatively short record length permitted calculations of the spectral densities only at harmonics of 0.0184 cpy and thus no detail could be resolved in the spectrum. With only 3 spectral lines between the half-power points even the estimate of the damping time is not too reliable.

For an ideal record the damping time (or relaxation time) can be determined from the power spectrum. The power is maximum at the cyclic

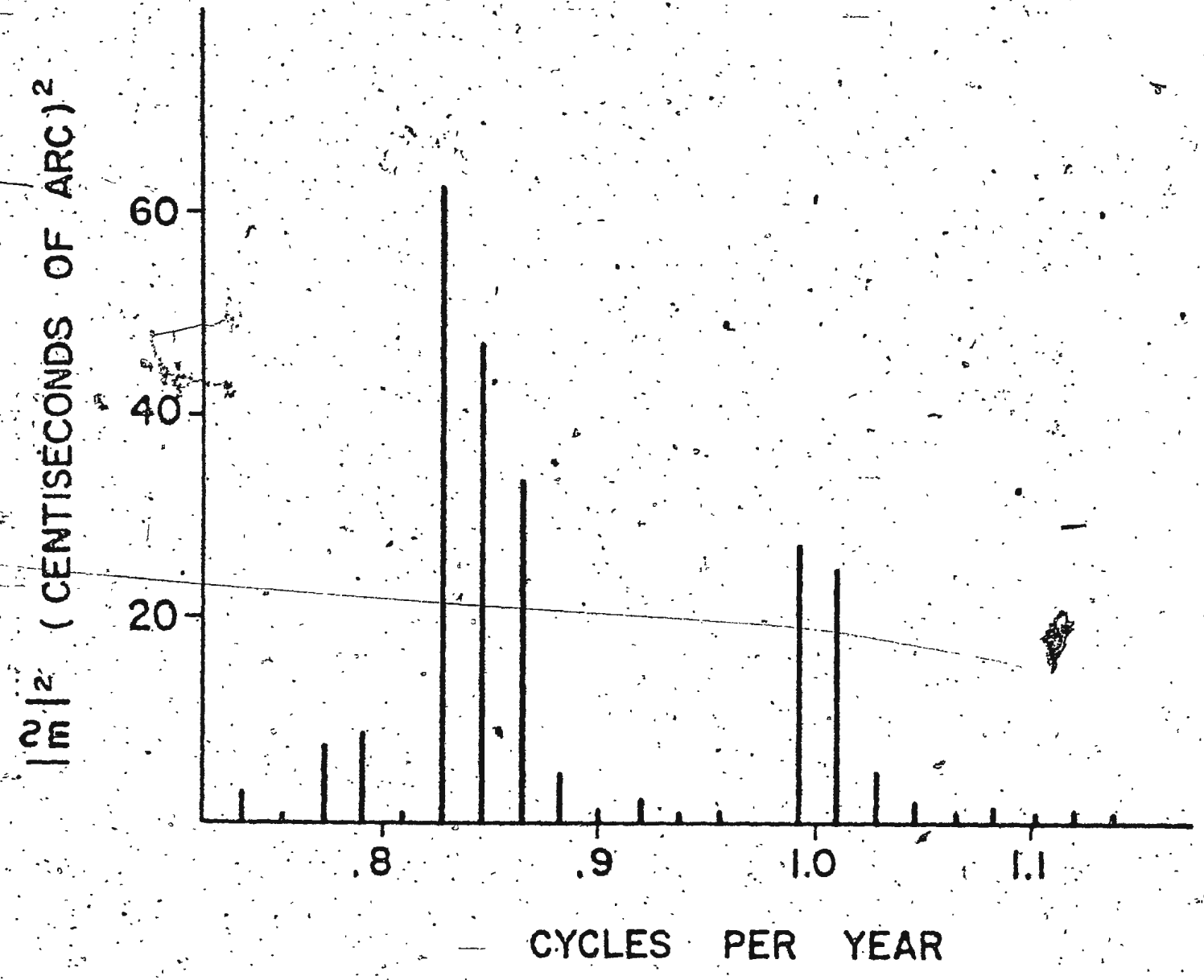

Fig. 1 Fourier spectrum of latitude variation. (From Rudnick, Table 1.)

frequency ω_0 and the half-width of the peak is the reciprocal of the damping time. The quality factor Q is then given by

$$Q = \omega_0/\Delta\omega_0$$

where the half-width $\Delta\omega_0$ is determined by the frequencies $(\omega_0 \pm \Delta\omega_0)$ at which the power is half of the maximum power.

The sparse sampling of the spectrum achieved by Rudnick (1956) was one reason for the lack of reliability in his estimate of the damping time of the Chandler process.

Furthermore the sampling process itself will be reflected in the spectral peak obtained. The use of a finite, discrete process to sample the record results in a spectral peak which is shorter and broader than the peak which would be obtained from an ideal record.

Departure from stationarity (such as isolated large changes in phase which may be accompanied by changes in the amplitude of the signal) also modifies the shape of the spectral peak (Federov & Yatskiv, 1965). Therefore in practice the width of the spectral peak will indicate some combination of the contributions of the effects of (i) the sampling process used to observe the event, (ii) the non-stationarity of the process and (iii) the anelasticity of the Earth. Neglect of the first two of these effects will lead to incorrect statements concerning the effects of anelasticity of the Earth.

In general, therefore, one can say that the Q inferred from the power spectrum is a lower limit to the real Q.

The gross features of the Chandler wobble which have been estimated from earlier spectral analyses and autoregressions (Rudnick,

1956; Walker & Young, 1957, Jeffreys, 1968) are its frequency (0.82 to 0.87 cpy) and its damping time (2 to 30 years).

Since these earlier analyses were published, several powerful tools and techniques have become available. First, the computer, and in 1965 the Fast Fourier Transform (FFT) technique (Cooley & Tukey, 1965) which allows spectra to be calculated in a more reasonable computational time and, secondly, interpolates the spectral densities between the frequencies determined by the record length. The actual observations for which the spectrum is required is supplemented by adding zeros to the end of the record until a total record length of 2^n data points is obtained and the FFT uses this supplemented record as its data base. The spectrum is thus interpolated to a finer frequency grid (the spectrum will now be calculated at frequencies which are multiples of $\omega = \frac{2\pi}{2^n \Delta t}$; the addition of zeros to the record makes no different assumption about the non-recorded signal than does the standard spectral technique and the spectrum is interpolated on to the new frequency grid). I note that in the traditional spectral analyses adjacent power estimates are uncorrelated, however the interpolated power estimates resulting from the use of FFT introduce correlation between adjacent interpolated power estimates. In 1968 the Maximum Entropy (a data adaptive) (MEM) method of spectral analysis was introduced (Burg, 1968, 1970, 1972) and the results of MEM studies of the Chandler wobble will be discussed later.

Spectral analyses of the variation of latitude data using FFT have been published by Yashkov (1965) and, nearly simultaneously with this study, Gaposchkin (1972). By splicing together various records these authors were able to produce records with lengths significantly longer

than that used by Rudnick (1956). A record constructed in this fashion will appear to give a much better resolution than a shorter record. However the hidden shortcomings must be noted. Earlier segments of the record represent data obtained from fewer stations using different methods of data reduction and independent observing programs, and these inconsistencies in the spliced record may largely offset any apparent gain in resolution. It is immediately noticeable in the power spectra obtained by these authors that there is a fine structure in the Chandler band or multiple Chandler peaks.

Yashkov and Gaposchkin have interpreted these peaks to be physically significant. Yashkov reported that this multiplicity of Chandler peaks would resolve the disparity between the Q estimated from the previous analyses of latitude data and that inferred for the Earth from seismic studies, thus indicating the mantle as a suitable energy sink for the Chandler wobble. He finds that the half-width of the individual peaks is less than 0.025 cpy which indicates a damping time of at least 80 years, corresponding to a Q of at least 200. The implication was that prior analyses had not been able to separate these Chandler components because of the shorter record lengths and consequent poorer resolution and had therefore resulted in spuriously large half-widths. However the existence of multiple peaks presents another problem; it implies that the mantle cannot be a single component system with regard to the wobble and must be re-investigated as a multiple component system with coupling between these components to find the corresponding free wobble modes of the Earth.

Gaposchkin also reached this conclusion as his analysis distinguished three wobble components in the Chandler region (at 0.898, 0.865 and 0.807 cpy) as well as the annual component.

Colombo & Shapiro (1968) removed the annual term from the latitude data and remarked that the plot of the remaining polar motion is contained in an envelope characteristic of a beat phenomenon with a period between 80 and 100 years the result of superposition of two wobbles with periods differing by 12 or 10 days, respectively. They also have suggested that, because of the low velocity zone, the upper mantle acts as a two-layer system with three degrees of freedom coupled by a viscous torque.

An alternative that has been suggested for the explanation of the multiple peaks resolved in such spectral analyses is that the Chandler period is variable by as much as 4% (Melchior, 1957). However, the Chandler frequency is determined by bulk properties of the Earth (such as the moments of inertia, the bulk elasticity and the dynamic ellipticity), and it is difficult to envisage any physical process which could substantially change these bulk properties over very short time intervals.

Following Yashkov's paper, Federov & Yatskiv (1965) gave still another alternative explanation for the multiple peaks of the Chandler region. Their interpretation of these peaks was illustrated by considering an extremely simplified model pole path where the effects of damping were neglected and where a phase shift of 180° was introduced in the middle of the record. Taking the frequency of the purely periodic term which described the pole path before or after the phase jump as σ and the record length as (2N-1) data points at time intervals Δt, the spectrum

produced had maximum power at frequencies of

$$\sigma \pm \frac{1}{N\Delta t}$$

and vanished at the assumed Chandler frequency of σ cpy.

From this illustration it is apparent that a single large phase shift in the middle of a record of an undamped periodic phenomenon produces a "bifurcation" or an apparent splitting of the true peak into two smaller peaks placed symmetrically about the true frequency. The implications of their model have been substantiated by a more detailed investigation which I have carried out, in which damping, arbitrary phase shifts, regeneration of the amplitude and non-symmetric records about the event have been modelled. In these cases the splitting into multiple peaks is observed but the symmetry of the spectra about the assumed frequency is destroyed.

Federov & Yatskiv attribute the multiple peaks to phase shifts and quote Orlov (1961): This interval (1924-1926) was characterized by a phenomenon which "essentially altered the nature of the Chandler wobble". This explanation appears to be borne out by Yashkov's investigation of shorter lengths of record; three subsets of the original data, each a record of 25 years, gave significantly different spectra, two records show only one peak whereas the record that spans the above mentioned interval clearly shows the multiple peak spectra.

One physical process consistent with the phase shift hypothesis advanced by Federov & Yatskiv is probably the excitation mechanism proposed by Mansinha & Smylie (1968) for the Chandler wobble. Neglecting forced precession and nutation, the Earth's angular momentum, angular velocity and principal axis of the inertia tensor will coincide in the absence of wobble. During wobble, the angular velocity and the principal axis

precess about the angular momentum vector; the semi-apex angle of the cone described by the principal axis being only about a fraction H of that described by the angular velocity. Due to dissipation and to mass readjustment these vectors would eventually spiral into coincidence with the angular momentum vector. The sudden large scale redistribution of mass due to an earthquake would change the components of the inertia tensor and hence the orientation of the principal axis. As angular momentum is conserved during this event, the angular velocity must change in accordance with the change in the inertia tensor. Viewed from a geographic frame, the inertia pole has undergone a sudden displacement and the angular velocity has begun precessing about a new position. This can constitute a change in both the amplitude and the phase of the variation of latitude data and would represent a non-stationary process. The phase shifts could be randomly distributed over long periods of time but could be cumulative over shorter time intervals to produce a spectral record similar to the results of the model proposed by Federov & Yatskiv. 1925 was a period of relative seismic inactivity with major earthquakes beginning again in 1926.

The present study is an extension of the work published by Yashkov. I chose to compute and compare spectral analyses of the ILS-IPMS data as this record comprises the longest continuous data set available from a single organization. Again I note that the apparent gain in record length and in resolution that might result from splicing data collected by independent observatories prior to the formation of the ILS on to this record would be questionable. The choice of this record, which I believe

was the optimum record available in 1971, gives a duration of about 70 years (December 1899 to October 1970) with 12 data points per year - the geographical coordinates of the rotation pole relative to the CIO. From this basic record I can produce the power spectrum, select subsets of the entire record to compare the resulting spectra and apply filters to the data which will decrease the uncertainty in the spectral estimates. In this investigation of the spectra of the wobble I shall show the basic uncertainties present in any attempt to extract parameters or to substantiate hypotheses concerning the Chandler motion by means of FFT.

CHAPTER 2

RESULTS

Using the entire ILS-IPMS data available in 1971 (Walker & Young, 1957; Jeffreys, 1968; Yumi, 1968, 1969, 1970) I computed the power spectrum of the prograde components of the variation of latitude data. I shall refer to this as the raw spectrum (Figure 2). This spectrum is in essential agreement with the spectra produced by Yashkov (1965) and Gaposchkin (1972), showing the annual peak clearly and also the fine structure of the Chandler region dominated by two sharp resonances near 0.84 cpy. I shall not consider the effect of observational errors on this spectrum but shall show the uncertainty which is directly due to the length of the record and, to a lesser extent, the discrete sampling of the variation of latitude signal. In Figure 2 the 80% confidence interval of the dominant peak extends from 10.5 to 230 $(0''.01)^2$/cpy; the bandwidth of the raw spectrum is narrow (hence the detail in the spectrum) and the corresponding variance of the spectral estimate is very large.

The confidence interval can be narrowed (at the expense of the bandwidth and resolution) by employing a suitable smoothing process and then recalculating the spectrum. I chose Parzen windows (Figure 3) to weight the data as these windows are sharply peaked in the frequency domain and thus average over a smaller frequency band than the common alternatives. For a Parzen window of width M in the time domain the data point is replaced by the smoothed data point (Jenkins and Watts, 1968, p. 244)

$$\bar{x}(t) = \sum_{j=-M}^{M} W_p(j)\, x(t + j\Delta t)$$

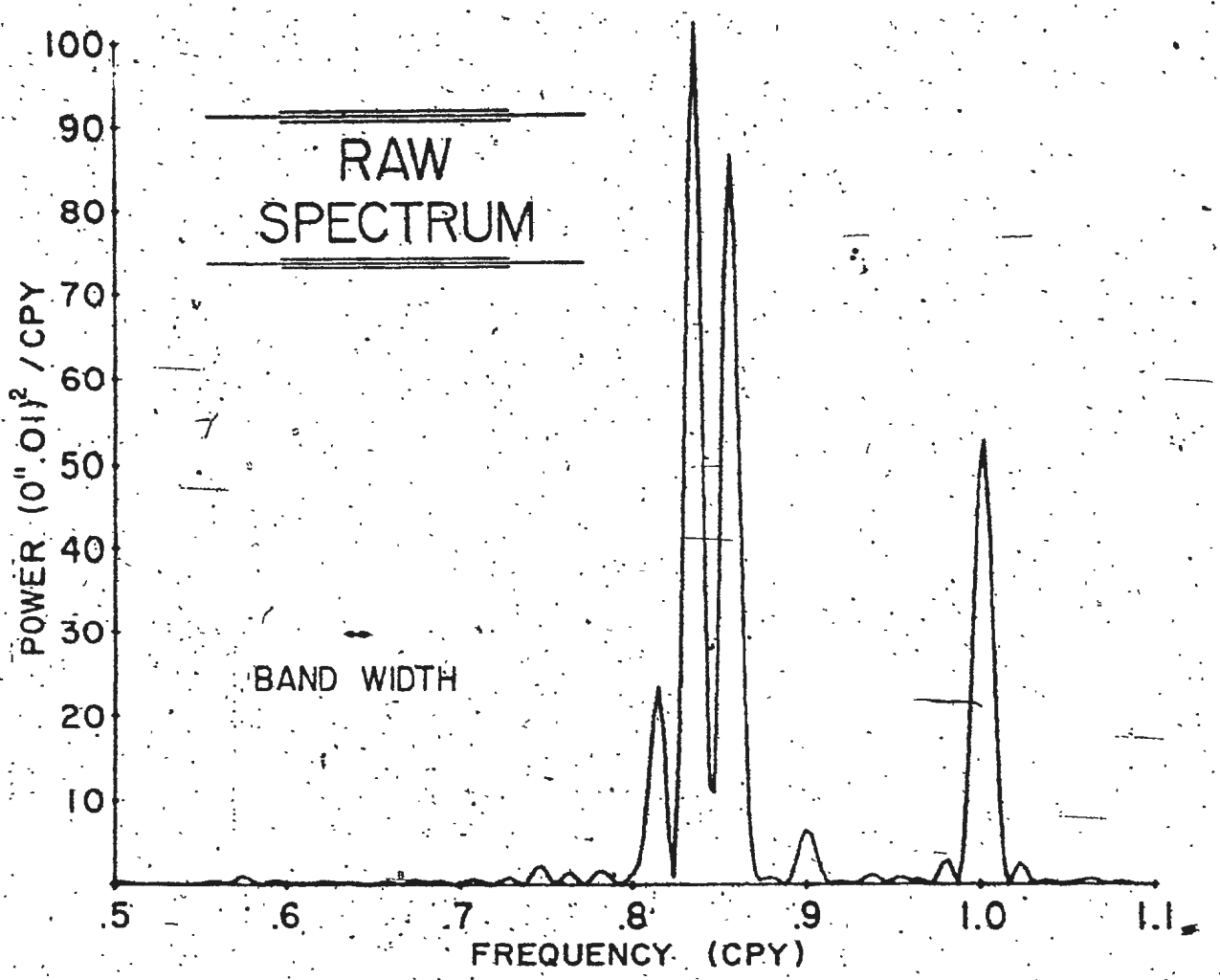

Fig. 2. Unsmoothed power spectrum of the polar motion, computed from ILS-IPMS monthly means, December 1899 - October 1970.

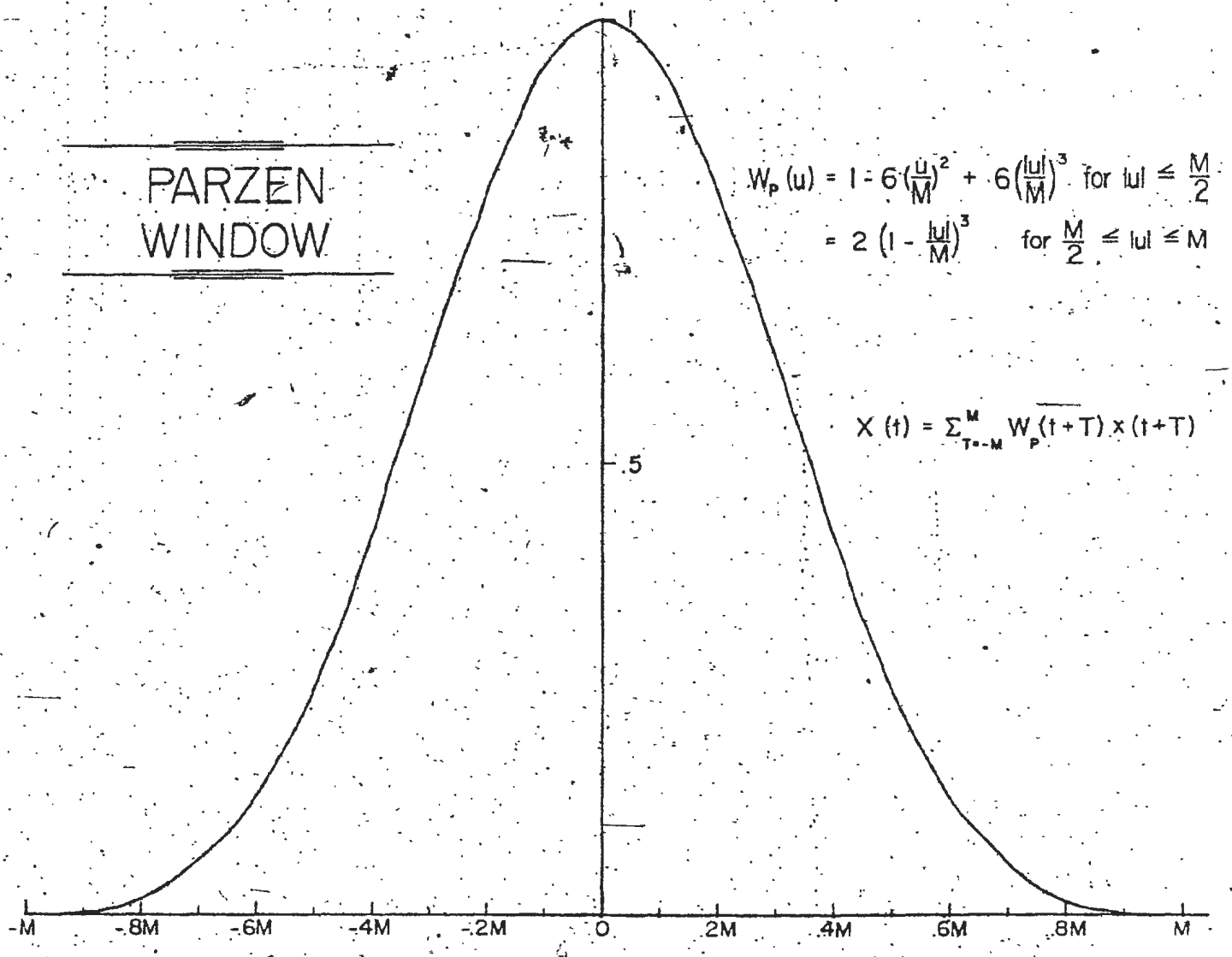

Fig. 3. The Parzen window used to smooth the spectrum.

where the weighting function or window of width M is defined by

$$W_p(j) \equiv \begin{cases} 1 - 6\left(\frac{|j|}{M}\right)^2 + 6\left(\frac{|j|}{M}\right)^3 & |j| \le M/2 \\ 2\left[1 - \frac{|j|}{M}\right]^3 & \frac{M}{2} \le |j| \le M \\ 0 & |j| \ge M. \end{cases}$$

The representation of this window in the frequency domain is

$$W_p(f) = \frac{3M}{4}\left[\frac{\sin(\pi f M/2)}{\pi f M/2}\right]^4$$

and the smoothing of the data in the time domain is equivalent to an averaging process over a bandwidth given by $\frac{1.86}{M}$ cpy. The values used for the window width were 20, 32, 50 and 70 years. Figures 4-7 show the effects of these windows on the spectrum with the 80% confidence limits indicated.

Only the last of these spectra exhibits a trace of the separation of the Chandler region into two peaks. This is to be expected since the bandwidth is only just small enough to resolve these two frequencies in this case; the confidence interval has increased to emphasize how little confidence can be placed in the reliability of this detail.

An alternative method which also demonstrates the lack of definite evidence in the spectral analysis of this data is the comparison of spectra obtained from different subsets of the ILS-IPMS data. When these subsets are taken with the same record length, the resulting spectra should be similar, provided that the wobble excitation resembles a

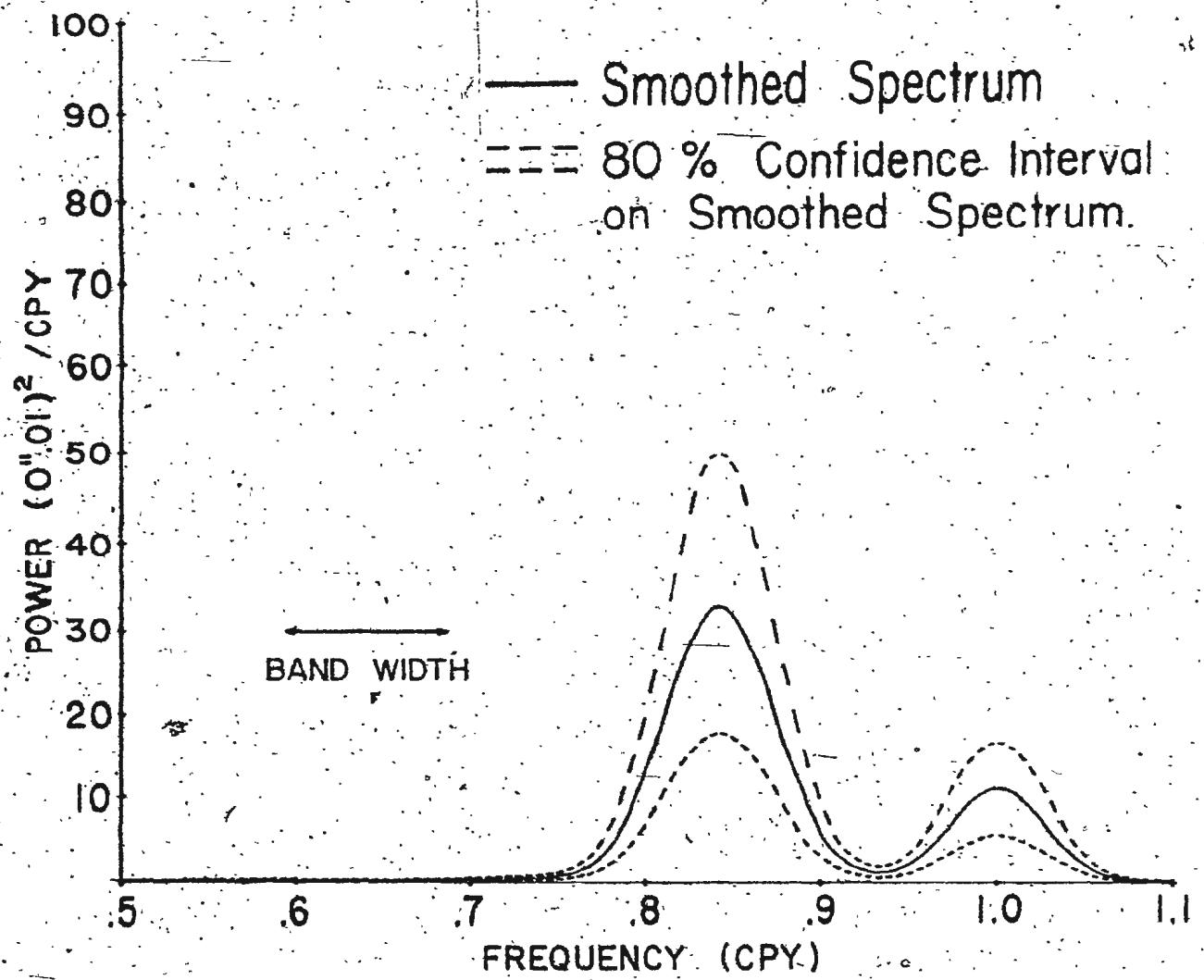

Fig. 4. Spectrum of the polar motion: 70-yr record smoothed with 20-yr Parzen window.

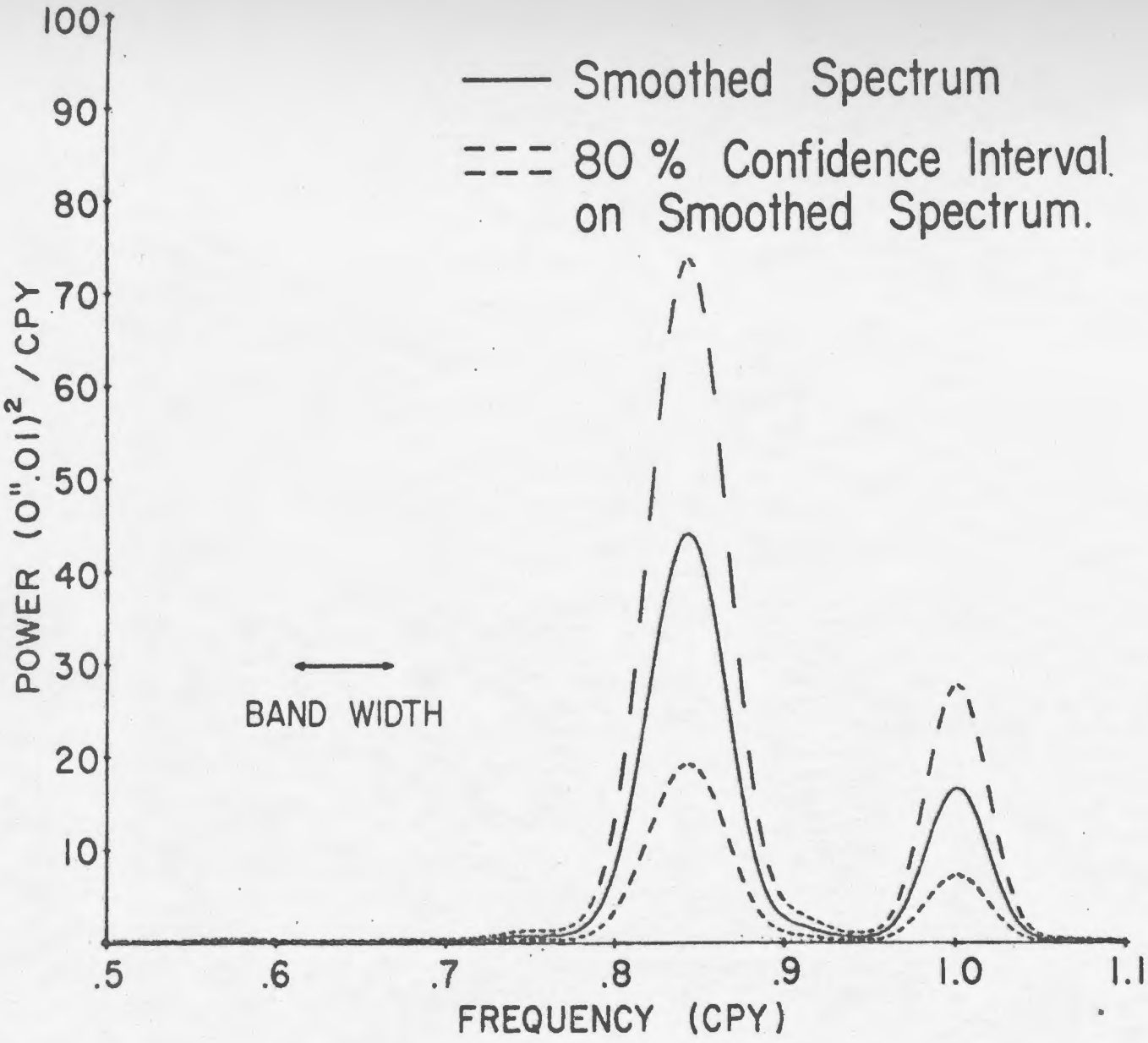

Fig. 5. Spectrum of the polar motion: 70-yr record smoothed with a 32-yr Parzen window.

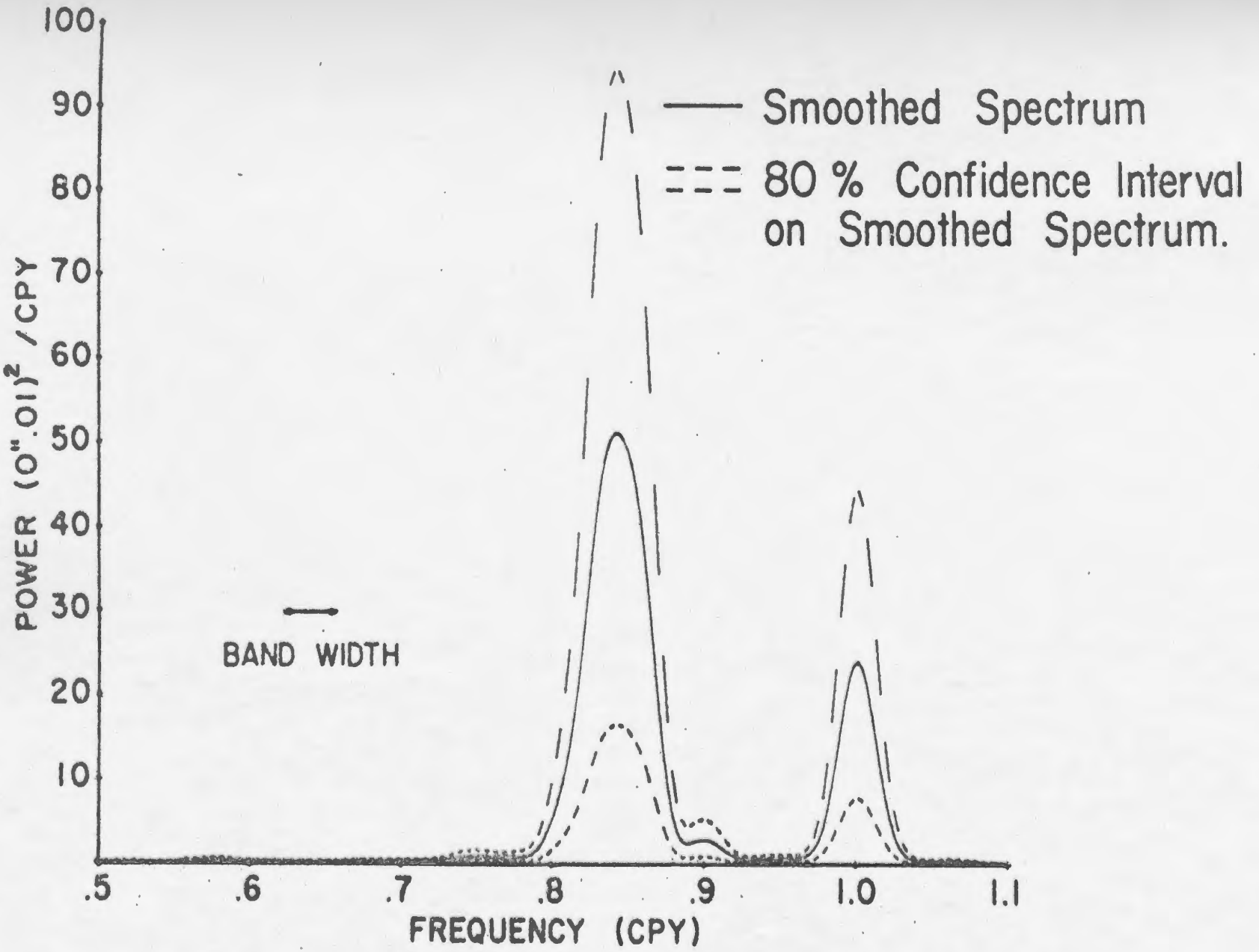

Fig. 6. Spectrum of the polar motion: 70-yr record smoothed with 50-yr Parzen window.

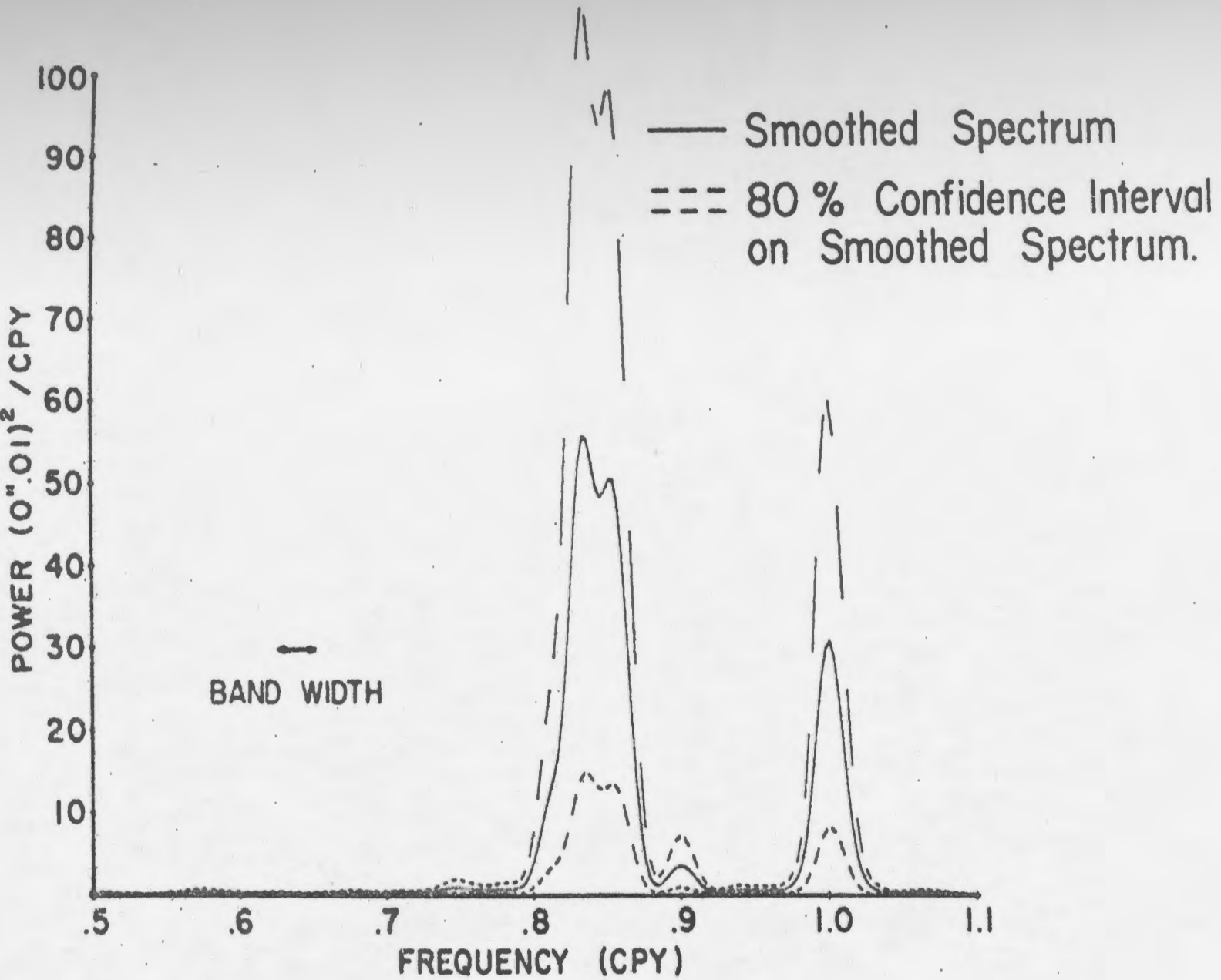

Fig. 7. Spectrum of the polar motion: 70-yr record smoothed with 70-yr Parzen window.

stationary random process. The resolution in the raw spectrum of each of these subsets is weaker than that of the full record, however, subsets of equal length will have equal resolutions and can then be compared among themselves.

This comparison has been made for record lengths of 20, 30, 40 and 60 years (Figures 8-11). Selecting the four spectra produced from records of 40-year duration (Figure 10), the unsmoothed spectra are remarkably variable in the Chandler region although the spectrum of the annual wobble is very persistent. Furthermore the observed half-width of the annual peak ($\sim$ 0.012 cpy) is the minimum half-width that can be obtained from a discrete 40-year record; narrower half-widths obtained in the Chandler region must be spurious.

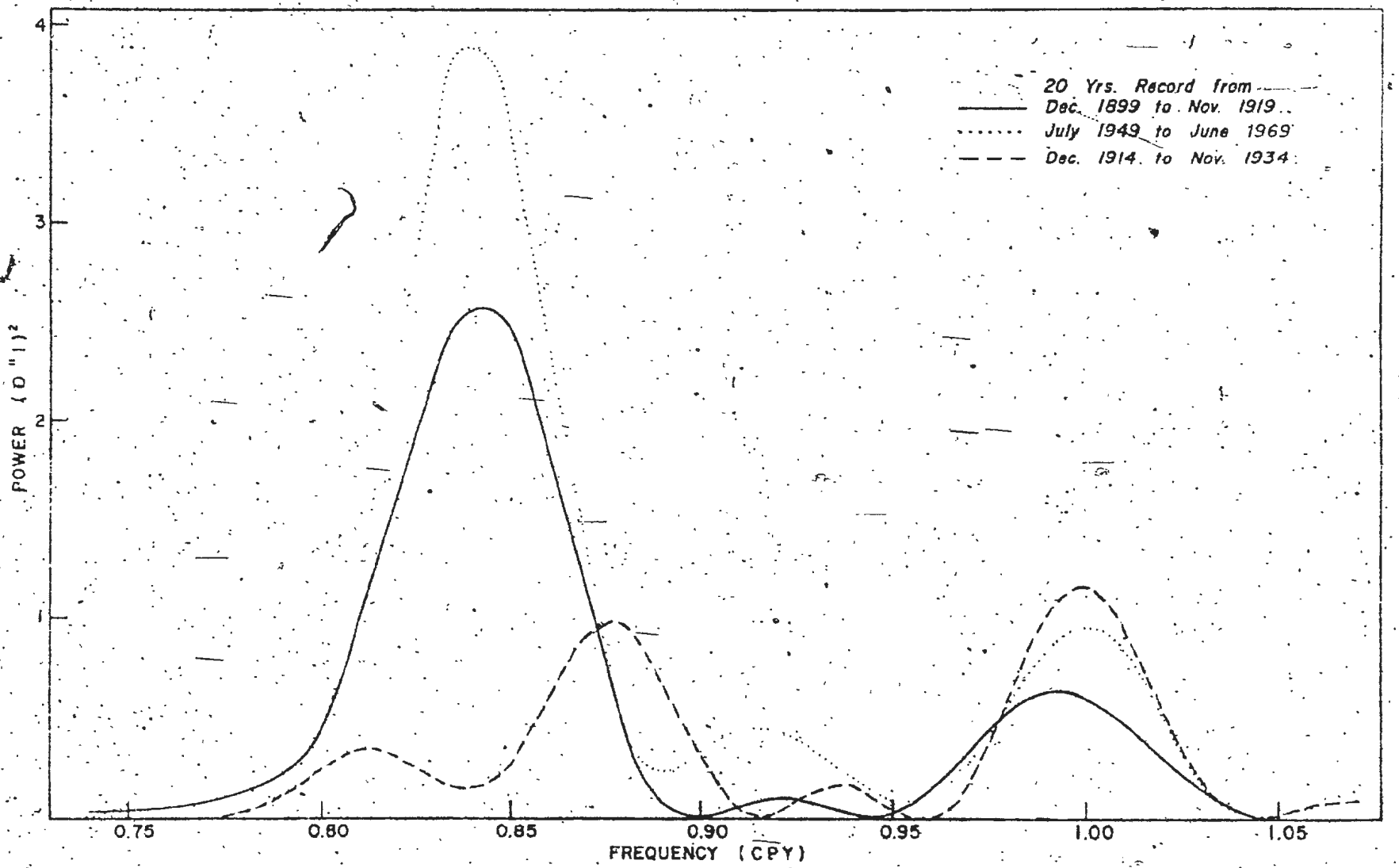

Fig. 8. Unsmoothed spectra of the polar motion, computed from 20-yr subsets of the 70-yr record.

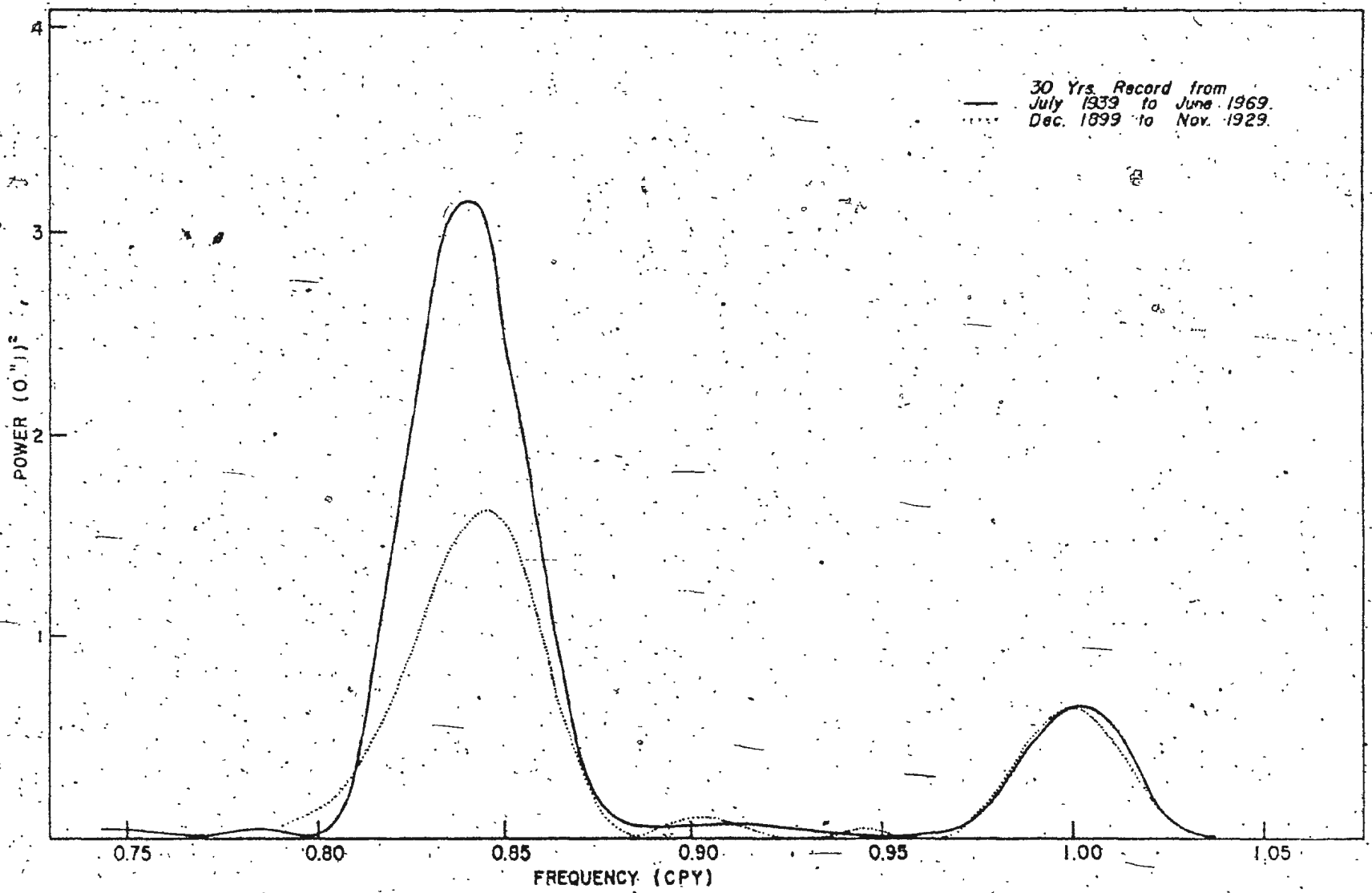

Fig. 9. Unsmoothed spectra of the polar motion, computed from 30-yr subsets of the 70-yr record.

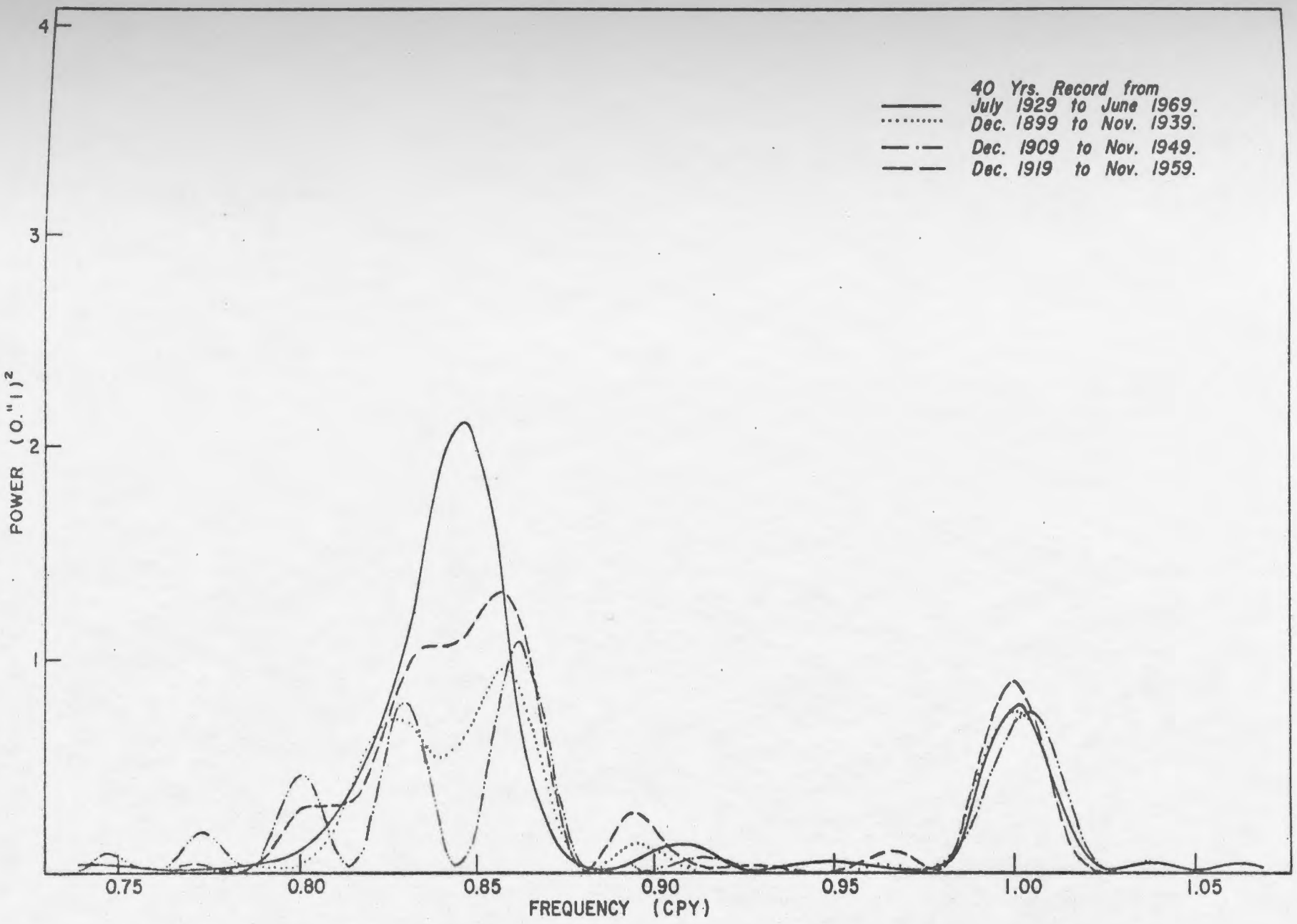

Fig. 10. Unsmoothed spectra of the polar motion, computed from 40-yr subsets of the 70-yr record.

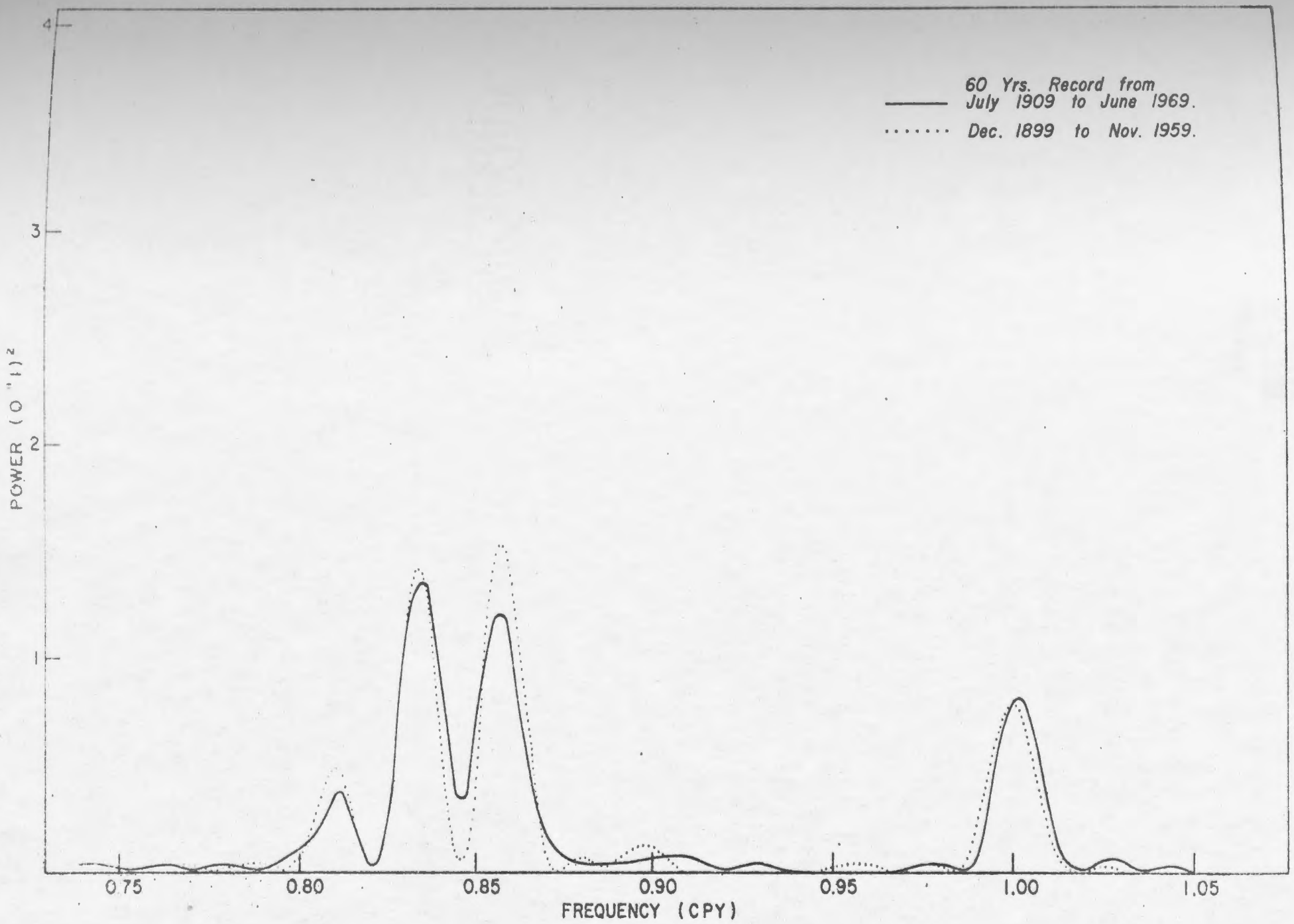

Fig. 11. Unsmoothed spectra of the polar motion, computed from 60-yr subsets of the 70-yr record.

CHAPTER 3

DISCUSSION AND CONCLUSIONS

The variability within the Chandler region lends support to the interpretation that the wobble excitation is not a stationary random process, and that the Chandler band structure is due to phase shifts. The conclusion forced by these tests is that there is neither definite evidence for nor against a double (or multiple) peak structure in the Chandler region.

Furthermore it is evident that neither the traditional nor the FFT spectral technique will succeed with the present data or even with a substantially increased record length. It is possible that in the near future better quality data (more accurate and at shorter time intervals) will be available using long baseline interferometry. However the confidence limits placed on the spectra in this paper have neglected any contributions due to noise in the data and thus reflect only the facts that the data points are discrete and that the record length is relatively short. For these methods to be decisive, for a stationary random process, a much longer record is necessary

The most important advance of this study over those of Yashkov (1965) and Gaposchkin (1972) is the investigation of the statistical aspects of the spectrum of the Chandler wobble as neither Yashkov nor Gaposchkin discussed the confidence limits placed on their spectral estimates nor the implications of the spectra with regard to stationarity.

A paper reporting this work has been published (Pedersen & Rochester, 1972).

Miller & Wunsch (1973) calculated the spectrum of the pole tide (excited by the Chandler wobble) using 65-year records of sea levels and have obtained only a single Chandler peak which again gives evidence against the existence of two or more Chandler wobble periods.

More recently MEM (Burg, 1968,1970,1972) has been applied to geophysical problems and to the Chandler wobble in particular. MEM uses a set of prediction error coefficients to pre-whiten the data before the spectral estimates are calculated and hence gives the true spectrum from a shorter record length even when the spectrum does change slowly with frequency (Lacoss, 1971). MEM also makes the least arbitrary assumption about continuing the data beyond the actual record. Claerbout (1969) used an ILS data set and Smylie et al. (1973) used 11 years of BIH data, applying MEM to obtain a single Chandler peak with a Q of 50. Currie (1974) applied MEM to the ILS-IPMS data (1900-1973) and obtained a single Chandler peak at a period of 432.95 ± 1.02 msd with a Q of 36 ± 10. Currie places an upper limit of 60 on the Q of the Chandler motion which would rule out the mantle as a possible sink of the Chandler energy; however, as I have previously noted, the half-width determined from spectral analyses will be greater than the true half-width due to the sampling technique and due to possible departures from stationarity. Currie concludes that the Chandler process is non-stationary and thus validates my own conclusions.

REFERENCES

Anderson, D. L., 1967. The anelasticity of the mantle, Geophys. J. R. astr. Soc., 14, 135.

Bodri, B., 1974. Influence of viscosity on the phase of Earth tides, Phys. Earth Planet. Interiors, 9, 141.

Buchbinder, G. G. R., 1971. A velocity structure of the Earth's core, Bull. seism. Soc. Am., 61, 429.

Burg, J. P., 1968. A new analysis technique for time series data, presented at NATO Advanced Study Institute on Signal Processing, August 1968, Enschede, Netherlands.

Burg, J. P., 1970. A new concept in power spectra estimation, presented at the 40th meeting, Soc. Explor. Geophys., New Orleans, November 1970.

Burg, J. P., 1972. The relationship between maximum entropy spectra and maximum likelihood spectra, Geophysics, 37, 375.

Claerbout, J. F., 1969. Frequency mixing in Chandler wobble data (abstract), Trans. Am. geophys. Un., 50, 119.

Colombo, G. and Shapiro, I. I., 1968. Theoretical model for the Chandler wobble, Nature, 217, 156.

Cooley, J. W. & Tukey, J. W., 1965. An algorithm for the machine calculation of complex Fourier series, Math. Comp., 19, 297.

Currie, R. G., 1974. The period and Q_w of the Chandler wobble, Geophys. J. R. astr. Soc., 38, 179.

Dahlen, F. A., 1971. The excitation of the Chandler wobble by earthquakes, Geophys. J. R. astr. Soc., 25, 157.

Doornbos, D. J., 1974. The anelasticity of the inner core, Geophys. J. R. astr. Soc., 38, 397.

Federov, E. P. & Yatskiv, Ya. S., 1965. The cause of the apparent "bifurcation" of the free nutation period, Soviet Astronomy, 8, 608.

Gaposchkin, E. M., 1972. Analysis of pole position from 1846-1970, in Rotation of the Earth, eds. P. Melchior, S. Yumi, D. Reidel Publishing Co., Dordrecht.

Hendershott, M. C., 1973. Ocean tides, EOS Trans. AGU, 54, 76.

Hough, S. S., 1895. The oscillations of a rotating, ellipsoidal shell containing fluid, Nature, 217, 156.

Israel, M., Ben-Menahem, A. & Singh, S. J., 1973. Residual deformation of real Earth models with application to the Chandler Wobble, Geophys. J. R. astr. Soc., 32, 219.

Jeffreys, H., 1968. The variation of latitude, Mon. Not. R. astr. Soc., 141, 255.

Jenkins, G. M. & Watts, D. G., 1968. Spectral Analysis and its applications, Holden-Day, San Francisco, California.

Kaula, W. M., 1968. An Introduction to Planetary Physics: The Terrestrial Planets, John Wiley Inc., New York.

Lacoss, R. T., 1971. Data adaptive spectral analysis methods, Geophysics, 36, 661.

Lagus, P. L. & Anderson, D. L., 1968. Tidal dissipation in the Earth and Planets, Phys. Earth Planet. Interiors, 1, 505.

Larmor, J., 1909. The relation of the Earth's free precessional nutation to its resistance against tidal deformation, Proc. R. Soc. London, A, 82, 89.

Larmor, J., 1915. The influence of the oceanic waters on the law of variation of latitudes, Proc. Lond. Math. Soc., Ser. 2, 14, 440.

Love, A. E. H., 1909. The yielding of the Earth to disturbing forces, Proc. R. Soc. London, A, 82, 73.

Mansinha, L. & Smylie, D. E., 1967. Effect of earthquakes on the Chandler wobble and the secular polar shift, J. geophys. Res., 72, 4731.

Mansinha, L. & Smylie, D. E., 1968. Earthquakes and the Earth's wobble, Science, 161, 1127.

Melchior, P., 1957. Latitude Variation, Progress in Physics and Chemistry of the Earth, 2, Pergamon Press.

Miller, S. P. & Wunsch, C., 1973. The pole tide, Nature, 246, 98.

Munk, W. & Hassan, E. S. M., 1961. Atmospheric exciation of the Earth's wobble, Geophys. J. R. astr. Soc., 4, 339.

Munk, W. & MacDonald, G. J. F., 1960. The rotation of the Earth, Cambridge University Press.

Newcomb, S., 1892. Remarks on Mr. Chandler's law of variation of terrestrial latitudes, Astr. J., 12, 49.

Pedersen, G. P. H. & Rochester, M. G., 1972. Spectral analyses of the Chandler wobble, in Rotation of the Earth, eds. P. Melchior, S. Yumi, D. Reidel Publishing Co., Dordrecht.

Qamar, A. & Eisenberg, A, 1974. The damping of core waves, J. geophys. Res., 79, 758.

Rochester, M. G. & Smylie, D. E., 1965. Geomagnetic core-mantle coupling and the Chandler wobble, Geophys. J. R. astr. Soc., 10, 289.

Rudnick, P. 1956. The spectrum of the variation of latitude, Trams. Am. geophys. Un., 37, 137.

Smith, S. W. & Anderson, D. L., 1967. Attenuation of the Earth's free oscillations (abstract), Intern. Union. Geol. Geophys.

Smylie, D. E. & Mansinha, L., 1971. The elasticity theory of dislocations in real Earth models and changes in the rotation of the Earth, Geophys. J. R. astr. Soc., 23, 329.

Smylie, D. E., Clarke, G. K. C. & Ulrych, T. J., 1973. Analysis of the irregularities in the Earth's rotation, in Methods of computational physics, eds. B. Alder, S. Feinbach, B. A. Bolt, vol. 13, Academic Press, New York.

Walker, A. & Young, A., 1957. Further results on the analysis of the variation of latitude, Mon. Not. R. astr. Soc., 117, 119.

Yashkov, V. Ya., 1965. Spectrum of the motion of the Earth's poles, Soviet Astronomy, 8, 605.

Yumi, S., 1968-1970. Monthly Notes Int. Polar Motion Serv.

PART II

UNDERTONES AND TIDES FOR A ROTATING EARTH

INTRODUCTION

The problem of theoretically deriving the response of the Earth to the tidal attraction of astronomical bodies has been under development for the last hundred years.

In 1863 Kelvin calculated the response of an incompressible sphere, homogeneous in density and rigidity, to a potential of external origin. Herglotz (1905) generalized this study by considering models with spherical symmetry and quadratic forms (Roche's law) for the density and rigidity profiles. The effects of compressibility on a homogeneous Earth were accounted for by Love (1909) and, on a Roche model Earth, by Hoskins (1920). The first investigation to incorporate a core (Jeffreys, 1926) modelled the Earth as an incompressible homogeneous mantle overlying a homogeneous incompressible core. Although each of these studies was an extension on previous work, all models considered were extremely simple; the computational difficulties inherent in a realistic Earth model were prohibitive and none of the above Earth models could be considered more than indicative.

The first work to incorporate a geophysically more realistic Earth model was undertaken by Takeuchi (1950). Taking varied Earth models consistent with Bullen's seismological results, he numerically integrated (by abacus) the set of differential equations which define the deformation field.

Within the last two decades, computers have made possible the investigation of Earth tides for increasingly more realistic Earth models.

Jeffreys & Vicente (1957) adopted a variational approach and treated the core as an incompressible fluid rather than as a solid with vanishing rigidity. In one model they specified a Roche law density profile within the core and in the other model they simulated the inner core to some extent by introducing a point mass at the Earth's centre. Molodenskii (1961) started with the Navier-Stokes equations and examined a model with a fluid core, where the density variation in the fluid was due to compression alone, and a model containing a solid inner core. Jeffreys & Vicente's approach has been reworked (Pedersen, 1967) with minor corrections and Kakuta (1970) has extended Molodenskii's work by accounting for the effects of compressibility within the fluid region on the boundary conditions at the core-mantle interface.

Until recently all geophysically acceptable models had been constructed under the assumption that the fluid core obeyed the Adams-Williamson condition; the fluid core had been assumed to be adiabatic and hence gravitationally neutrally stable against convection. The investigation of the static deformation of the fluid core of the Earth by Smylie & Mansinha (1971) has emphasized the importance of this assumption. Subsequently, Pekeris & Accad (1972) introduced a polytropic model for the fluid core which admits departures from the above adiabatic model to a sub- or super-adiabatic fluid and investigated the resulting tidal deformation of the Earth; however their work neglected the Earth's rotation.

Inversion of free oscillation data has refined Earth models and the accompanying free oscillation theory has recast the governing equations

of the deformation into six first-order differential equations appropriate to high speed computation, I extend the governing equations to include rotational couplings. The specific model under consideration was initially developed by Landisman et al. (1965), modified by Pekeris & Accad (1972) to incorporate a sub- or super-adiabatic fluid core and then by Smylie (1974) to include a solid inner core.

In the first chapter I will specify the Earth model under consideration in greater detail and note the simplifications which were taken to ensure that the computations were manageable. I also derive the differential equations which govern the spatial variation of the deformation. The development undertaken in this chapter is an extension of work previously done in the theory of elastic free oscillations (Alterman et al., 1959), the static deformation of the Earth (Smylie & Mansinha, 1971) and the externally driven bodily tides of the solid Earth (Pekeris & Accad, 1972). Smylie (1974) attempted to improve on Pekeris & Accad by taking the effects of rotation into account but ignored the excitation of torsional modes through Coriolis coupling. Crossley (1975b) has investigated the effects of Coriolis coupling and has calculated undertone periods. This work is an improvement over the results of Pekeris & Accad and Smylie due to the inclusion of the Earth's rotation and specifically because of the retention of the Coriolis coupling which excites the torsional modes of oscillation.

The second chapter contains the specific numerical methods necessary to initiate and to propagate the solution through the Earth from the geocentre. The initialization is an extension of the techniques described by Smylie & Mansinha (1971) and have been obtained independently

by Crossley (1975a) for a non-rotating Earth. My initialization scheme accommodates the Earth's rotation. Due to the excitation of the torsional modes and of the spheroidal modes of other degrees than the degree of the exciting potential, the propagation technique is most simply described by matrices and 4-dimensional arrays rather than by vectors and matrices. Because of the rotational coupling it is also necessary to test the solutions obtained for stability against changes in the truncation level retained to compute the responses.

The numerical results are presented in the third chapter. I find that the inclusion of the rotational effects, especially within the fluid core, greatly perturbs the motions from the solutions obtained by Pekeris & Accad (1972) and Smylie (1974), to the extent that a practical upper limit of 11 hours is placed on the forcing period for the procedure developed in this study to be applicable; Crossley (1975b) presents quasi-empirical evidence that for core undertone oscillations there is a theoretical upper limit on the period of 12 hours; both his results and mine demonstrate that the number of modes which must be considered increase rapidly as this limit is approached. Within the above period range only one bodily tide has been observed (the ter-diurnal M_3). I calculate the solutions for this tide and the Love numbers that result. However it is also possible to predict two free oscillations of degree 2, order 2, with periods less than 12 hours by investigating the variation of the Love numbers as functions of the period of the exciting potential.

The discussion of the results of this analysis is presented in the final chapter.

The detailed mathematical developments have been described in appendices in an attempt to retain continuity through the main text of the thesis.

CHAPTER 1

EQUATIONS GOVERNING THE TIDAL RESPONSE OF THE ROTATING EARTH

1. The Earth Model

The Earth model consists basically of three regions: an elastic solid envelope - the mantle, an outer fluid core and an inner elastic solid core. In each region the model is defined in terms of the density profile, the gravitational field strength, and the shear and compressional velocities of the seismic waves (or alternatively the Lamé constants). Although I can formulate the general problem to include the ellipticities of these surfaces implicitly, in order to evaluate the solution I have allowed the model to degenerate to spherical symmetry. The initial condition that is imposed on this model Earth is an equilibrium configuration of balance between the elastic stresses and the gravitational field (hydrostatic equilibrium).

The conditions investigated in this thesis are the reactions of the Earth, while rotating uniformly, to a harmonic potential of external origin.

The governing equations I derive follow most closely those of Alterman et al. (1959) and Smylie & Mansinha (1971) but incorporate fully the effects of the external potential and of the rotation. Pekeris & Accad (1972) have also attempted a study of Earth tides using the equations in the above mentioned works but they did not include the effects of rotation. Smylie (1974) included the Coriolis self-coupling but neglected the excitation of other modes by the Coriolis effect.

The major shortcoming of this model is the relaxation of the ellipticity of the internal surfaces to provide a spherically symmetric model.

As previously mentioned the actual profiles of the Earth parameters have been taken to indicate the response of a sub-adiabatic fluid core with constant stability factor $\beta = -0.2$. The model was initially described by Landisman et al. (1965). Pekeris & Accad (1972) then recalculated the density and gravity profile in the inner core consistent with the above stability factor, and Smylie (1974) provided the data in Table 1 which takes the solid inner core of the Earth into account.

The choice of a constant $-\beta$ profile has limited the model so that only the constraint on the mass of the core (and not the constraint on the core's moment of inertia) is satisfied.

TABLE 1

THE PARAMETERS OF THE EARTH MODEL WITH A SUB-ADIABATIC OUTER CORE ($\beta(r) = -0.2$) (SMYLIE, 1974)

r (km)	ρ_o (gm/cm^3)	g_o (cm/s^2)	v_p (km/s)	v_s (km/s)
0	13.030	0	11.15	4.90
173.5	13.023	63.1	11.15	4.89
347.0	13.003	126.2	11.16	4.88
520.5	12.968	189.0	11.17	4.88
694.0	12.921	251.4	11.17	4.86
867.5	12.860	313.3	11.15	4.85
1041.0	12.786	374.7	11.13	4.84
1075.7	12.770	386.9	11.12	4.84
1110.4	12.753	399.0	11.09	4.84
1145.1	12.736	411.2	11.04	4.84
1179.8	12.717	423.3	10.93	4.83
1214.5	12.697	435.3	10.76	4.83
1214.5	12.697	435.3	10.76	
1249.2	12.677	447.4	10.48	
1283.9	12.654	459.4	10.17	
1297.8	12.645	464.2	10.11	
1318.6	12.630	471.3	10.11	
1388.0	12.581	495.1	10.08	
1735.0	12.293	610.8	9.88	
2082.0	11.939	720.8	9.63	
2429.0	11.517	824.0	9.31	
2776.0	11.023	919.1	8.90	
3123.0	10.449	1004.8	8.44	
3473.0	9.795	1080.2	8.04	
3473.0	5.279	1080.2	13.65	7.20
3491.0	5.239	1077.0	13.70	7.20

TABLE 1, continued

r (km)	ρ_0 (gm/cm^3)	g_0 (cm/s^2)	v_p (km/s)	v_s (km/s)
3571.0	5.086	1063.1	13.70	7.25
3771.0	5.092	1034.2	13.45	7.20
3971.0	5.090	1013.7	13.20	7.10
4171.0	5.085	1000.1	13.00	7.00
4371.0	5.072	992.0	12.80	6.95
4571.0	5.066	988.4	12.55	6.85
4771.0	5.040	988.5	12.30	6.75
4971.0	4.955	991.0	12.05	6.60
5171.0	4.852	994.8	11.80	6.50
5371.0	4.619	998.6	11.40	6.35
5471.0	4.502	999.9	11.30	6.30
5571.0	4.373	1000.9	10.90	6.15
5671.0	4.215	1001.3	10.50	5.90
5771.0	4.047	1000.9	10.10	5.60
5871.0	3.812	999.4	9.60	5.30
5958.0	3.569	997.0	9.06	5.00
6071.0	3.374	992.5	8.50	4.60
6171.0	3.413	988.6	8.05	4.40
6221.0	3.462	987.0	7.85	4.35
6271.0	3.488	985.8	8.00	4.40
6311.0	3.474	984.9	8.15	4.60
6338.0	3.386	984.3	8.16	4.65
6338.0	2.840	984.3	6.30	3.55
6371.0	2.840	981.9	6.30	3.55

2. List of Symbols

I have adopted the standard representation used in the theory of free oscillations and of forced tidal response of the Earth. A list of the main symbols used with their physical meaning is presented here. In general I shall distinguish a unit vector by a circumflex (^), a vector by an arrow (→) and a tensor by a tilda (~) over the symbol.

$i = \sqrt{-1}$	the imaginary unit
$\tilde{1}$	the identity tensor
$\dot{x} = \frac{\partial x}{\partial t}$	the partial derivative with respect to time
D	the distance from the Earth to the Moon
$\tilde{e}$	the elastic strain tensor
$f = \frac{\sigma}{\Omega}$	the driving frequency in cycles/day
$\vec{g}_o$	the equilibrium value for gravity at $\vec{r}$
G	the universal constant of gravitation
h,k,l	Love numbers
k,n	indices indicating the degree of a spherical harmonic
l,m	indices indicating the order of a spherical harmonic
p_o	the equilibrium hydrostatic pressure
P_n^m	the associated Legendre function of degree n and order m
$\vec{r}$	the position or radius vector

R	the radius of the Earth
S_n^m	the surface spherical harmonic of degree n and order m
t_n^m, u_n^m, v_n^m	the radial factors in the displacement modes
$\vec{u}$	the vector displacement from the equilibrium position
V, V_o	the instantaneous and equilibrium gravitational potential
v_p, v_s	the compressional and shear seismic velocities
y_i	the radial factors in the expansions of the fields
β	stability factor
Δ	dilatation or relative change in volume
θ	geocentric co-latitude
λ	Lamé constant (adiabatic incompressibility within the fluid)
μ	rigidity
ρ, ρ_o	instantaneous and equilibrium density
σ	frequency of the driving potential
$\tilde{\tau}, \tilde{\tau}_o$	initial and instantaneous stress tensors
$\tilde{\tau}_1$	elastic stress tensor
ϕ	geocentric longitude
Φ	the induced potential resulting from the deformations
ψ	the external forcing potential
$\vec{\Omega}$	the angular velocity of the Earth

Other symbols may be introduced and used briefly for explicitly stated purposes.

3. Equations of Motion for the Rotating Earth

Within the model Earth defined, consider a mass element which undergoes a small displacement $\vec{u}$ to the point $\vec{r}$. This displacement is directly due to the application of an external (harmonic) potential, but it is also necessary to consider the indirect effects of rotation, the differences in gravity and the initial stress between the initial and instantaneous particle position, the establishment of additional elastic stress and the induced gravitational field due to these displacements. At this stage it is not yet necessary to insist on spherical symmetry.

In a geographic frame rotating with uniform angular velocity $\vec{\Omega} = \Omega \hat{k}$, that is a frame rotating on the average with the Earth, the equation of motion of an element of mass is:

$$\rho\left[\ddot{\vec{u}} + 2\vec{\Omega}\times\dot{\vec{u}} + \vec{\Omega}\times(\vec{\Omega}\times\vec{r})\right] = \vec{\nabla}\cdot\tilde{\tau} + \rho\vec{\nabla}V + \rho\vec{\nabla}\psi \tag{1.1}$$

where ρ, $\tilde{\tau}$, V and ψ are the instantaneous density, stress tensor, gravitational potential and externally produced potential at $\vec{r}$. These quantities are related to their equilibrium values at $\vec{r}$: ρ_0, $\tilde{\tau}_0$, V_0 by

$$\begin{aligned} \rho &= \rho_0 + \rho_1 \\ \tilde{\tau} &= \tilde{\tau}_0 + \tilde{T} \\ V &= V_0 + \Phi \quad \text{with} \quad \vec{\nabla}V_0 \equiv \vec{g}_0 \end{aligned} \tag{1.2}$$

The change in the density of the mass element as it is carried from $\vec{r} - \vec{u}$ to $\vec{r}$ is due to the dilation, $\Delta \equiv \vec{\nabla}\cdot\vec{u}$, (either expansion or contraction) during its displacement and hence

$$\begin{aligned} \rho(\vec{r}) &= \rho_o(\vec{r}-\vec{u}) - \rho_o \Delta \\ &= \rho_o(\vec{r}) - \vec{u}\cdot\vec{\nabla}\rho_o - \rho_o\Delta \\ &= \rho_o(\vec{r}) - \vec{\nabla}\cdot(\rho_o\vec{u}) \\ &= \rho_o + \rho_1 \end{aligned} \tag{1.3}$$

The instantaneous stress existing at $\vec{r}$ is due to that carried by the mass element from $\vec{r} - \vec{u}$ plus that due to the elastic stresses associated with the shear motions and volume changes. Therefore

$$\begin{aligned} \tilde{\tau}(\vec{r}) &= \tilde{\tau}(\vec{r}-\vec{u}) + \tilde{\tau}_1 \\ &= \tilde{\tau}(\vec{r}) - \vec{u}\cdot\vec{\nabla}\tilde{\tau} + \tilde{\tau}_1 \end{aligned} \tag{1.4}$$

where $\tilde{\tau}_1$ incorporates the stresses due to the deformation.

The assumption that the original stress distribution is isotropic, i.e. $\tilde{\tau}_o = -p_o \tilde{1}$, allows the equilibrium condition (which can be extracted from the equation of motion by simply allowing the external potential and the displacement field to vanish) to be written

$$\rho_o \vec{\Omega}\times(\vec{\Omega}\times\vec{r}) = \vec{\nabla}\cdot\tilde{\tau}_o + \rho_o\vec{\nabla}V_o = -\vec{\nabla}p_o + \rho_o\vec{\nabla}V_o. \tag{1.5}$$

This is the condition of hydrostatic equilibrium for a rotating Earth, a balance between the effects of the initial stress and the geopotential. A consequence of the condition of isotropy in this model is that the equipotential surfaces and the isopecnic surfaces coincide in the undeformed configuration:

$$\vec{\nabla}\rho_o \parallel \vec{\nabla}V_o' - \vec{\Omega}\times(\vec{\Omega}\times\vec{r}). \tag{1.5a}$$

Rewriting the equations of motion to first order in the displacements, and using (1.5):

$$\rho_0 \ddot{\vec{u}} + 2\rho_0 \vec{\Omega} \times \dot{\vec{u}} = \vec{\nabla} \cdot \tilde{\tau}_1 - \rho_0 \Delta [\vec{\nabla} V_0 - \vec{\Omega} \times (\vec{\Omega} \times \vec{r})] + \rho_0 \vec{\nabla} [\psi + \Phi + \vec{u} \cdot \vec{\nabla} V_0 - \vec{u} \cdot \vec{\Omega} \times (\vec{\Omega} \times \vec{r})]. \tag{1.6}$$

I note here that if the rotational effects and the presence of the tide-producing potential are simultaneously set to zero the above equation properly degenerates to the equation defining the displacement field obtained in free oscillation theory:

$$\rho_0 \ddot{\vec{u}} = \vec{\nabla} \cdot \tilde{\tau}_1 - \rho_0 \Delta \vec{\nabla} V_0 + \rho_0 \vec{\nabla} [\Phi + \vec{u} \cdot \vec{\nabla} V_0]$$

(Alterman et al., 1959, p. 83, eqs. 7-9).

Alternatively, if the time dependence is also neglected the above equation reduces to the displacement equation investigated by Smylie & Mansinha in their study of the static deformation of the Earth:

$$\vec{\nabla} \cdot \tilde{\tau}_1 + \rho_0 \vec{\nabla} [\Phi + \vec{u} \cdot \vec{\nabla} V_0] - \rho_0 \Delta \vec{\nabla} V_0 = 0$$

(Smylie & Mansinha, 1971, p. 331, eq. 10).

If only the rotational terms are neglected the displacement equation I have developed degenerates to that obtained and used by Pekeris & Accad in their study of tidal deformations:

$$\rho_0 \ddot{\vec{u}} = \vec{\nabla} \cdot \tilde{\tau}_1 + \rho_0 \vec{\nabla} [\Phi' + \vec{u} \cdot \vec{\nabla} V_0] - \rho_0 \Delta \vec{\nabla} V_0$$

(Pekeris & Accad, 1972, p. 238, eqs. 5,6). In their paper they have included the external potential in the term Φ' rather than carrying this forcing potential explicitly. This is equivalent to our procedure providing that there is a corresponding modification in the boundary condition placed on Φ at the Earth's surface.

Finally the displacement equation degenerates to that used by Smylie to investigate the undertones of the Earth if the centrifugal terms in the displacement equation are set to zero:

$$\rho_0 \ddot{\vec{u}} + 2\rho_0 \vec{\Omega} \times \dot{\vec{u}} = \vec{\nabla} \cdot \tilde{\tau}_1 + \rho_0 \vec{\nabla} [\Phi + \vec{u} \cdot \vec{\nabla} V_0] - \rho_0 \Delta \vec{\nabla} V_0$$

(Smylie, 1974, eqs. 1,17).

The periods of elastic free oscillation are all less than 1 hour, so the neglect of the Coriolis effect is justifiable as I shall show numerically; however these effects become crucial in the consideration of the Earth tide phenomena and core undertones.

Smith (1974) has not only taken into account the full effects of rotation but also the departure of the Earth from spherical symmetry. He has also noted the excitation of the torsional modes and the coupling between modes which arises due to the departure of the Earth from a spherically symmetric, non-rotating body. Although his theoretical work is thus more complete than the results of this thesis, he has done no numerical calculations to show the effects of the coupling. Secondly, Smith's thesis requires knowledge of the variation of the ellipticity of

the isopecnic, equipotential surfaces and the normal derivatives of density, the geopotential and the seismic velocities; the retention of the centrifugal term will give rise to couplings between modes governed by the same selection rules as the ellipticity effects and of the same order since the ellipticity $\epsilon \simeq \Omega^2 a/g_0$. In comparison with the effects of the ellipticity, the centrifugal term is simply given and can be taken into account readily as I have done in this thesis.

In order to be able to solve for the deformation field it is necessary to supplement the displacement equation derived above with Laplace's equation for the forcing potential, Poisson's equation for the gravitational and the induced potentials and to postulate a stress-strain dependence. The decomposition of the displacements into radial spheroidal, transverse spheroidal, and torsional vectors and the subsequent expansion of these and the other field quantities into surface spherical harmonics is a standard and very useful technique.

4. Spherical Harmonic Expansion of the Equations of Motion

To proceed further I use the surface spherical harmonics

$$S_n^m(\theta,\phi) \equiv P_n^m(\cos\theta)\, e^{im\phi} \tag{1.7}$$

of degree n and order m where θ is the geocentric co-latitude and ϕ is the longitude. These are normalized such that they satisfy the relation

$$\int S_k^m S_k^{-m} \sin\theta\, d\theta\, d\phi = 2\pi \int P_k^m P_k^{-m} \sin\theta\, d\theta = \frac{4\pi(-1)^m}{2k+1} \tag{1.7a}$$

These surface spherical harmonics form a complete orthogonal basis for a spherical surface. The induced and the external potential can now be written in terms of this basis set as

$$\Phi = \sum_{n=0}^{\infty}\sum_{m=-n}^{n} \Phi_n^m(r) S_n^m(\theta,\phi) \;;\quad \phi = \sum_{n=2}^{\infty}\sum_{m=-n}^{n} \psi_n^m(r) S_n^m(\theta,\phi). \tag{1.8}$$

For the representation of a vector this is extended to the orthogonal vector basis with the triad

$$\hat{r} S_n^m \;,\quad r\vec{\nabla} S_n^m \;,\quad \vec{r}\times\vec{\nabla} S_n^m \tag{1.7b}$$

which are mutually perpendicular, orthogonal over the sphere and complete (Backus, 1958). Therefore the displacement field is written as a combination of spheroidal and torsional vector components:

$$\vec{u} = \sum_{n=0}^{\infty}\sum_{m=-n}^{n} \left\{ u_n^m \hat{r} S_n^m + v_n^m r\vec{\nabla} S_n^m + t_n^m \vec{r}\times\vec{\nabla} S_n^m \right\}. \tag{1.9}$$

In standard free oscillation theory the torsional component is completely decoupled from the spheroidal modes. It is excited independently of the spheroidal modes and can be studied independently. Again in the static deformation of the Earth, it is decoupled from the spheroidal modes and is solved independently. As the forcing potential is purely spheroidal, Pekeris & Accad (1972) and Smylie (1974) assumed that there was no coupling between the torsional oscillations and the spheroidal excitation and completely neglected any study of the torsional response. In the situation here considered the torsional modes are excited through rotational (Coriolis) coupling to the spheroidal modes; they also feed energy back into the spheroidal modes and consequently they must be retained in the description of the displacements for a complete solution. Neglect of the torsional modes also leads to a violation of the conservation of angular momentum (Appendix F).

From the structure assumed above for the displacements and the properties of the surface spherical harmonics the dilatation can be written as

$$\Delta = \sum_{n=0}^{\infty} \sum_{m=-n}^{n} \left\{ \frac{du_n^m}{dr} + 2\frac{u_n^m}{r} - n(n+1)\frac{v_n^m}{r} \right\} S_n^m \quad . \tag{1.10}$$

Therefore, for simplicity, I shall omit the summation signs and the indices unless ambiguity would result. In keeping with previous works (Alterman et al., 1959) I shall also adopt the equivalent variables

$$y_1 = u_n^m \quad , \quad y_3 = v_n^m \quad , \quad y_5 = \Phi_n^m \tag{1.11a}$$

and introduce

(1.11b) $$y_7 = i t_n^m \quad , \quad y_9 = \psi_n^m \, .$$

Since its sources are external to the Earth the tide-producing potential satisfies Laplace's equation

$$\nabla^2 \psi_n^m = 0$$

and since the potential must be finite through the Earth the relevant solution satisfies the first-order differential equation

(1.12) $$\frac{dy_9}{dr} = n \frac{y_9}{r} \, .$$

Poisson's equation governs the initial and the instantaneous gravitational potentials, hence

(1.13) $$\nabla^2 V_0 = \vec{\nabla} \cdot \vec{g}_0 = -4\pi G \rho_0$$
$$\nabla^2 V = -4\pi G \rho \, .$$

Therefore the induced potential satisfies

(1.14a) $$\nabla^2 \Phi = -4\pi G \rho_1 = 4\pi G \vec{\nabla} \cdot (\rho_0 \vec{u})$$

or, equivalently,

(1.14b) $$\vec{\nabla} \cdot [\vec{\nabla} \Phi - 4\pi G \rho_0 \vec{u}] = 0$$

so that the term, $\vec{\nabla}\Phi - 4\pi G \rho_0 \vec{u}$, is solenoidal and its normal component is continuous across boundaries, provided that $\vec{r} \cdot \vec{u}$ is continuous there (Crossley & Gubbins, 1975).

At this point I shall neglect the ellipticities of the isopecnic, equipotential surfaces and assume spherical symmetry, whence

$$\rho_0 = \rho_0(r) \quad , \quad g_0 = g_0(r).$$

I retain the centrifugal terms which are of the same order as the ellipticity since it will be necessary in any further study which does incorporate the ellipticity to include these effects.

I expand the radial (normal) component of the solenoidal vector obtained from (1.14b) in spherical harmonics by the relationship

$$\hat{r} \cdot [\vec{\nabla}\Phi - 4\pi G \rho_0 \vec{\xi}] = \sum_{n=0}^{\infty} \sum_{m=-n}^{n} y_6(r)\, S_n^m(\theta,\phi)$$

from which

$$y_6 = \frac{d\Phi_n^m}{dr} - 4\pi G \rho_0 u_n^m$$

or

$$\frac{dy_5}{dr} = y_6 + 4\pi G \rho_0 y_1 \quad , \tag{1.15}$$

where y_6, the normal component of the solenoidal vector, is the gravitational flux density.

Poisson's equation for the induced potential (1.14a) can then be expanded in the spherical harmonic basis set as

$$\vec{\nabla} \cdot \{ y_6 \hat{r} S + y_5 \vec{\nabla} S - 4\pi G \rho_0 (y_3 r \vec{\nabla} S - i y_7 \vec{r} \times \vec{\nabla} S) \} = 0.$$

Hence

$$\left[\frac{dy_4}{dr} + 2\frac{y_4}{r}\right] S + \left[y_5 - 4\pi G \rho_0 r y_3\right] \nabla^2 S = 0 .$$

As the surface spherical harmonics satisfy

$$\nabla^2 S + \frac{n(n+1)}{r^2} S = 0$$

the above expression is equivalent to

$$\frac{dy_4}{dr} = -4\pi G \rho_0 n(n+1)\frac{y_3}{r} + n(n+1)\frac{y_5}{r^2} - \frac{2y_4}{r} \tag{1.16}$$

for each spherical harmonic mode.

The set of equations derived above is still incomplete for the solution of the response of the Earth model. The additional postulate necessary to complete this set is a specific relation expressing the dependence of the stress tensor, $\tilde{\tau}_1$, on the displacements. In the following two sections I proceed to define this dependence in the solid regions and in the fluid outer core.

5. The Stress-Displacement Equations within an Elastic Solid

I assume that the solid under consideration is isotropic, elastic and subject only to small displacements. Then

$$\tilde{\tau} = \lambda \Delta \tilde{I} + 2\mu \tilde{e}$$

where λ and μ are the Lamé constants and the components of the strain tensor, $\tilde{e}$, are

$$e_{ij} = \frac{1}{2}\left[\frac{\partial u_i}{\partial x_j} + \frac{\partial u_j}{\partial x_i}\right].$$

The shear modulus, or rigidity, is given by

$$\mu = \rho_0 v_s^2$$

and λ by

$$\lambda + 2\mu = \rho_0 v_p^2$$

where v_s and v_p are the shear and compressional seismic velocities, respectively.

At this stage I am dealing with the simplified spherically symmetric Earth model or specifically

$$\rho_0 = \rho_0(r) \quad , \quad v_p = v_p(r) \quad , \quad v_s = v_s(r) \; .$$

I show (Appendix A.1) that the divergence of the stress tensor can be written in terms of spheroidal and torsional vector components:

$$\vec{\nabla}\cdot\tilde{\tau}_1$$

$$= \left\{\frac{d}{dr}\left[(\lambda+2\mu)\frac{du}{dr} + \frac{2\lambda u}{r} - n(n+1)\frac{\lambda v}{r}\right] + \frac{2\mu}{r}\left[2\frac{du}{dr}\right.\right.$$

$$\left.\left. - \frac{2u}{r} + n(n+1)\frac{v}{r}\right] - n(n+1)\frac{\mu}{r}\left[\frac{dv}{dr} + \frac{u}{r} - \frac{v}{r}\right]\right\}\hat{r}S$$

$$+ \left\{\frac{d}{dr}\left[\mu\left(\frac{dv}{dr} + \frac{u}{r} - \frac{v}{r}\right)\right] + \frac{3\mu}{r}\left(\frac{dv}{dr} + \frac{u}{r} - \frac{v}{r}\right) + \frac{2\mu v}{r^2}\right.$$

$$\left. + \frac{\lambda}{r}\left[\frac{du}{dr} + \frac{2u}{r} - n(n+1)\frac{v}{r}\right] - \frac{2\mu}{r}(n^2+n-1)v\right\} r\vec{\nabla}S$$

$$+ \left\{\frac{d}{dr}\left[\mu\left(\frac{dt}{dr} - \frac{t}{r}\right)\right] + \frac{3\mu}{r}\left(\frac{dt}{dr} - \frac{t}{r}\right) - \frac{\mu}{r}(n^2+n-2)t\right\}\vec{r}\times\vec{\nabla}S.$$

I introduce the variables y_2, y_4 and y_8:

$$y_2 = (\lambda+2\mu)\frac{dy_1}{dr} + 2\lambda\frac{y_1}{r} - n(n+1)\lambda\frac{y_3}{r},$$

(1.17)
$$y_4 = \mu\left[\frac{dy_3}{dr} + \frac{y_1}{r} - \frac{y_3}{r}\right],$$

$$y_8 = \mu\left[\frac{dy_3}{dr} - \frac{y_3}{r}\right].$$

These variables are directly related to the radial components of the elastic stress:

$$\tau_{rr} = \sum_{n,m} y_2^{nm}(r)\, S_n^m(\theta,\phi) ,$$

$$\tau_{r\theta} = \tau_{\theta r} = \sum \left\{ y_4 \frac{\partial S}{\partial \theta} - \frac{i y_8}{\sin\theta} \frac{\partial S}{\partial \phi} \right\} ,$$

$$\tau_{r\phi} = \tau_{\phi r} = \sum \left\{ \frac{y_4}{\sin\theta} \frac{\partial S}{\partial \phi} + i y_8 \frac{\partial S}{\partial \theta} \right\} .$$

These definitions allow the stress force to be rewritten

$$\vec{\nabla}\cdot\tilde{\tau}_1 =$$

$$\left\{ \frac{dy_2}{dr} + \frac{4\mu}{\lambda+2\mu}\frac{y_2}{r} - \frac{4\mu k}{r^2} y_1 + \frac{2\mu k}{r^2} n(n+1) y_3 \right.$$

$$\left. - \frac{n(n+1)}{r} y_4 \right\} \hat{r} S + \left\{ \frac{dy_4}{dr} + \frac{3y_4}{r} + \frac{\lambda}{\lambda+2\mu}\frac{y_2}{r} \right. \tag{1.18}$$

$$\left. + \frac{2\mu k}{r^2} y_1 - \frac{4\mu}{r^2}\frac{\lambda+\mu}{\lambda+2\mu} n(n+1) y_3 + \frac{2\mu}{r^2} y_3 \right\} r\vec{\nabla} S$$

$$- i \left\{ \frac{dy_8}{dr} + \frac{3y_8}{r} - \mu\frac{(n^2+n-2)}{r^2} y_4 \right\} \vec{r}\times\vec{\nabla} S ,$$

with

$$k = \frac{3\lambda+2\mu}{\lambda+2\mu} = \frac{3k}{\lambda+2\mu} .$$

where k is the incompressibility. Writing the displacement equation in the expanded form utilizing the orthogonal vector basis $\hat{r}S$, $r\vec{\nabla}S$ and $\vec{r}\times\vec{\nabla}S$:

$$
\begin{aligned}
&\rho_0\left[\ddot{y}_1\hat{r}S + \ddot{y}_3 r\vec{\nabla}S - i\ddot{y}_7\vec{r}\times\vec{\nabla}S\right] \\
&+2\rho_0\vec{\Omega}\times\left[\dot{y}_1\hat{r}S + \dot{y}_3 r\vec{\nabla}S - i\dot{y}_7\vec{r}\times\vec{\nabla}S\right] \\
&= \left\{\frac{dy_2}{dr} + \frac{4\mu}{\lambda+2\mu}\frac{y_2}{r} - \frac{4\mu k}{r^2}y_1 + \frac{2\mu k}{r^2}n(n+1)y_3 - \frac{n(n+1)}{r}y_4\right\}\hat{r}S \\
&+\left\{\frac{dy_3}{dr} + \frac{3y_3}{r} + \frac{2\mu k}{r^2}y_1 + \frac{\lambda}{\lambda+2\mu}\frac{y_2}{r} + \frac{2\mu}{r^2}y_3\right. \\
&\qquad \left. - n(n+1)\frac{4\mu}{r^2}\frac{\lambda+\mu}{\lambda+2\mu}y_3\right\} r\vec{\nabla}S \\
&-i\left\{\frac{dy_8}{dr} + \frac{3y_8}{r} - \mu\frac{(n^2+n-2)}{r^2}y_7\right\}\vec{r}\times\vec{\nabla}S \\
&+\rho_0\left[\left(\frac{dy_5}{dr} + \frac{dy_9}{dr}\right)\hat{r}S + (y_5+y_9)\vec{\nabla}S\right] \\
&+\rho_0\vec{\nabla}\left\{(y_1\hat{r}S + y_3 r\vec{\nabla}S - iy_7\vec{r}\times\vec{\nabla}S)\cdot\left[\vec{g}_0 - \vec{\Omega}\times(\vec{\Omega}\times\vec{r})\right]\right\} \\
&+\frac{\rho_0}{\lambda+2\mu}\left\{y_2 + \frac{4\mu}{r}y_1 - n(n+1)\frac{2\mu}{r}y_3\right\}S\left[\vec{g}_0 - \vec{\Omega}\times(\vec{\Omega}\times\vec{r})\right]
\end{aligned}
\tag{1.19}
$$

with

$$\vec{g}_0 \equiv \vec{\nabla}V_0 = -g_0(r)\,\hat{r}$$

because of the relaxation of the model to spherical symmetry.

Using the orthogonality of the basis vectors, the orthogonality of the spherical harmonics, the definitions and the relations already derived, I extract three first-order differential equations for the vector components of each spherical harmonic mode (Appendix A.2).

The radial component gives:

$$\begin{aligned}\frac{dy_2^k}{dr} &= \rho_0 \ddot{y}_1^k - 4\left[\frac{\rho_0 g_0}{r} - \frac{\mu k}{r^2}\right] y_1^k - \rho_0\Omega^2\left[A_1^{kn} + A_2^{kn}\right] y_1^n \\ &\quad - \frac{4\mu}{\lambda+2\mu}\frac{y_2^k}{r} + k(k+1)\left[\frac{\rho_0 g_0}{r} - \frac{2\mu k}{r^2}\right] y_3^k - 2im\rho_0\Omega \dot{y}_3^k \\ &\quad - \rho_0\Omega^2\left[n(n+1)A_1^{kn} + 2A_2^{kn}\right] y_1^n + \frac{k(k+1)}{r} y_4^k \\ &\quad - \frac{\rho_0\Omega^2}{\mu} r A_2^{kn} y_4^n - \rho_0 y_6^k + 2i\rho_0\Omega A_3^{kn} \dot{y}_7^n + 2m\rho_0\Omega^2 A_4^{kn} y_7^n \\ &\quad + m\frac{\rho_0\Omega^2}{\mu} r A_4^{kn} y_8^n - \rho_0 \frac{k}{r} y_9^k ,\end{aligned} \tag{1.20}$$

the rest of the spheroidal component is

$$\begin{aligned}k(k+1)\frac{dy_4^k}{dr} &= k(k+1)\left\{\left[\frac{\rho_0 g_0}{r} - \frac{2\mu k}{r^2}\right] y_1^k - \frac{\lambda}{\lambda+2\mu}\frac{y_2^k}{r} - \frac{3y_4^k}{r}\right. \\ &\quad + \frac{2\mu}{r^2}\left[2k(k+1)\frac{\lambda+\mu}{\lambda+2\mu} - 1\right] y_3^k - \frac{\rho_0 y_5^k}{r} - \frac{\rho_0 y_9^k}{r} \\ &\quad \left. - \rho_0\Omega^2\left[A_1^{kn} y_1^n + A_2^{kn} y_3^n - m A_4^{kn} y_7^n\right] + \rho_0 \ddot{y}_3^k\right\} \\ &\quad - 2i\rho_0\Omega\left[m\dot{y}_1^k + m\dot{y}_3^k - B_1^{kn}\dot{y}_7^n\right] \\ &\quad + \frac{\rho_0\Omega^2}{\lambda+2\mu} B_2^{kn}\left[4\mu y_1^n + r y_2^n - 2n(n+1)\mu y_3^n\right],\end{aligned} \tag{1.21}$$

and the torsional component is

$$k(k+1)\frac{dy_8^k}{dr} = k(k+1)\left\{(k^2+k-2)\frac{\mu}{r^2}y_7^k - \frac{3}{r}y_8^k + \rho_0 \ddot{y}_7^k\right\}$$
$$+ 2i\rho_0\Omega\left[B_1^{kn}\dot{y}_3^n + B_4^{kn}\dot{y}_1^n - m\dot{y}_7^k\right]$$
$$- \frac{m\rho_0\Omega^2}{\lambda+2\mu}A_4^{kn}\left[4\mu y_1^n + r y_2^n - 2n(n+1)\mu y_3^n\right]. \qquad (1.22)$$

The coupling coefficients A_1^{kn}, A_2^{kn}, A_3^{kn}, A_4^{kn}, B_1^{kn}, B_2^{kn} and B_4^{kn} are defined in Appendix A and calculated in Appendix C. The angular velocity $\vec{\Omega}$ is

$$\vec{\Omega} = \Omega[\cos\theta\,\hat{r} - \sin\theta\,\hat{\theta}].$$

If I neglect the effects of rotation ($\Omega \to 0$) the above set of equations again degenerates to the set used in free oscillation theory (with $\psi = 0$) and to those used by Pekeris & Accad (with $\Phi + \psi \to \Phi$).

The complete set of first-order differential equations that define the deformation field throughout the solid regions of the Earth are (1.17), (1.20), (1.21) and (1.22), together with the defining equations for the potentials (1.12), (1.15) and (1.16) from section 4.

A parallel development must now be done for the fluid outer core.

6. The Navier-Stokes Equations within the Fluid Core

I assume that the fluid composing the outer core of the Earth is inviscid and isotropic (I also neglect any geomagnetic effects), and hence the stress within the fluid is due only to the expansion or compression of the local volume element. Under this consideration

$$\tilde{\tau}_1 = \lambda \Delta \tilde{I} ,$$

where again the Lamé constant (also the bulk modulus within the fluid) is

$$\lambda = \rho_0 v_p^2 = \rho_0 v^2 .$$

For the moment I return to the more exact, rotationally flattened model of the Earth, although later I shall relax this to spherical symmetry.

With the above specification of the stress tensor, the displacement equation (1.6) can be written as

$$\ddot{\vec{u}} + 2\vec{\Omega} \times \dot{\vec{u}} = \frac{1}{\rho_0}\vec{\nabla}(\lambda\Delta) - \Delta\left[\vec{g}_0 - \vec{\Omega}\times(\vec{\Omega}\times\vec{r})\right] + \vec{\nabla}\left[\phi + \Phi + \vec{u}\cdot\vec{g}_0 - \vec{u}\cdot\vec{\Omega}\times(\vec{\Omega}\times\vec{r})\right]. \tag{1.23}$$

From the condition of initial hydrostatic equilibrium, the isopecnic and geopotential surfaces in the equilibrium configuration coincide, or equivalently, the density gradient is parallel to the gravitational field. I adopt an analytic form for the hydrostatic condition as introduced by Pekeris & Accad (1972, p. 239, eq. 13)

$$\lambda\vec{\nabla}\left(\frac{1}{\rho_0}\right) = -(1-\beta(r))\left\{\vec{\nabla}V_0 - \vec{\Omega}\times(\vec{\Omega}\times\vec{r})\right\} \doteq (1-\beta)\left\{g_0\hat{r} + \vec{\Omega}\times(\vec{\Omega}\times\vec{r})\right\}. \tag{1.24}$$

Smylie & Mansinha (1971) have shown the extent to which the static response of the fluid depends on its departure from the Adams-Williamson condition and this has since been discussed by Smylie (1974) and Crossley (1975b). In all models considered to date the stability factor, β, has been taken as a constant. The above expression degenerates to the Adams-Williamson condition (in the absence of rotation) when $\beta(r) = 0$ everywhere and to a uniform density distribution when $\beta(r) = 1$. The model published by Pekeris & Accad (and supplemented by Smylie to allow for the presence of the inner core) has $\beta(r) = -0.2$ throughout the fluid core. I use the same model for purposes of comparison.

The stability factor is related to the thermodynamic properties of the fluid. Under the assumption of isotropy the equilibrium density profile will be the result of the pressure and the temperature distributions. Therefore

$$\frac{d\rho_0}{dr} = \left(\frac{\partial \rho_0}{\partial p}\right)_S \frac{dp}{dr} + \left(\frac{\partial \rho_0}{\partial S}\right)_p \frac{dS}{dr}$$

$$= \left(\frac{\partial \rho_0}{\partial p}\right)_S \frac{dp}{dr} + \left(\frac{\partial \rho_0}{\partial T}\right)_p \Big/ \left(\frac{\partial T}{\partial S}\right)_p \frac{dS}{dr}$$

where p is the pressure, T is the temperature and S is the specific entropy.

The thermodynamic definition of the adiabatic incompressibility or the bulk modulus of the fluid is

$$\lambda = \rho_0 \Big/ \left(\frac{\partial \rho_0}{\partial p}\right)_S$$

and the difference between the actual temperature gradient present at r and

the adiabatic temperature gradient which would prevail at $\vec{r}$ in a perfect fluid in thermodynamic equilibrium

$$\delta = \frac{dT}{dr} - \left(\frac{\partial T}{\partial r}\right)_S$$
$$= \frac{dT}{dr} - \left(\frac{\partial T}{\partial p}\right)_S \frac{dp}{dr}$$
$$= \left(\frac{\partial T}{\partial S}\right)_p \frac{dS}{dr} .$$

The coefficient of thermal volume expansion at constant pressure is defined as

$$\alpha_p \equiv \frac{1}{V}\left(\frac{\partial V}{\partial T}\right)_p = -\frac{1}{\rho_0}\left(\frac{\partial \rho_0}{\partial T}\right)_p .$$

Hence the density gradient can be written using the above relations and definitions as

$$\frac{d\rho_0}{dr} = \frac{\rho_0}{\chi}\frac{dp}{dr} + (-\rho_0 \alpha_p)\delta$$

and the condition of initial hydrostatic equilibrium allows

$$\frac{d\rho_0}{dr} = -\frac{\rho_0}{\chi}\rho_0 g_0 - \rho_0 \alpha_p \delta .$$

Again these can be regrouped to give

$$\frac{d}{dr}\left(\frac{1}{\rho_0}\right) = \frac{g_0}{\chi}\left[1 - \beta\right]$$

with the stability factor

$$\beta \equiv -\frac{\chi \alpha_p \delta}{\rho_0 g_0} .$$

If a fluid element, initially at a radius r from the centre of the Earth and with density, $\rho_o(r)$, moves suddenly to r + u then its density change will be adiabatic:

$$d\rho = \left(\frac{\partial \rho_o}{\partial p}\right)_s dp = -\frac{\rho_o^2 g_o}{\lambda} u .$$

The fluid now surrounding the particle has an *in situ* density determined by the equation of state within the fluid, $\rho_o(r+u)$, and hence differs from the initial density of the fluid element by

$$d\rho_o = -\frac{\rho_o^2 g_o}{\lambda}(1-\beta)u$$

and from the final density of the element by

$$d\rho_o - d\rho = \left[\frac{\beta \rho_o^2 g_o}{\lambda}\right] u .$$

The buoyant force on this displaced fluid element is then

$$\beta\left[\frac{\rho_o^2 g_o}{\lambda}\right] u$$

and will determine its subsequent behaviour.

If the stability factor is negative, $\beta < 0$, the buoyant force acts as a restoring force and the element will oscillate about its initial position with frequency $N = g_o\sqrt{-\beta}/v_p$ (the Väisälä frequency). The initial density distribution is uniformly stable against convection. For $\beta = 0$ the Adams-Williamson condition holds (and the temperature gradient is adiabatic), the buoyant force vanishes and the element is stable in its new position. The configuration is then neutrally or marginally stable

with respect to the onset of convection. For $\beta > 0$ the temperature gradient is superadiabatic and the buoyant force causes the element to move farther from the initial position. The fluid is unstable and convection can occur.

The stress force can now be rewritten with the aid of the equation of state (1.24) as

$$\frac{1}{\rho_0}\vec{\nabla}\cdot\tilde{\tau}_1 = \frac{1}{\rho_0}\vec{\nabla}(\lambda\Delta)$$

$$= \vec{\nabla}\left(\frac{\lambda\Delta}{\rho_0}\right) - \lambda\Delta\vec{\nabla}\left(\frac{1}{\rho_0}\right)$$

$$= \vec{\nabla}\left(\frac{\lambda\Delta}{\rho_0}\right) + (1-\beta)\Delta\left\{\vec{g}_0 - \vec{\Omega}\times(\vec{\Omega}\times\vec{r})\right\}$$

and the displacement equation can be transformed into

$$\ddot{\vec{u}} + 2\vec{\Omega}\times\dot{\vec{u}}$$

$$= -\vec{\nabla}\left[\frac{\lambda\Delta}{\rho_0} + \psi + \Phi + \vec{u}\cdot\vec{g}_0 - \vec{u}\cdot\vec{\Omega}\times(\vec{\Omega}\times\vec{r})\right] \tag{1.25}$$

$$-\beta\Delta\left[\vec{g}_0 - \vec{\Omega}\times(\vec{\Omega}\times\vec{r})\right].$$

The curl of this equation is

$$\vec{\nabla}\times\left[\ddot{\vec{u}} + 2\vec{\Omega}\times\dot{\vec{u}}\right] = -\vec{\nabla}(\beta\Delta)\times\left[\vec{g}_0 - \vec{\Omega}\times(\vec{\Omega}\times\vec{r})\right] \tag{1.26}$$

which immediately gives the result obtained by Smylie & Mansinha (1971) for the static deformation of a (in this case, uniformly rotating) fluid: either

the fluid must be exactly Adams-Williamson or adiabatic throughout or the dilatation vanishes (with the exception of the lowest degree mode - the purely normal expansion or contraction of the fluid).

Now I revert to a spherically symmetric model.

Generally for the dynamic case I define within the fluid the variable

$$Z^{nm} \equiv \frac{\lambda}{\rho_0}\Delta^{nm} = V^2\Delta = y_2/\rho_0$$

whence

$$\frac{dy_1}{dr} = -\frac{2y_1}{r} + \frac{Z}{V^2} + \frac{k(k+1)}{r}y_3 \tag{1.27}$$

In Appendix B I show that the components of the displacement equation produce a differential equation involving the dilatation and two analytic equations constraining the transverse motions. These are

$$\begin{aligned}\frac{dZ^k}{dr} &+ \Omega^2 A_2^{kn}\frac{d}{dr}\left(ry_3^n\right) - m\Omega^2 A_4^{kn}\frac{d}{dr}\left(ry_7^n\right)\\ &= -\frac{4g_0}{r}y_1^k + \ddot{y}_1^k - y_6^k - \frac{k}{r}y_9^k + (1-\beta)\frac{g_0}{V^2}Z^k\\ &+ k(k+1)\frac{g_0}{r}y_3^k - 2im\Omega\dot{y}_3^k + 2i\Omega A_3^{kn}\dot{y}_7^n\\ &+ \Omega^2 A_1^{kn}\left[y_1^n - (1-\beta)\frac{rZ^n}{V^2} - n(n+1)y_3^n\right],\end{aligned} \tag{1.28}$$

$$\ddot{y}_3^k - \frac{2im\Omega\epsilon}{k(k+1)}\dot{y}_3^k - \Omega^2 A_2^{kn} y_3^n + m\Omega^2 A_4^{kn} y_7^n + \frac{2i\Omega B^{kn}}{k(k+1)}\dot{y}_7^n$$

$$= \frac{1}{r}\left[Z^k + y_5^k + y_9^k - q_0 y_1^k\right] + \frac{2im\Omega}{k(k+1)}\dot{y}_1^k + \Omega^2 A_1^{kn} y_1^n - \beta\frac{\Omega^2 r B_2^{kn}}{k(k+1)V^2} Z^n \quad (1.29)$$

and

$$\ddot{y}_7^k - \frac{2im\Omega}{k(k+1)}\dot{y}_7^k + \frac{2i\Omega B_1^{kn}}{k(k+1)}\dot{y}_3^n = \frac{1}{k(k+1)}\left[-2i\Omega B_4^{kn}\dot{y}_1^n + \beta\frac{\Omega^2 r}{V^2} m A_4^{kn} Z^n\right]. \quad (1.30)$$

Because of the second and third terms on the LHS of the first of the above equations, it is also necessary to give the components of the curl of the equation of motion (1.26). These components are derived in Appendix B.

$$\frac{d}{dr}\left(r\ddot{y}_3^k\right) - \frac{2im\Omega}{k(k+1)}\frac{d}{dr}\left(r\dot{y}_3^k\right) + \frac{\beta\Omega^2 r B_2^{kn}}{k(k+1)V^2}\frac{dZ^n}{dr} + \frac{2i\Omega B_1^{kn}}{k(k+1)}\frac{d}{dr}\left(r\dot{y}_7^n\right) - 2i\Omega A_3^{kn}\dot{y}_7^n$$

$$= \ddot{y}_1^k - \frac{2im\Omega}{k(k+1)}\dot{y}_1^k - \frac{\beta q_0 Z^k}{V^2} + \frac{2im\Omega r}{k(k+1)}\frac{\dot{Z}^k}{V^2} + \frac{\beta\Omega^2 r B_3^{kn}}{k(k+1)V^2} Z^n \quad (1.31a)$$

and

$$\frac{d}{dr}\left(r\dot{y}_7^k\right) - \frac{2im\Omega}{k(k+1)}\frac{d}{dr}\left(r\dot{y}_7^k\right) + \frac{2i\Omega B_1^{kn}}{k(k+1)}\frac{d}{dr}\left(r\dot{y}_3^n\right)$$

$$+ \frac{2i\Omega n(n+1)B_4^{kn}}{k(k+1)}\dot{y}_3^n - \frac{m\beta\Omega^2 r^2 A_4^{kn}}{k(k+1)v^2}\frac{d\dot{z}^n}{dr} \tag{1.31b}$$

$$= \frac{2\Omega}{k(k+1)}\left[iB_4^{kn}\dot{y}_1^n + \frac{m\beta\Omega r}{v^2}A_4^{kn}\dot{z}^n - \frac{iB_4^{kn}r}{v^2}\dot{z}^n\right].$$

The third component of this equation is simply a repetition of (1.30).

I will treat the above two equations as analytic equations defining the variables $\frac{d}{dr}(ry_3)$ and $\frac{d}{dr}(ry_7)$ in terms of the remaining variables and then these with the other analytic equations can be solved for the non-radial motions and their derivatives. Finally I will be left with only five first-order differential equations (for each spherical harmonic mode) which involve only the radial displacement, the dilatation and the potential equations.

This then completes the definition of the problem insofar as explicitly stating the governing differential equations of the displacement fields in both the elastic solid regions of the Earth and in the fluid outer core.

Having the governing equations above, I shall investigate the tide-raising potential and the coupling terms due to rotation to determine the selection rules which govern the set of the modes of the deformation which this tide-raising potential will excite indirectly.

7. The Tide-Raising Potential and the Selection Rules for the Excited Modes

The sources of the tide-raising potential under consideration are the Moon and the Sun. For either source it is possible to specify its position relative to the centre of the Earth as $\vec{D} = (D, \lambda, \zeta)$ and its mass as M. At a field point, $\vec{r}$, within the Earth, the tide-raising potential is

$$\psi = GM\left(\frac{1}{R} - \frac{1}{D}\right)$$

where

$$R = |\vec{D} - \vec{r}|.$$

A standard expansion of this in Legendre polynomials gives

$$\psi = \frac{GM}{D} \sum_{n=2}^{\infty} \left(\frac{r}{D}\right)^n P_n(\cos\gamma)$$

where γ is the angle between $\vec{r}$ and $\vec{D}$.

In terms of the coordinates of the field point $\vec{r} = (r, \theta, \phi)$ (it should again be noted here that θ is the co-latitude),

$$\psi = \frac{GM}{D} \sum_{n=2}^{\infty} \left(\frac{r}{D}\right)^n \sum_{m=-n}^{n} (-1)^m S_n^{-m}(\lambda, \zeta) S_n^m(\theta, \phi)$$

and within the Earth the ratio $\frac{r}{D} \leq \frac{1}{60}$ so that I need only retain leading terms. I explicitly do not consider any external driving forces on the Earth other than the leading terms (n=2 and n=3).

As I have truncated the tide-raising potential to only the second and third harmonics, for a non-rotating Earth only second and third degree harmonic responses would be excited. The effect of rotation is then, by coupling other modes to these modes, to excite these other modes. It is

chiefly for this reason that I am investigating a rotating Earth model. Considering the coupling coefficients defined in Appendix A and used in the equations which govern the displacement fields in both the solid and fluid regions of the Earth, A_1, A_2, B_2 and B_3 couple even degree spheroidal terms to even degree spheroidal terms and odd degree spheroidal terms to odd degree spheroidal terms. The remaining coupling coefficients A_3, A_4, B_1 and B_4 couple even degree spheroidal terms to odd degree torsional terms and odd degree spheroidal terms to even degree torsional terms. All coupling coefficients couple modes of the same order so that it is not necessary to carry this index explicitly. Only if the Earth model were extended to include the possibility of azimuthal variations would coupling between different orders be excited. If I consider only the second degree external tide-raising potential as the source of the deformations, it is evident that the Coriolis and centrifugal couplings will excite only even degree spheroidal components and odd degree torsional components. The results of the rotational coupling are shown schematically below (Fig. 1). Alternatively, if I consider only the third degree excitation only odd degree spheroidal and even degree torsional modes will be excited. The coupling effect of ellipticity will be similar to that of centrifugal force.

Since this is an infinite chain it will be necessary to truncate the set of equations at various levels and compare the results to test the convergence of the set of solutions at chosen forcing periods.

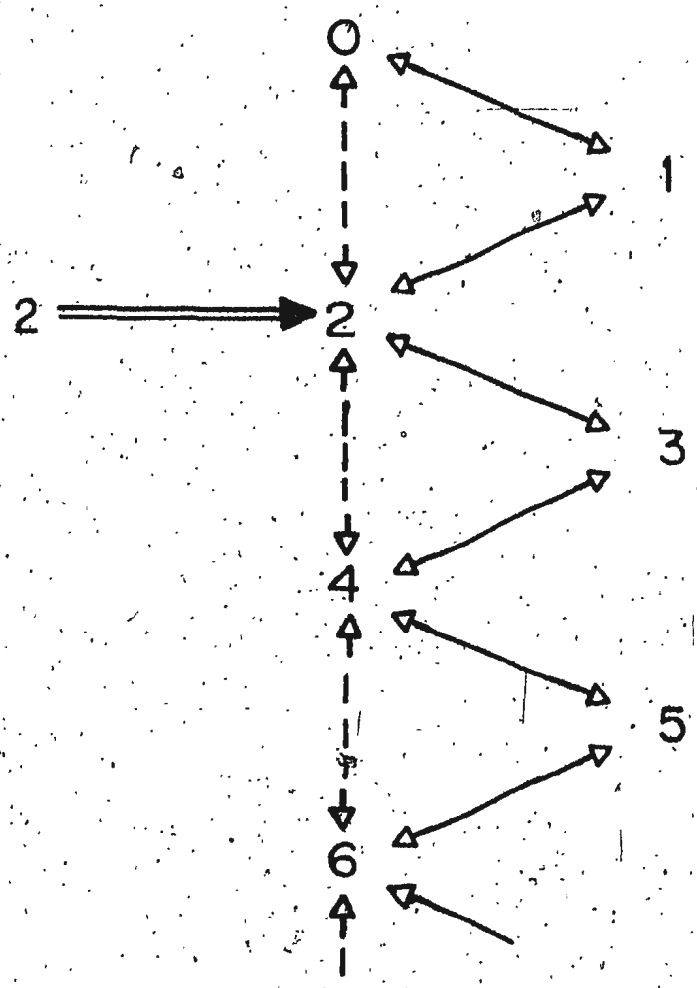

direct excitation by the tide producing potential

coupling due to Coriolis effects

coupling due to centrifugal effects

Fig. 1. Schematic of the exchanges of energy between the spheroidal modes and the torsional modes due to rotational coupling for tide-raising potential of degree 2.

8. The Time Dependence of the Forcing Motion

In this section the simplifying assumption that the exciting potential has a sinusoidal time dependence is made. A more complicated temporal variation can then be considered a simple Fourier sum of these sinusoidal time variations. The time dependence chosen is simply $e^{i\sigma t}$ for all variables since dissipative processes within the Earth have been neglected.

Under this assumption the equations governing the deformations can be rewritten simply by replacing a partial derivative with respect to time by $i\sigma$, e.g.

$$\dot{y}_i \longrightarrow i\sigma y_i$$
$$\ddot{y}_i \longrightarrow -\sigma^2 y_i \quad .$$

In this form the set of first-order differential equations for the solid regions and the corresponding set of analytic and first-order differential equations in the fluid are now complete and phrased in terms of real (not complex) variables. The solution to these equations will be subject to the boundary conditions on the variables at (or across) interfaces between the solid and fluid regions and at the surface.

9. Boundary Conditions

All the variables under consideration must be regular at the origin (centre of the Earth) and the displacements must vanish at the origin to leave the stresses finite. The single exception to this statement is the spheroidal displacements of degree one, which must satisfy the condition that the centre of mass of the Earth remain fixed.

The potentials are continuous across all internal boundaries and, since the gravitational flux is solenoidal, its normal component is also continuous across all boundaries provided $\hat{r}\cdot\vec{u}$ is itself continuous.

As I am dealing with dynamic displacements rather than the static case, the radial displacement and the radial stress are also continuous across all internal boundaries. The shear stresses must vanish at the surface of the Earth ($r = R$) and also at the internal solid-fluid interfaces.

Returning to the induced gravitational potential and the normal component of the gravitational flux, these must be continuous at the surface of the Earth and the induced potential becomes harmonic outside the Earth.

$$y_6^k(R^-) = y_5^k(R^+),$$
$$y_6^k(R^-) = y_6^k(R^+),$$
$$y_5^k(r) = \left(\frac{R}{r}\right)^{k+1} y_6^k(R) \quad ; \quad r \geq R$$

Therefore

$$R\,y_6^k + (k+1)\,y_6^k = 0 \quad \text{at } r = R. \tag{1.32}$$

I note that this differs from the constraint placed on these terms by Pekeris & Accad (1972). However they were dealing not with the induced potential but with the combination of the induced and inducing potentials; furthermore their condition (p. 239, eq. 10) should read:

(1.33) $$R\, y_6^k + (k+1)\, y_5^k = (2k+1)\, U^k(R)$$

where their U^k is equivalent to my y_9^k.

The problem is now completely specified, with the Earth model defined, the governing differential equations formulated and the constraining boundary conditions stated. In the next chapter I shall discuss the initialization, the scaling and the numerical propagation technique.

CHAPTER 2

NUMERICAL PROCEDURES

1. Initialization

In order to start the solutions at the geocentre it is necessary to examine the behaviour of the deformations, stresses, potentials and gravitational flux near there for each mode under consideration.

As a first approximation, the defining equations governing the deformations within the elastic inner core are simplified by neglecting the rotational and the dynamic terms (set $\sigma = \Omega = 0$). The set of equations I have developed then degenerates to the set obtained by Smylie & Mansinha (1971) for the solid part of the Earth. In this approximation the torsional modes are completely decoupled from the spheroidal modes and from each other, and the spheroidal modes are also completely decoupled from the torsional modes and from each other. In order to produce the behaviour of the solutions as $r \to 0$, I also assume that the variation in density and in the Lamé constants is negligible and write each variable in a regular power series expansion. The procedure used here is similar to that used by Smylie & Mansinha (1971) where they considered the entire core of the Earth as fluid. Crossley (1975a) has independently used this technique and obtained results consistent with mine.

The leading term in each variable can then be calculated (Appendix D). For the terms of degree zero these are

$$\begin{aligned} y_1^0 &= \alpha_0 r + \cdots \\ y_2^0 &= (3\lambda + 2\mu)\alpha_0 + \cdots \\ y_5^0 &= \gamma_0 + \cdots \end{aligned} \tag{2.1}$$

All other variables of degree zero vanish throughout the Earth. For degrees $k \geq 1$ the above procedure gives

$$
\begin{aligned}
y_1^k &= \alpha_k r^{k-1} + \cdots \\
y_2^k &= 2\mu(k-1)\alpha_k r^{k-2} + \cdots \\
y_3^k &= \frac{\alpha_k}{k} r^{k-1} + \cdots \\
y_4^k &= 2\mu\left(\frac{k-1}{k}\right)\alpha_k r^{k-2} + \cdots \\
y_5^k &= \gamma_k r^k + \cdots \\
y_6^k &= [k\gamma_k - 3\Gamma\alpha_k] r^{k-1} + \cdots \\
y_7^k &= \nu_k r^k \\
y_8^k &= \mu(k-1)\nu_k r^{k-1} \\
y_9^k &= c_k r^k
\end{aligned}
\tag{2.2}
$$

where the coefficients include three undetermined constants (α_k, γ_k and ν_k), the strength of the external potential (c_k is known in terms of the mass of the source and its distance from the Earth) and the constant

$$
\Gamma \equiv \lim_{r \to 0}\left[\frac{g_0(r)}{r}\right] = \frac{4\pi G \rho_0(0)}{3} . \tag{2.3}
$$

As stated in Appendix D, each mode except the degree zero response involves one other arbitrary constant to uniquely determine the solutions and I have chosen the coefficient of r^{k+1} in the expansion of y_1^k; i.e. I have taken

(2.4) $$y_i^k = \alpha_k r^{k-1} + \beta_k r^{k+1} + \cdots$$

At this stage the results are in agreement with the initialization procedure developed for the spheroidal components by Crossley (1975a) although they are formulated differently.

For numerical accuracy, I now define the variables x_i^k within the solid inner core of the Earth related to the variables y_i^k by the definitions

(2.5a) $$x_1^0 = y_1^0/r \quad , \quad x_2^0 = y_2^0 \quad , \quad x_5^0 = y_5^0$$

and for $k \neq 0$

(2.5b) $$x_i^k = y_i^k/r^{k-1} \qquad i = 1, 3, 6, 8$$
$$x_i^k = y_i^k/r^{k-2} \qquad i = 2, 4$$
$$x_i^k = y_i^k/r^k \qquad i = 5, 7, 9 .$$

Each of these variables will then have, within the inner core, the form

$$x_i^k = \text{constant} + O(r^2)$$

near the origin.

To improve on these conditions and take into account the cross coupling between torsional modes and spheroidal modes fully, I have rewritten the full dynamic equations in terms of these new variables, retained the approximation that the inner core is homogeneous near the geocentre and calculated the first and second derivatives of these variables at $r = 0$. The details are in Appendix D.

I find the first derivative at the origin vanishes and that the leading term in each expansion is again given by (2.1) and (2.2) with the definitions in (2.5) taken into account.

It is now possible to initialize the solution for an excitation of either degree 2 or degree 3 by taking the representation

$$\chi_i^n(0) = B_{ij}^{nk}(0)\, z_j^k \tag{2.6}$$

where the matrix of unknown coefficients is simply

$$Z \equiv \begin{bmatrix} x_1^0 & x_1^2 & x_1^4 \cdots \\ 0 & \ddot{x}_1^2 & \ddot{x}_1^4 \cdots \\ x_5^0 & x_5^2 & x_5^4 \cdots \\ x_7^1 & x_7^3 & x_7^5 \cdots \\ 0 & x_7^2 & 0 \cdots \end{bmatrix}_{r=0} = \begin{bmatrix} \alpha_0 & \alpha_2 & \alpha_4 \cdots \\ 0 & \beta_2 & \beta_4 \cdots \\ \gamma_0 & \gamma_2 & \gamma_4 \cdots \\ \nu_1 & \nu_3 & \nu_5 \cdots \\ 0 & c_2 & 0 \cdots \end{bmatrix} \tag{2.7a}$$

(where the dot over a variable now represents a radial derivative) for the degree 2 excitation, or as

$$Z \equiv \begin{bmatrix} x_1^1 & x_1^3 & x_1^5 \cdots \\ \ddot{x}_1^1 & \ddot{x}_1^3 & \ddot{x}_1^5 \cdots \\ x_5^1 & x_5^3 & x_5^5 \cdots \\ x_7^2 & x_7^4 & x_7^6 \cdots \\ 0 & x_7^3 & 0 \cdots \end{bmatrix}_{r=0} = \begin{bmatrix} \alpha_1 & \alpha_3 & \alpha_5 \cdots \\ \beta_1 & \beta_3 & \beta_5 \cdots \\ \gamma_1 & \gamma_3 & \gamma_5 \cdots \\ \nu_2 & \nu_4 & \nu_6 \cdots \\ 0 & c_3 & 0 \cdots \end{bmatrix} \tag{2.7b}$$

for the degree 3 excitation.

The matrix $\mathcal{X}$ is defined with the same number of columns as $\mathcal{E}$ where each column is the transpose of the row vector

$$(2.8) \quad (x_1^p, x_2^p, x_3^p, x_4^p, x_5^p, x_6^p, x_7^{p+1}, x_8^{p+1}, x_9^p)$$

with the index p ranging over the even integers for the degree 2 excitation and over the odd integers for the degree 3 excitation.

For the degree 2 excitation the non-zero elements of the array $\mathcal{B}$ are

$$(2.9a) \quad B_{11}^{nn} = B_{53}^{nn} = B_{74}^{nn} = B_{98}^{22} = 1$$

$$(2.9b) \quad B_{21}^{11} = 3\lambda + 2\mu$$

and for $n \neq 1$ $(N \neq 0)$

$$(2.9c) \quad B_{21}^{nn} = 2\mu(N-1) \; ; \; B_{31}^{nn} = \frac{1}{N} \; ; \; B_{41}^{nn} = \mu\frac{N-1}{N} \; ;$$
$$B_{61}^{nn} = -3\Gamma \; ; \; B_{63}^{nn} = N \; ; \; B_{84}^{nn} = N\mu$$

where n is the index referring to the spheroidal variables of degree N and the torsional variables of degree N+1 represented in the n'th column of $\mathcal{X}$.

For the degree 3 excitation the array $\mathcal{B}$ is constructed in an identical fashion with the exception that (2.9c) holds for n = 1 rather than (2.9b). Again the spheroidal variables of degree N (= 2n-1) and the torsional variables of degree N+1 are represented in the n'th column of $\mathcal{X}$.

For either case the first derivatives of all variables vanish at the origin and from Appendix D where I calculated the second derivatives at the origin the further relation

$$\ddot{x}_i^n(0) = C_{ij}^{nk} z_j^k \tag{2.10}$$

is obtained by solving these equations.

Hence a quadratic prediction from the origin r = 0 to an arbitrary radius r = Δ can be taken as

$$\begin{aligned} x(\Delta) &= x(0) + \Delta \dot{x}'(0) + \tfrac{1}{2}\Delta^2 \ddot{x}(0) \\ &= x(0) + 0 + \tfrac{1}{2}\Delta^2 \ddot{x}(0) \\ &= B z + \tfrac{1}{2}\Delta^2 C z \\ &= \left[B + \tfrac{1}{2}\Delta^2 C\right] z \end{aligned}$$

That is, the solution set at a finite distance from the origin is extrapolated from the solution at the origin using the derivatives of the solution at the origin. The solution can now be represented in terms of the array of undetermined constants as

$$x(\Delta) = B(\Delta) z \tag{2.11a}$$

where the array $B(\Delta)$ is defined as

$$B(\Delta) \equiv B(0) + \tfrac{1}{2}\Delta^2 C. \tag{2.11b}$$

As noted in Appendix D, special care has to be taken for the evaluation of the derivatives since individual coefficients behave as r^{-1}; however, these are multiplied by variables in such a manner as to cancel out.

Once the solution is obtained at some arbitrary non-zero radius the coefficients in the derivatives are individually well-behaved and the second derivatives are obtainable immediately. Using the complete fully dynamic set of differential equations, which can now be written in the form

$$\dot{X}_i^n = A_{ij}^{nk} X_j^k \quad \text{or} \quad \dot{X} = AX,$$

and which can be supplemented by forming

$$\ddot{X} = A\dot{X} + \dot{A}X = [AA + \dot{A}]X,$$

a quadratic predictor has been formed which allows the solution to be propagated through small increments in radius from the initial arbitrary radius to the outer boundary of the inner core. This quadratic extrapolation gives

$$\begin{aligned} X(r+\Delta) &= X(r) + \Delta \dot{X}(r) + \tfrac{1}{2}\Delta^2 \ddot{X}(r) \\ &= X(r) + \Delta A X(r) + \tfrac{1}{2}\Delta^2 [AA + \dot{A}] X(r) \\ &= [I + \Delta A + \tfrac{1}{2}\Delta^2 (AA + \dot{A})] X(r) \end{aligned}$$

In practice only the array B is calculated at each step and this is given by

$$B(r+\Delta) = [I + \Delta A + \tfrac{1}{2}\Delta^2 (AA + \dot{A})] B(r) \tag{2.12}$$

and in practice the radial derivative of the array A is sufficiently well approximated for small steps by treating the density and the Lamé constants as constant during this step. The major improvement due to the retention of this term is gained near the origin where the coefficients of A behave as r^{-1}.

The propagation technique described above in principle allows the calculation of the solutions of all modes excited either directly by the external potential or indirectly through rotational couplings to be determined at any radius within the inner core in terms of the set of undetermined constants describing the behaviour at the origin. When the solution has been propagated to the outer boundary of the solid inner core the condition that the shear stresses vanish is applied and the unknowns $\ddot{x}_1^k$ and x_7^k are determined in terms of the remaining variables. The array $\mathbf{B}$ is then rewritten in terms of this reduced set of undetermined coefficients, and passed into the fluid region.

Since the propagation technique uses matrices and 4-dimensional arrays, a Runge-Kutta method was not used. The use of a Runge-Kutta method would have entailed storage of at least two test arrays and comparison of each element in these arrays. The alternative of selecting a small step size was used.

For computational accuracy it is also convenient to scale the variables for the calculations from rationalized MKS units.

In the following two sections both the scaling procedure and the propagation through the fluid and through the mantle are discussed.

In practise it is neither possible nor necessary to consider all the modes which may be excited to some extent through rotational coupling. In the final section of this chapter I discuss the truncations chosen for the propagation of the solution.

2. Scaling

For computational accuracy and for convenience the system of units described below is used rather than rationalized MKS units: the unit of distance is taken to be 10^7 m = 10^4 km, the unit of time is taken to be 10^3 seconds, the unit of mass is 10^{24} kilograms. The physical parameters are now scaled in agreement with the scheme used by Smylie (1974) and Crossley (1975b).

In the above system the numerical values of the physical quantities are related to the MKS values by

$$\begin{aligned}
\rho &= 10^{-3}\rho_{MKS} && \sim 10 \\
v &= 10^{-4}v_{MKS} && \sim 1 \\
\lambda &= 10^{-12}\lambda_{MKS} && \sim 10 \\
g &= 10^{-3}g_{MKS} && \sim 1 \\
\Omega &= 10^{3}\Omega_{MKS} && \sim .1 \\
G &= 10^{9}G_{MKS} && \sim .1
\end{aligned}$$

The rationale for the above scaling procedure is that the parameters and variables within the Earth no longer span over 15 orders of magnitude, as attempts prior to the use of this scaling procedure had incurred numbers which were too large.

3. Propagation of the Solutions through the Fluid Core and Mantle

The initialization of the solution, the propagation of this solution through the inner core and the application of the boundary conditions at the inner core-fluid interface has been discussed in the first section of this chapter. As a result of these calculations the radial variables (y_1, y_2, y_5, y_6 and y_9 which are continuous across the boundary) are known at the bottom of the fluid region in terms of the set of unknown constants introduced initially. These are written in the form

$$Y = BZ \qquad \text{i.e.} \qquad Y_i^n(r) = B_{ij}^{nk}(r)\, z_j^k$$

where the matrix Z has been reduced to

$$Z \equiv \begin{bmatrix} \alpha_0 & \alpha_2 & \alpha_4 & \cdots \\ 0 & 0 & 0 & \cdots \\ \gamma_0 & \gamma_2 & \gamma_4 & \cdots \\ 0 & 0 & 0 & \cdots \\ 0 & c_2 & 0 & \cdots \end{bmatrix} \quad \text{or} \quad \begin{bmatrix} \alpha_1 & \alpha_3 & \alpha_5 & \cdots \\ 0 & 0 & 0 & \cdots \\ \gamma_1 & \gamma_3 & \gamma_5 & \cdots \\ 0 & 0 & 0 & \cdots \\ 0 & c_3 & 0 & \cdots \end{bmatrix}$$

for the degree 2 or 3 excitation, respectively, and the tangential displacements at the bottom of the fluid are obtained from the analytic conditions (1.29 and 1.30).

As I have previously stated the above analytic conditions, with two other "analytic" conditions (1.31) obtained from the curl of the displacement equation, are used within the fluid to eliminate the transverse displacements and their derivatives, from the remaining differential equations. Again it is neither feasible nor necessary to retain all modes which may be excited and a choice of the maximum degree to be retained

in the elimination procedure must be made. To ensure accuracy in the elimination of the transverse displacements from the differential equations I have retained more modes for this step than have been kept in the propagation.

Once this reduction of the differential equations has been accomplished the result is a set of first-order differential equations relating only the radial displacement, the dilatation, the potentials and the gravitational flux represented in the form

$$\dot{Y}(r) = -A(r)\,Y(r)$$

which can be propagated through the fluid in small steps, Δ , to obtain

$$Y(r+\Delta) = Y(r) + \Delta\,\dot{Y}(r) = [I + \Delta A]\,Y(r)$$

in terms of the values at r or alternatively

$$B(r+\Delta) = [I + \Delta A]\,B(r).$$

The solution is then propagated to the fluid-mantle interface and passed into the mantle.

At the lower boundary of the mantle ($r = \alpha$), I restructure the matrix Z as

$$Z \equiv \begin{bmatrix} x_1^0(\alpha) & x_1^2(\alpha) \cdots \\ 0 & y_2^2(\alpha) \cdots \\ x_5^0(\alpha) & x_5^2(\alpha) \cdots \\ y_7^1(\alpha) & y_7^3(\alpha) \cdots \\ 0 & x_9^2(\alpha) \cdots \end{bmatrix} \quad \text{or} \quad \begin{bmatrix} x_1^1(\alpha) & x_1^3(\alpha) \cdots \\ y_3^1(\alpha) & y_3^3(\alpha) \cdots \\ x_5^1(\alpha) & x_5^3(\alpha) \cdots \\ y_7^2(\alpha) & y_7^4(\alpha) \cdots \\ 0 & x_9^3(\alpha) \cdots \end{bmatrix}$$

depending on whether the tide-raising potential is of degree 2 or 3.

The matrix reflects the fact that the transverse displacements need not be continuous across the solid-fluid boundary. The continuity of the other variables is taken into account in the array $\mathbf{B}$. Specifically the boundary condition that the shear stresses vanish at the interface is taken into account by setting

$$B^{nk}_{4j} = 0$$

and

$$B^{nk}_{6j} = 0 .$$

The components B^{nk}_{ij} for $i = 1, 2, 5, 6$ and 9 with $j = 1, 3$ or 5 are identical to those at the top of the fluid and with $j = 2$ or 4 are zero.

Within the mantle the system of differential equations is again simply of the form

$$\dot{Y}(r) = A(r)\, Y(r)$$

which is propagated through the mantle in a procedure identical to that previously described;

$$Y(r+\Delta) = [I + \Delta A]\, Y(r)$$

or

$$B(r+\Delta) = [I + \Delta A]\, B(r) .$$

Application of the boundary conditions on the stresses and the potentials at the surface of the Earth permits solving for all the arbitrary constants (the elements of the matrix Z) in terms of the amplitude of the tide-raising potential. The displacements at the surface are then known, as are the induced potential and the gravitational flux. The variations of the displacements, the stresses, the potentials and the gravitational flux throughout the Earth can then be determined.

At the surface of the Earth it is generally more convenient to measure the response in terms of Love numbers, dimensionless quantities which relate the deformations in the real Earth to the corresponding deformations of simplified Earth models. The Love number h is the ratio of the radial displacement at the surface of the Earth to the radial displacement at the surface of a fluid Earth, k is the ratio of the potential due to the deformations to the inducing potential, and ℓ (introduced by Shida) is the ratio of the horizontal displacement at the surface of the Earth to the corresponding horizontal (spheroidal) displacement on a fluid Earth.

4. The Stability of the Solution

As I have indicated in Figure 1, the effect of rotation is to couple other modes to the mode being driven directly by the tide-raising potential. In standard investigations of the free oscillations of the Earth at periods of less than one hour, only one mode at a time need be considered. Pekeris & Accad (1972) considered only one mode at a time due to their neglect of all rotational couplings. Smylie (1974) included the Coriolis self-coupling but neglected the torsional modes and the rotational excitation of other spheroidal modes. I show that these couplings must be taken into account as the period of the motion increases and hence I need to consider the effect of truncating the full solution (which would contain an infinite number of modes) to a subset which can be handled numerically yet will still give credible results.

There are two decisions on truncation to be made. The first of these is simply a choice of the truncation which is generally carried throughout the integration; in effect this is a choice of the size of the matrix of arbitrary constants which has been referred to as Z in this chapter. As a standard I take Z as a 5x3 matrix and verify these results (or improve on them) by supplementing this to a 5x4 matrix. Also Z can be reduced to a 5x2 matrix for more direct comparison with the results of Pekeris & Accad (1972). The standard choice for an excitation of degree 2 implies a retention of the spheroidal degrees 0, 2 and 4, and the torsional degrees 1, 3 and 5, and I shall refer to this as a 'propagation truncation' of level 3. The results obtained with the 5x4 matrix includes the modes above as well as the spheroidal degree 6 and the torsional degree 7 response and is referred to as a 'propagation truncation' of level 4. The 5x2 matrix

specifies a 'propagation truncation' of level 2 and retains only degree 0 and 2 spheroidal response and degree 1 and 3 torsional response.

The second choice is generated by the need to solve for the transverse displacements (y_3 and y_7) and their derivatives within the fluid and to then eliminate these variables from the differential equations. In principle one again has an infinite set of coupled equations which one would like to be able to solve analytically. Again in practise one must solve these numerically and hence choose some truncation level for the computations. Fortunately it is necessary to perform this solution only once (for a specified driving period) and it is therefore possible to retain a much higher number of modes to solve for the transverse motions and to eliminate these from the differential equations. After this elimination the resulting set of differential equations is then truncated to the 'propagation truncation' level consistent with that retained in the solid regions of the Earth.

The standard truncation level chosen for this step was an inclusion of all spheroidal modes up to degree 26 and torsional modes up to degree 27 (a choice made by computer core available) with relaxations to a maximum degree of 5 or 3 torsional mode (in the latter choice a 'propagation truncation' level of 3 is the maximum consistent choice) for a comparison with previous results and with the results of other authors. This truncation is referred to as an 'elimination truncation' and the choices indicated above are levels 14, 3 and 2, respectively.

As a final check on the numerical solution obtained it is necessary to repeat the calculations with different step sizes chosen for

the integrations. This allows an optimization of step size with respect to both accuracy and speed.

The numerical method can also be tested to some extent by comparing the numerical solutions to an analytic solution. By neglecting all rotational coupling except the Coriolis self-coupling and assuming an Earth model of uniform density, an analytic solution can be obtained in terms of spherical Bessel functions and modified spherical Bessel functions (Appendix E). The resulting analytic solution can then be compared with the numerical solution derived by using the techniques used for the complete case (after removing all coupling coefficients) for the equivalent Earth model. These solutions are compared in Appendix E and show excellent agreement.

CHAPTER 3

NUMERICAL RESULTS

In the preceding two chapters I have derived the necessary set of differential equations, specified the boundary conditions and discussed the numerical procedure that I have used to investigate the Earth tide problem. Using these methods I have been able to calculate the deformations produced by a tide-raising potential of either second or third degree.

For purposes of comparison with the results of Pekeris & Accad (1972), Smylie (1974) and Crossley (1975b), the model that I have adopted has a sub-adiabatic fluid core which will exhibit the free oscillations which Smylie has called undertones. Where Smylie and Crossley have only calculated the periods of these undertones, Pekeris & Accad also calculated the Love numbers as functions of frequency; however they neglected all rotational couplings (in essence, they have simply extended the standard free oscillation theory into a frequency regime where it is inapplicable). Smylie's investigation of the undertones of a rotating Earth included only the self-coupling term due to the Coriolis effect of all the rotational couplings which apply (Fig. 1) but Crossley has subsequently included the torsional modes in the fluid which are also excited through Coriolis forces.

The advantage of my approach is twofold: an arbitrary number of modes can (in principle) be retained to describe the response, and the behaviour of the displacements and stresses throughout the Earth and at the surface (in terms of the Love numbers) can be calculated at arbitrary periods.

To illustrate the above points I display the results obtained for the radial stress functions (y_2^k, the degree k response in the radial stress) that is obtained through the Earth (for k = 2 and for k = 4) in response to an extenal potential of degree and order two (n = m = 2). The radial stress functions have been chosen as representative since they are continuous across all internal boundaries and vanish at the surface. These are plotted for periods of 1, 2, 3, 4, 5, 6, 7, 8, 9, 10, 11 and 12 hours in Figures 2-13. These solutions have been obtained by retaining an 'elimination truncation' level of 14 and a 'propagation truncation' level of 3 which includes all modes of the response up to and including the degree 5 (and order 2) torsional components. For comparison the corresponding solution resulting from changing the 'propagation truncation' level to 4 (which includes the degree 6 spheroidal and degree 7 toroidal modes of order two) has been graphed for periods of 1, 3, 5, 7, 9, 11 and 12 hours.

The units on the vertical scale of these graphs are those described in Chapter 2, section 2, such that the externally prescribed potential is unity at a unit distance (10^4 km). The horizontal axis is marked in steps of 10^3 km with the inner core-fluid boundary and the core-mantle boundary indicated.

From these solutions it is evident that the description of the response in the fluid region is very sensitive to the numerical procedure for periods approaching the semi-diurnal. Not only are the solutions obtained dependent upon the step size used to propagate the solution through the fluid outer core but also upon the number of modes retained in the approximation of the full solution. The investigation of the variation of the solution with respect to the step size is a purely empirical

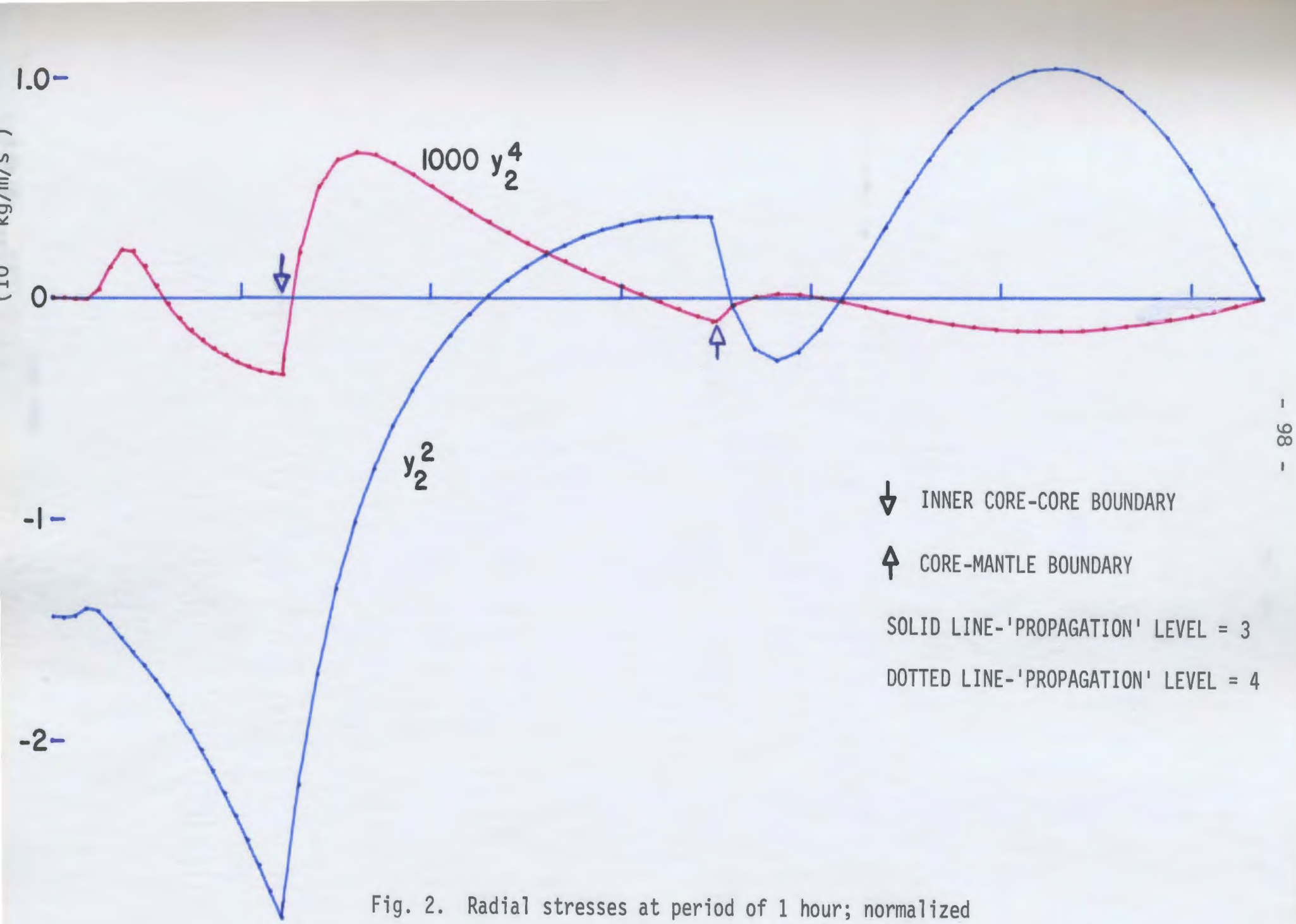

Fig. 2. Radial stresses at period of 1 hour; normalized to an inducing potential of 10^8 m^2/s^2 at 10^7 m.

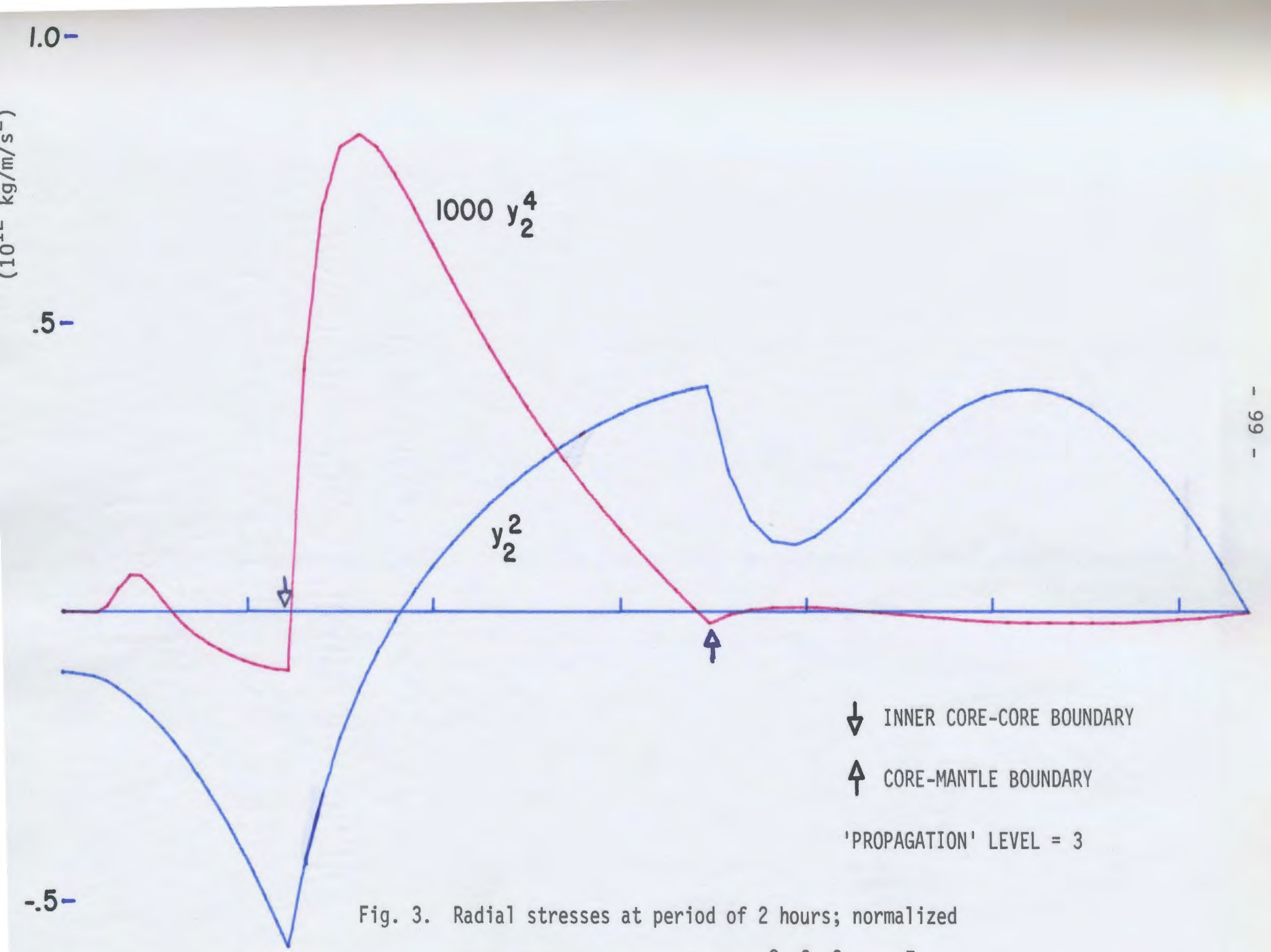

Fig. 3. Radial stresses at period of 2 hours; normalized to an inducing potential of 10^8 m^2/s^2 at 10^7 m.

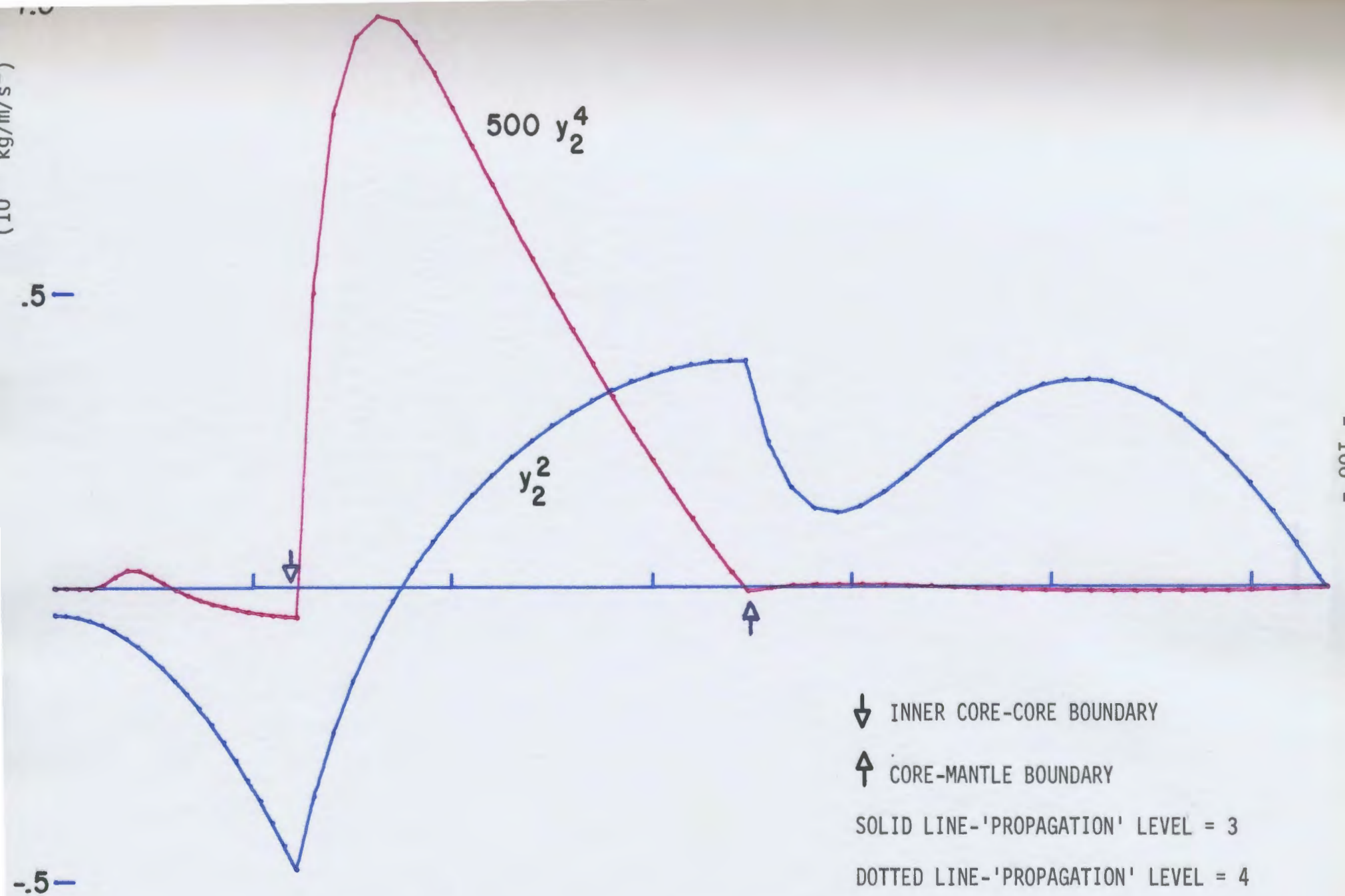

Fig. 4. Radial stresses at period of 3 hours; normalized to an inducing potential of 10^8 m^2/s^2 at 10^7 m.

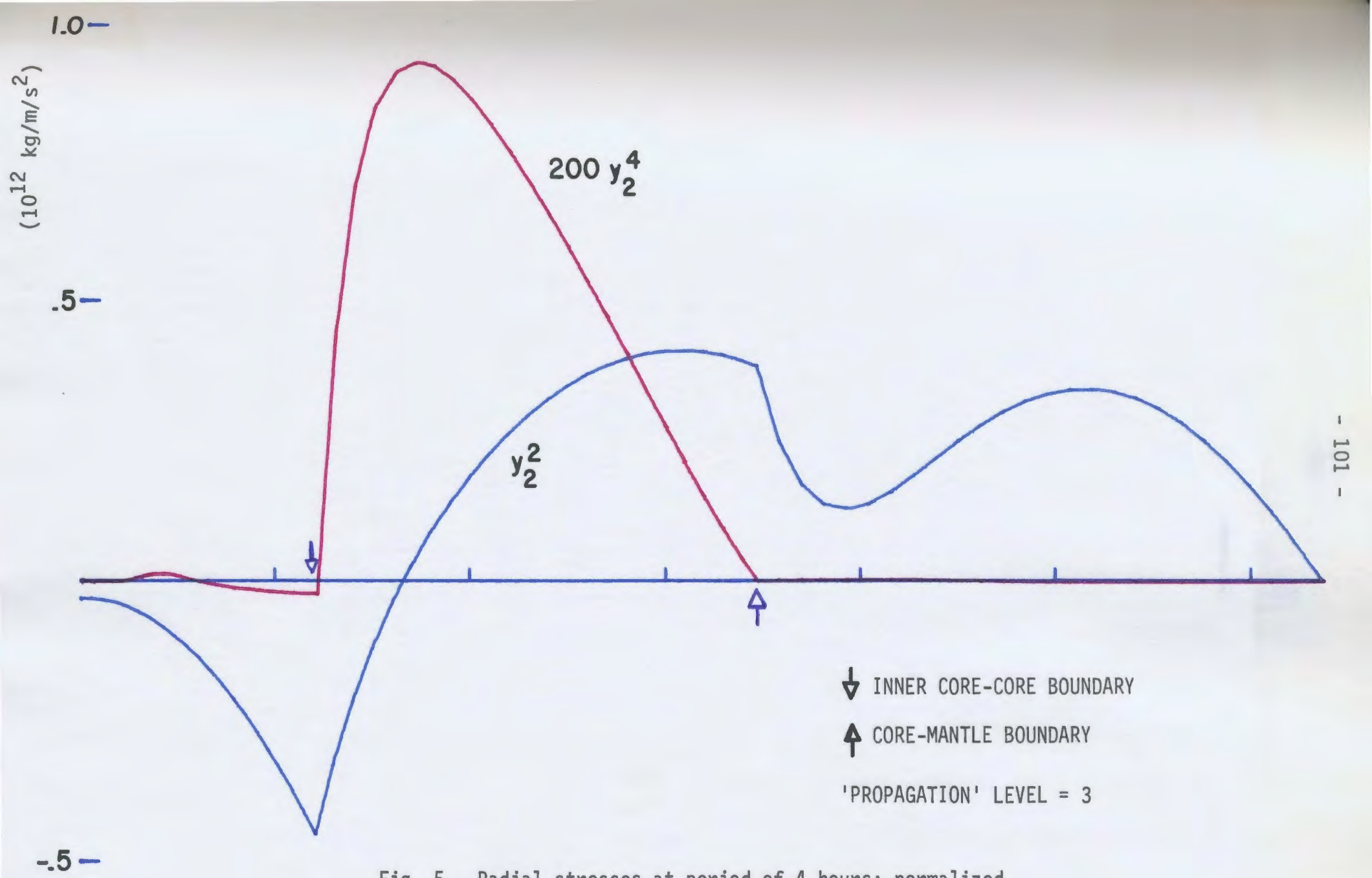

Fig. 5. Radial stresses at period of 4 hours; normalized to an inducing potential of 10^8 m^2/s^2 at 10^7 m.

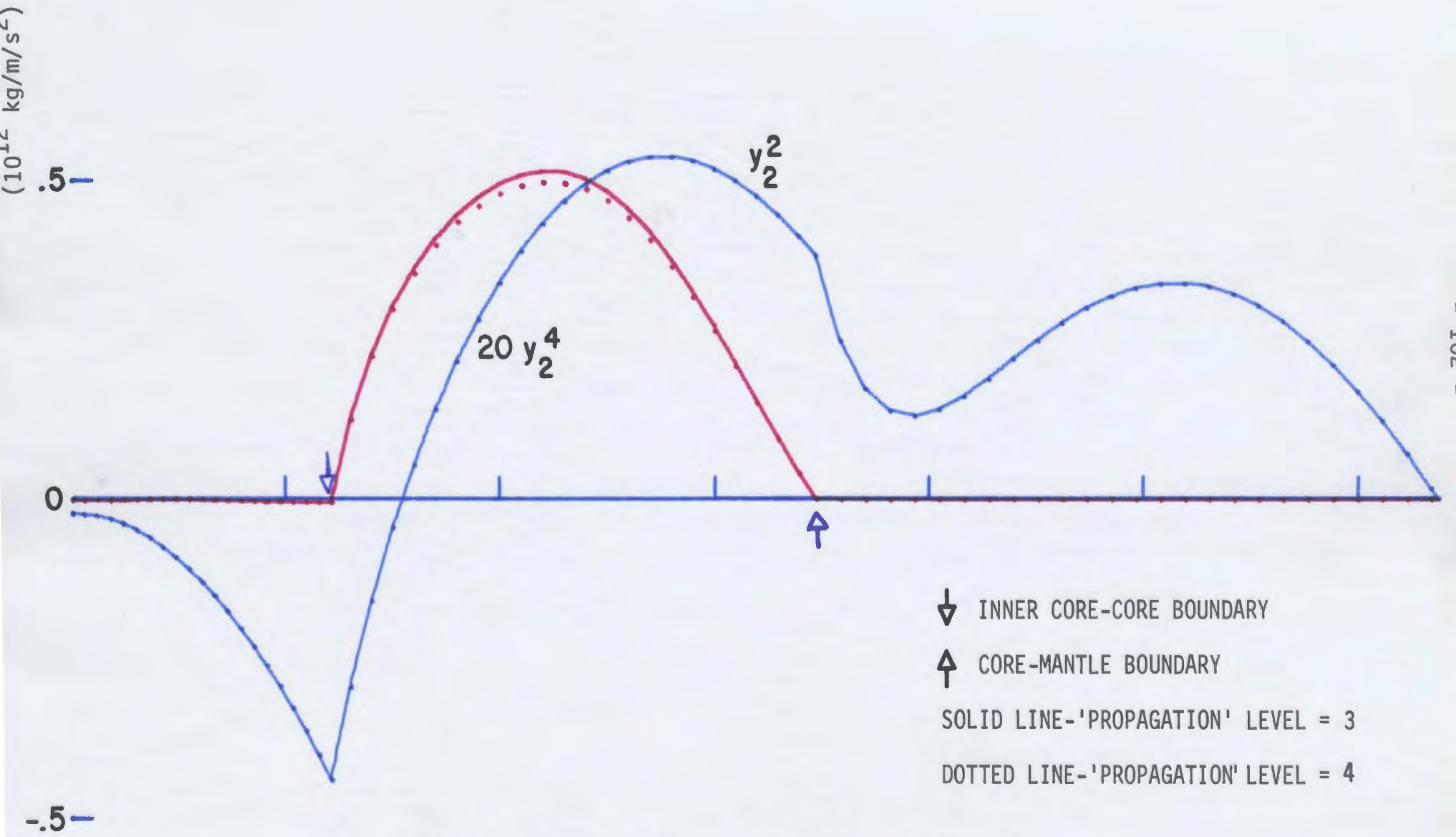

Fig. 6. Radial stresses at period of 5 hours; normalized to an inducing potential of 10^8 m^2/s^2 at 10^7 m.

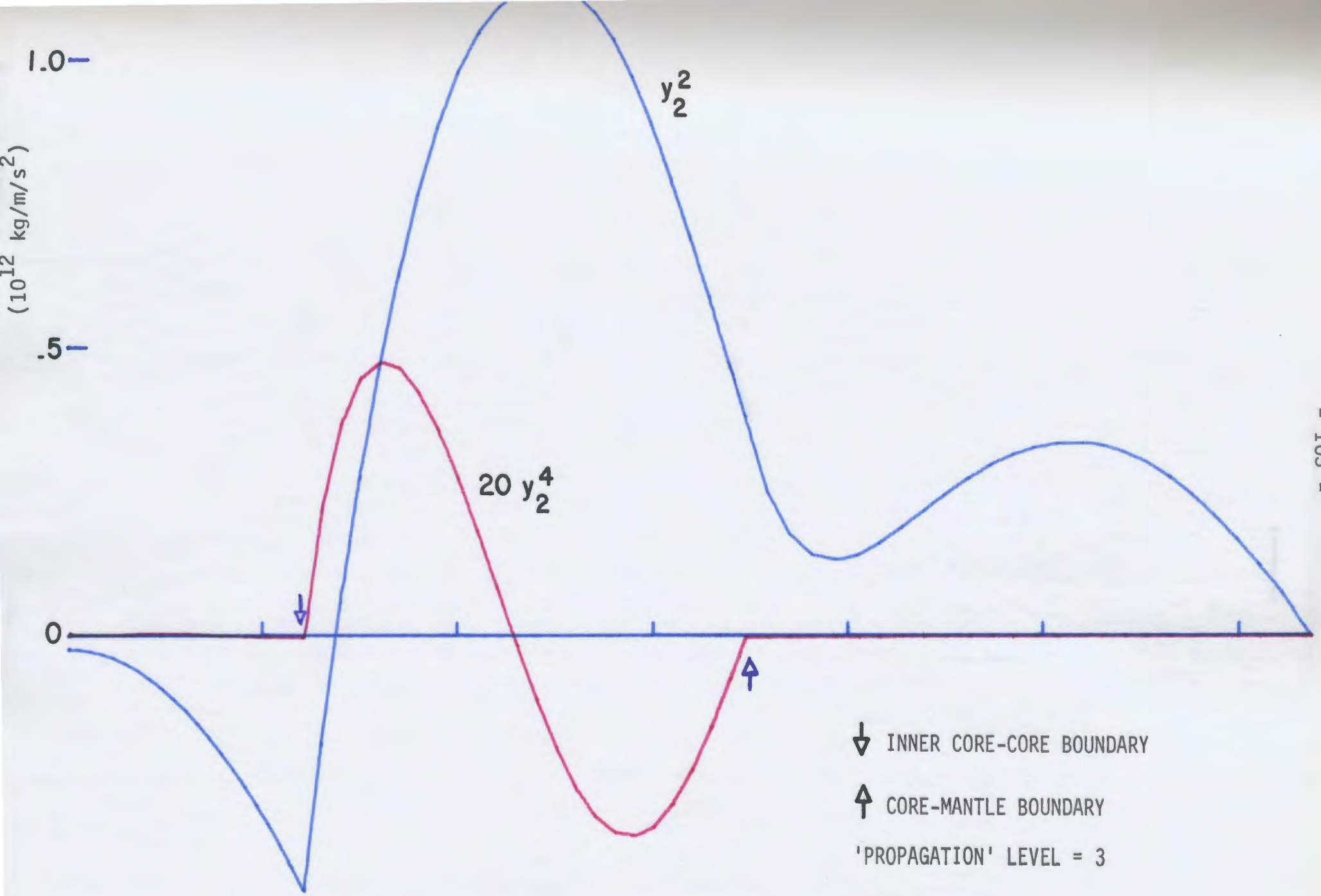

Fig. 7. Radial stresses at period of 6 hours; normalized to an inducing potential of 10^8 m^2/s^2 at 10^7 m.

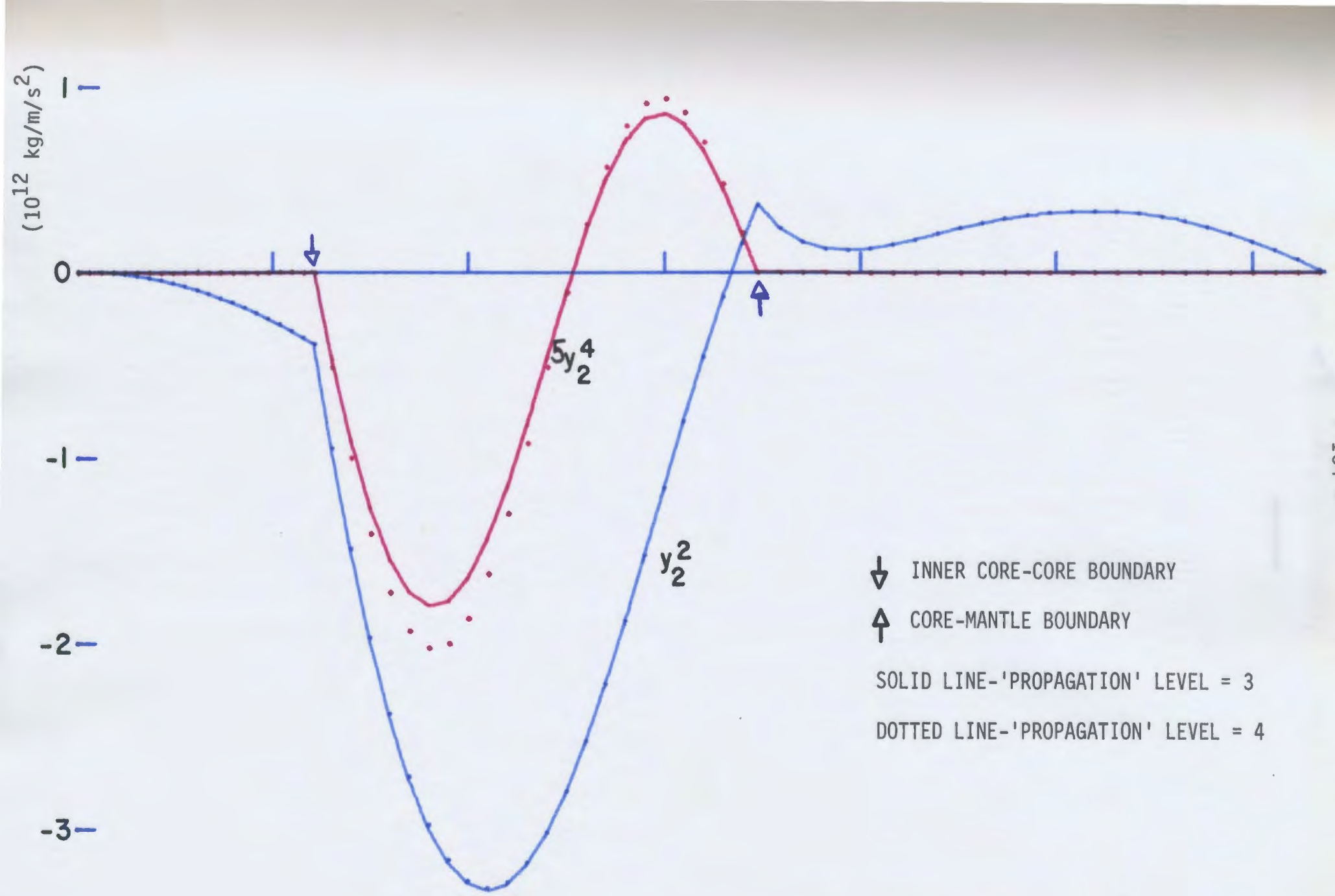

Fig. 8. Radial stresses at period of 7 hours; normalized to an inducing potential of 10^8 m^2/s^2 at 10^7 m.

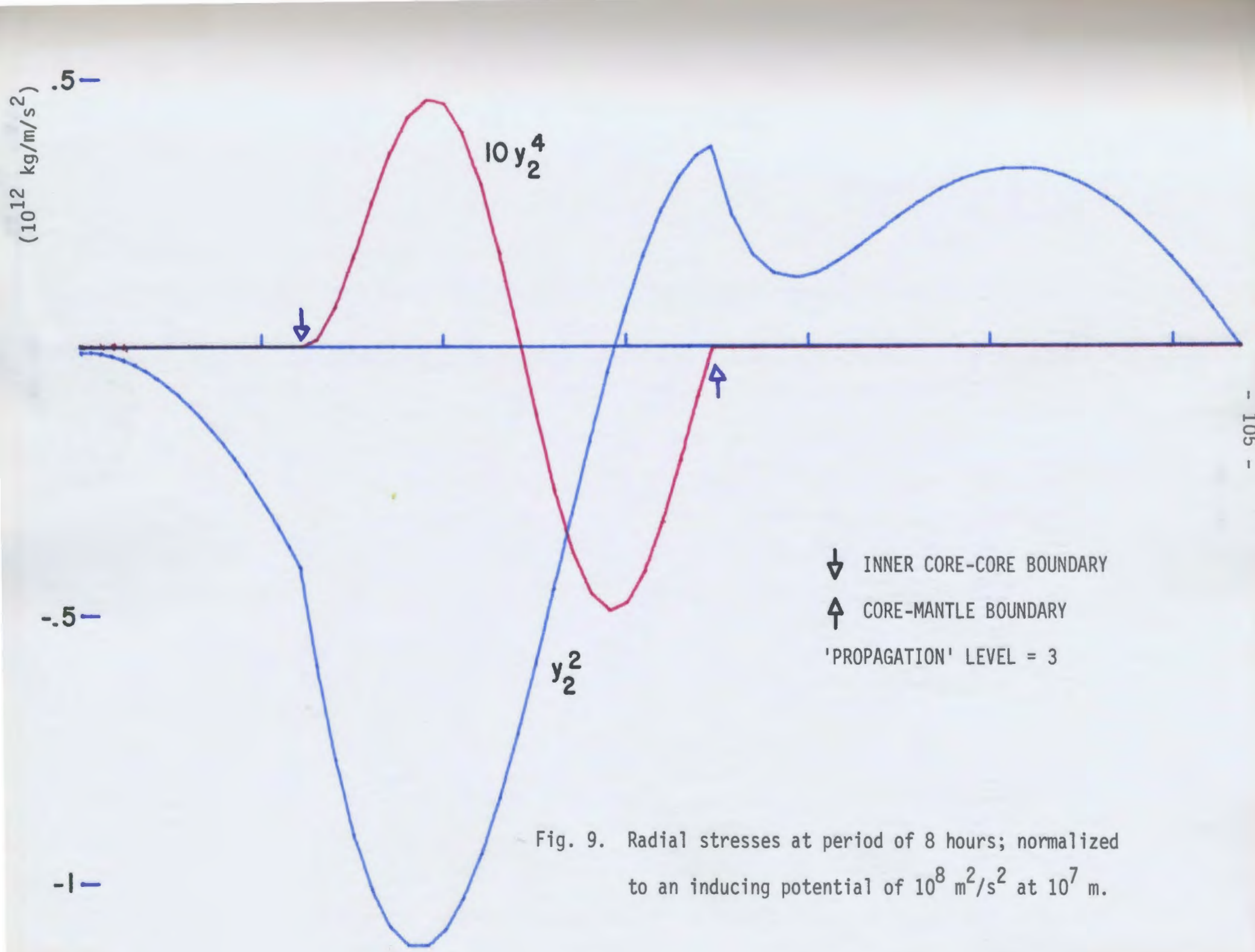

Fig. 9. Radial stresses at period of 8 hours; normalized to an inducing potential of 10^8 m^2/s^2 at 10^7 m.

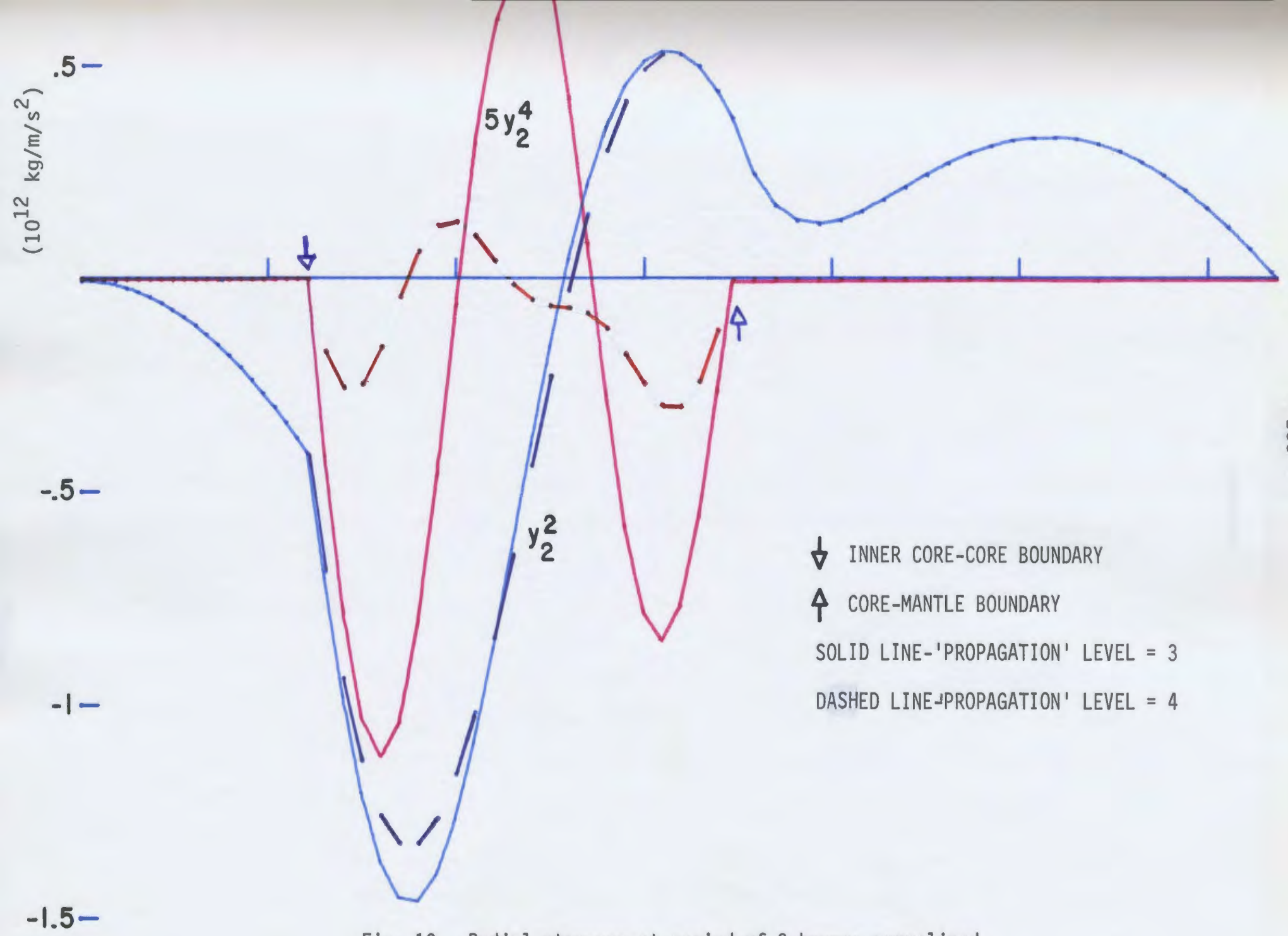

Fig. 10. Radial stresses at period of 9 hours; normalized to an inducing potential of 10^8 m^2/s^2 at 10^7 m.

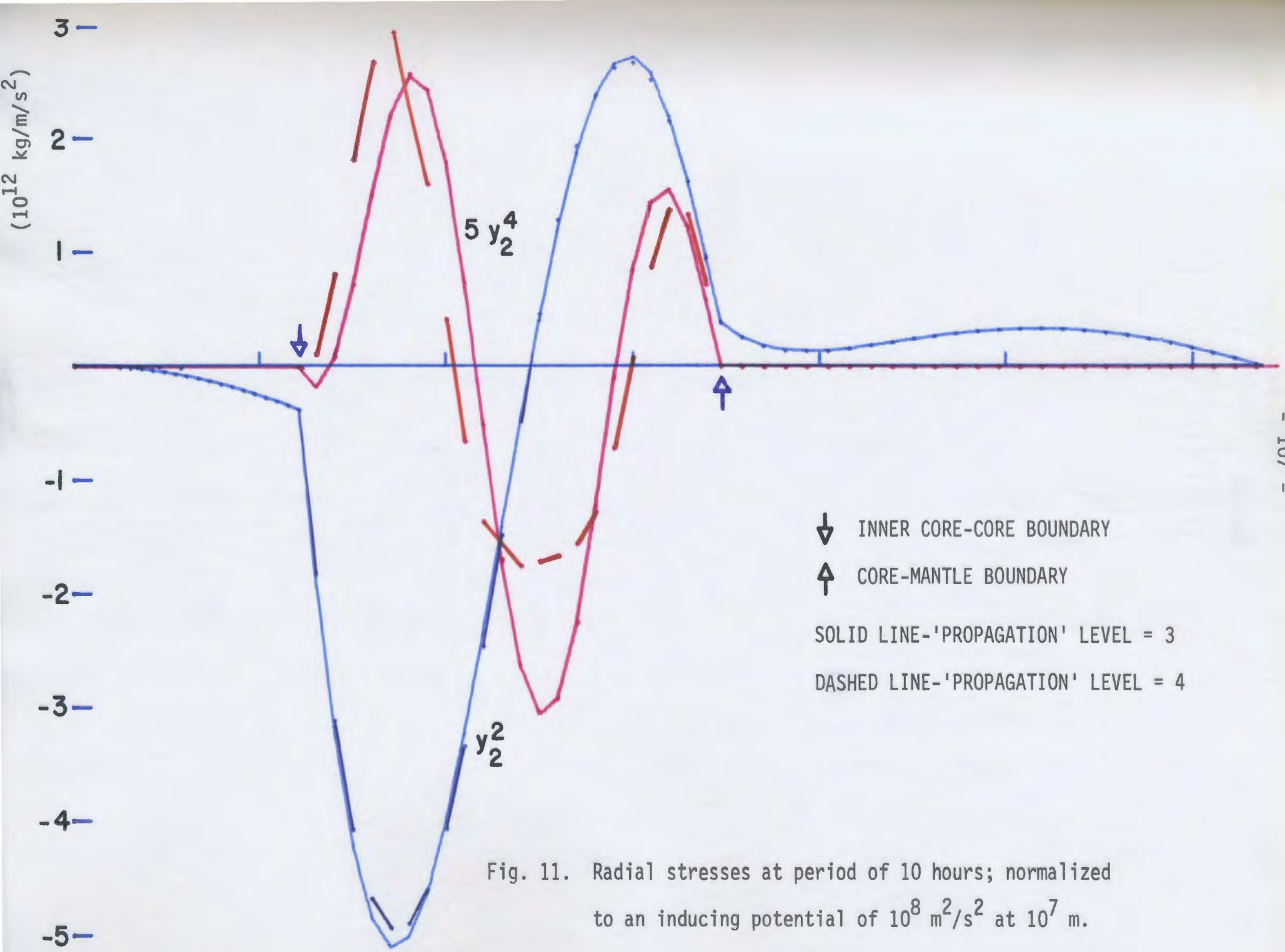

Fig. 11. Radial stresses at period of 10 hours; normalized to an inducing potential of 10^8 m^2/s^2 at 10^7 m.

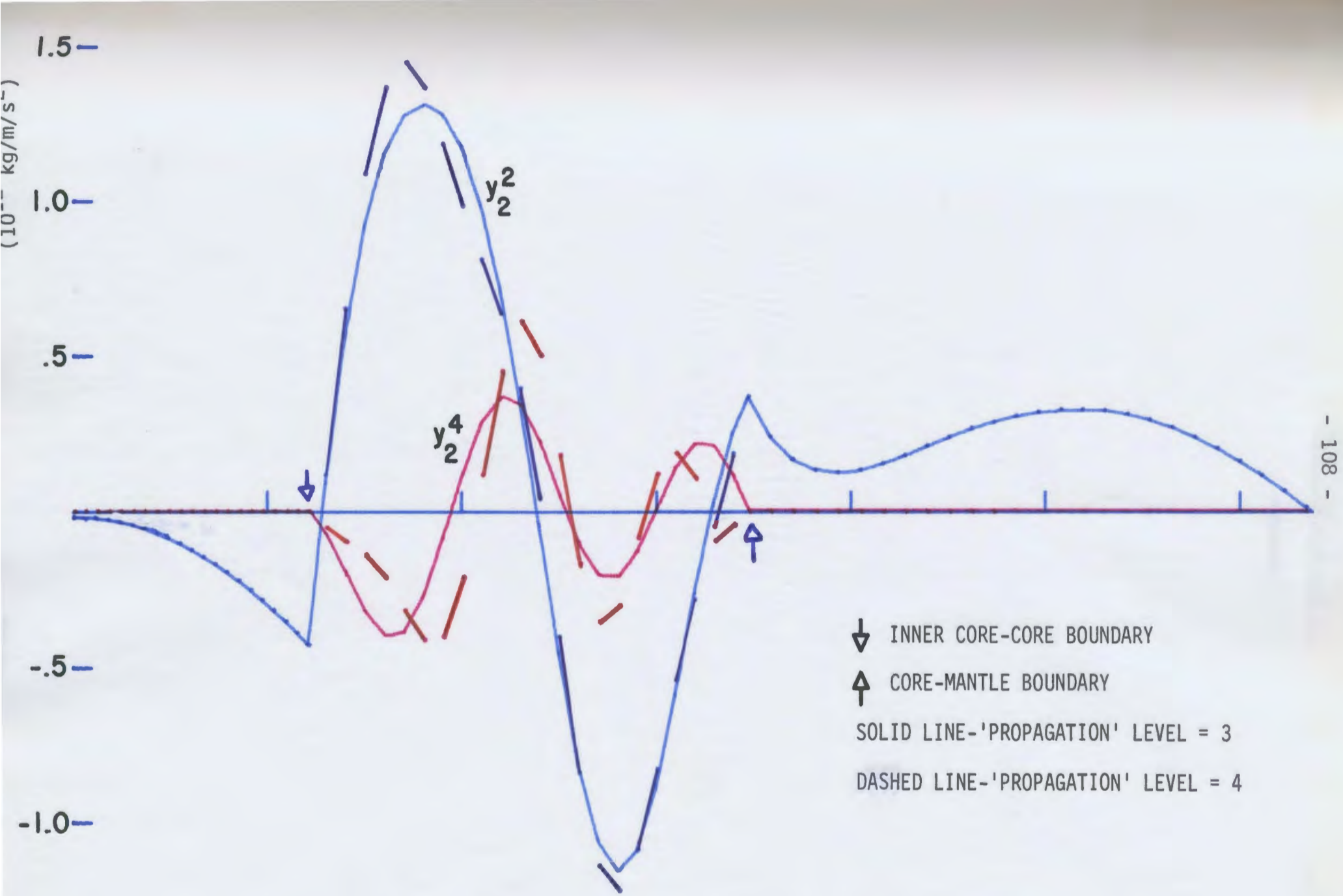

Fig. 12. Radial stresses at period of 11 hours; normalized to an inducing potential of 10^8 m^2/s^2 at 10^7 m.

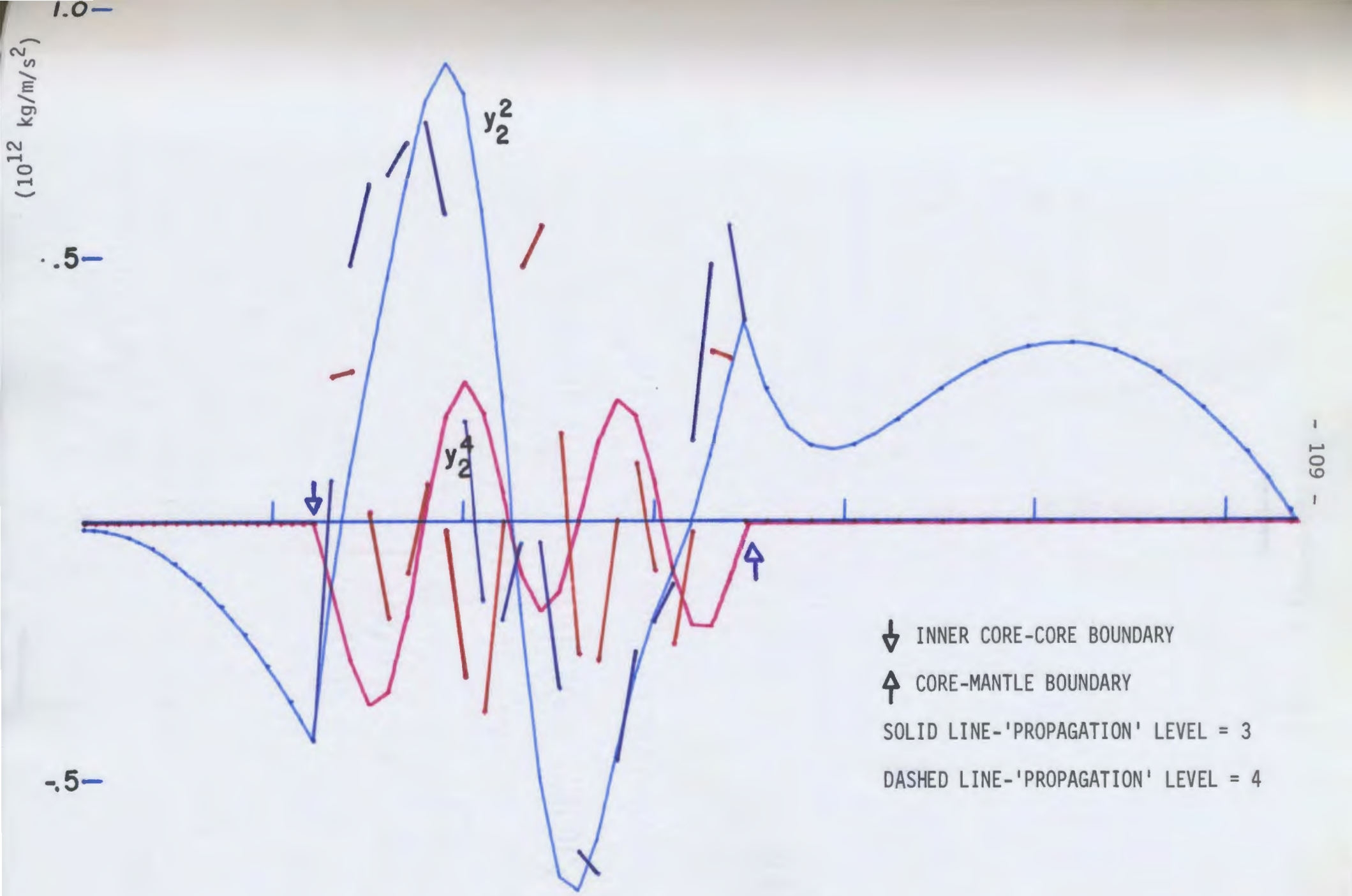

Fig. 13. Radial stresses at period of 12 hours; normalized to an inducing potential of 10^8 m^2/s^2 at 10^7 m.

numerical procedure and the results of these tests are given in Appendix G; the indication of these tests is that a step size of approximately 1 km. through the fluid region produces a realistic result.

However, even with this small step size used for propagating the solution through the fluid region, the solutions are deteriorating as the semi-diurnal period is approached. Using the convergence of the radial stress functions as a test, the applicability of the solutions is limited to periods less than the semi-diurnal. To illustrate the behaviour of the variables throughout the Earth I display the displacements (y_1^2, y_3^2 and y_7^3, Figures 14-17), the shear stresses (y_4^2 and y_8^3, Figures 18-21) and the potentials and gravitational flux (y_5^2, y_6^2 and y_9^2, Figures 22-25) for periods of 1 hour, 5 hours, 7 hours and 11 hours. The solutions for the 1-hour and 5-hour driving potential are those obtained with a 'propagation truncation' level of 3 whereas the longer period solutions were those derived by retaining a level of 4.

The spheroidal displacements at the 1-hour period are similar to the solutions obtained by Alterman et al. (1959, p. 88; Fig. 2) and by Pekeris & Accad (1972, p. 256, Fig. 10) for the fundamental spheroidal oscillation (except for the obvious differences due to the inclusion of an inner core in this model) showing that the free oscillation theory is sufficient for modelling the short period response of the Earth.

Within the solid regions of the Earth the elastic forces completely dominate any rotational effects and hence very little variation of the solutions with respect to the period of the driving potential is expected. This is borne out by the stability of the calculated solutions. The constraints imposed by the boundary conditions at the geocentre,

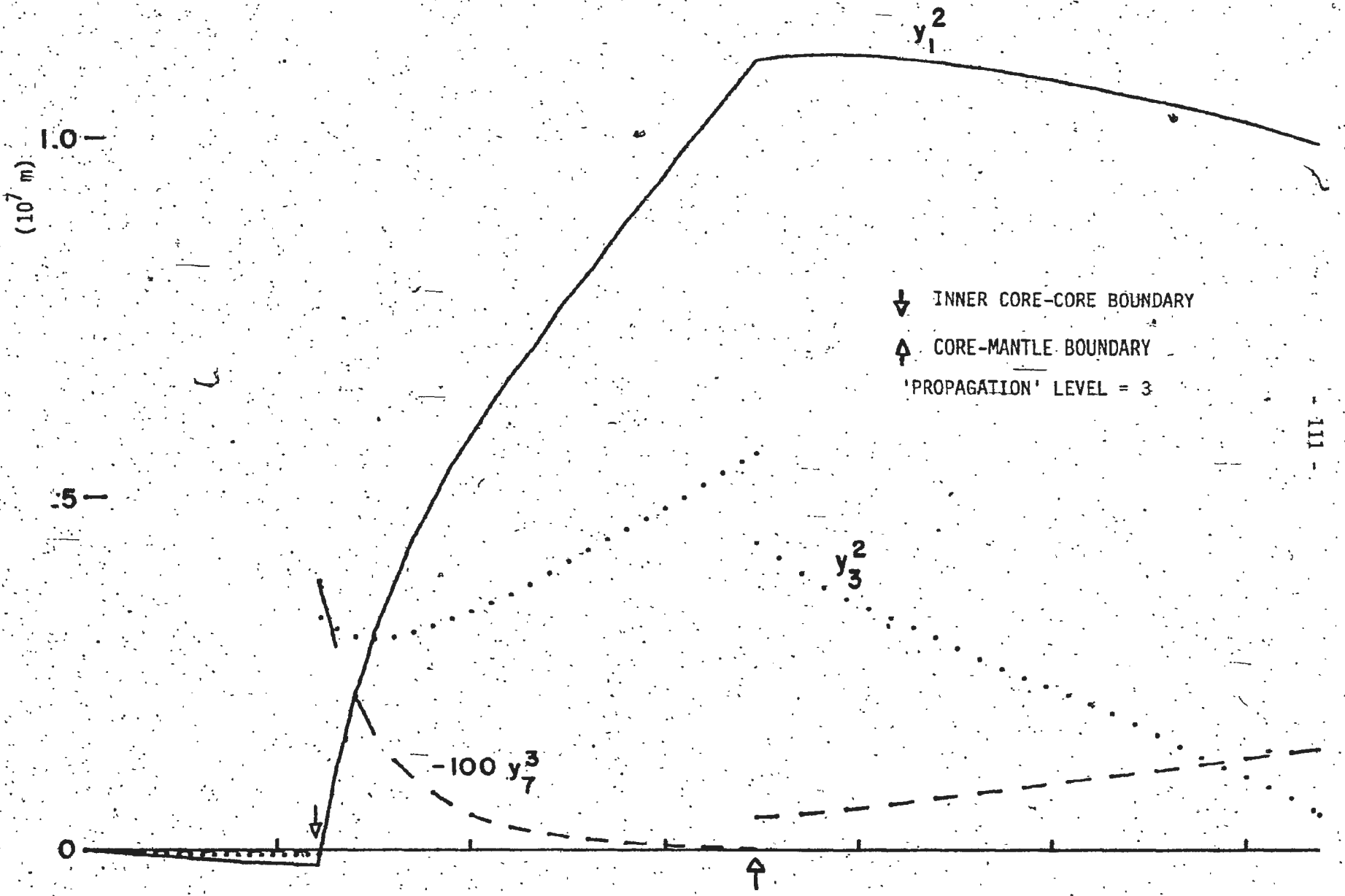

Fig. 14. Displacements at period of 1 hour; normalized to an inducing potential of 10^8 m^2/s^2 at 10^7 m.

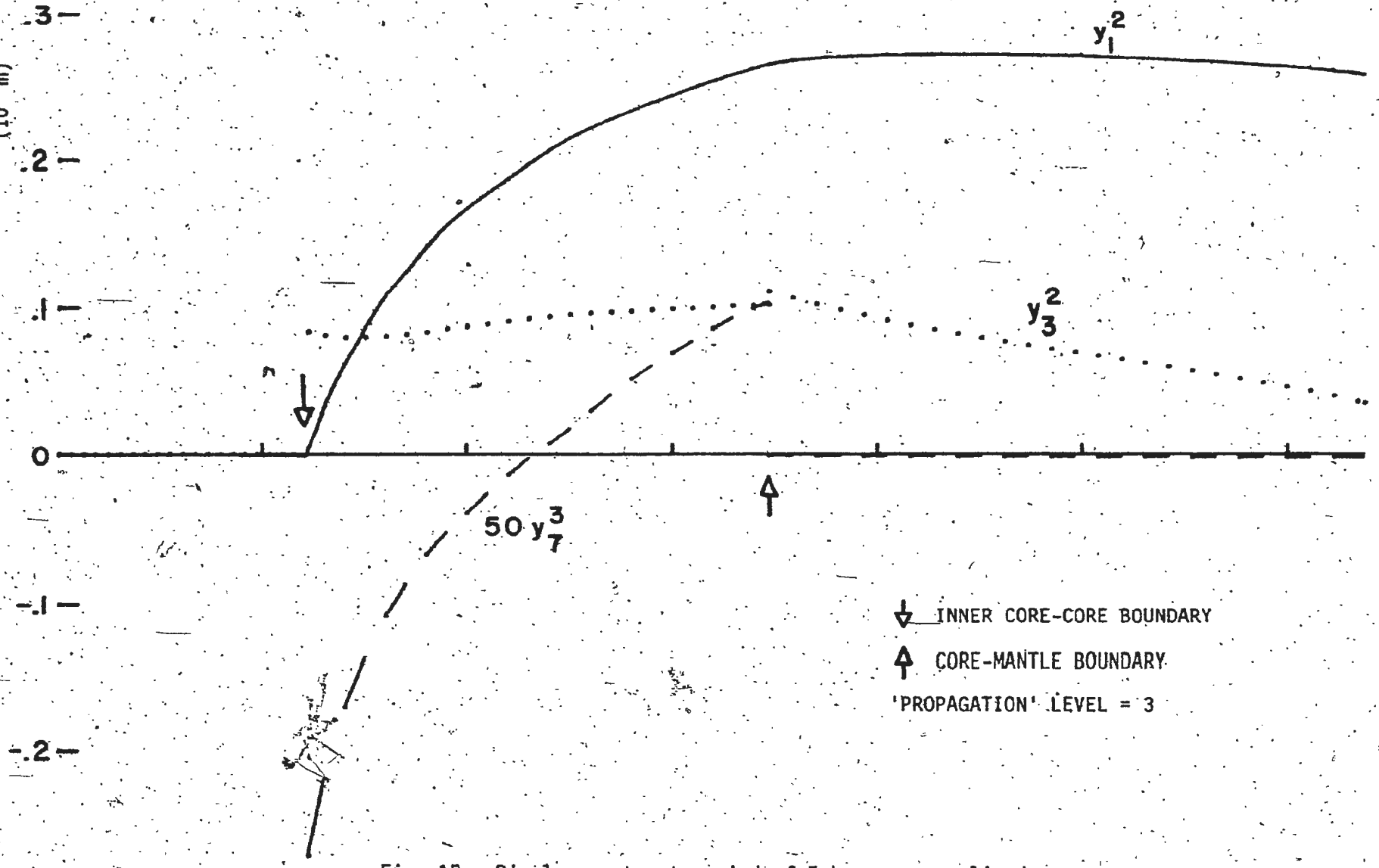

Fig. 15. Displacements at period of 5 hours; normalized to an inducing potential of 10^8 m^2/s^2 at 10^7 m.

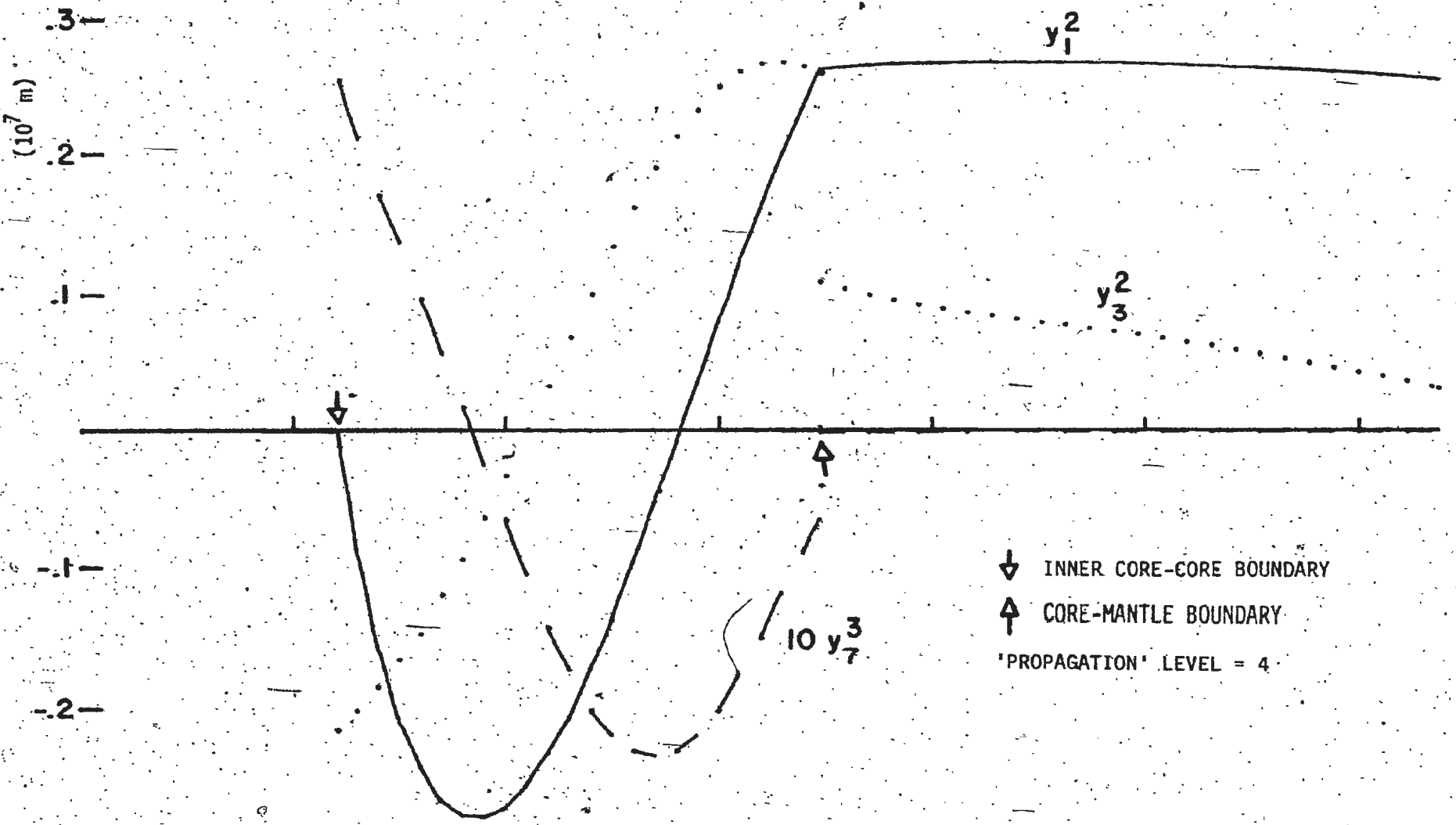

Fig. 16. Displacements at period of 7 hours; normalized to an inducing potential of 10^8 m^2/s^2 at 10^7 m.

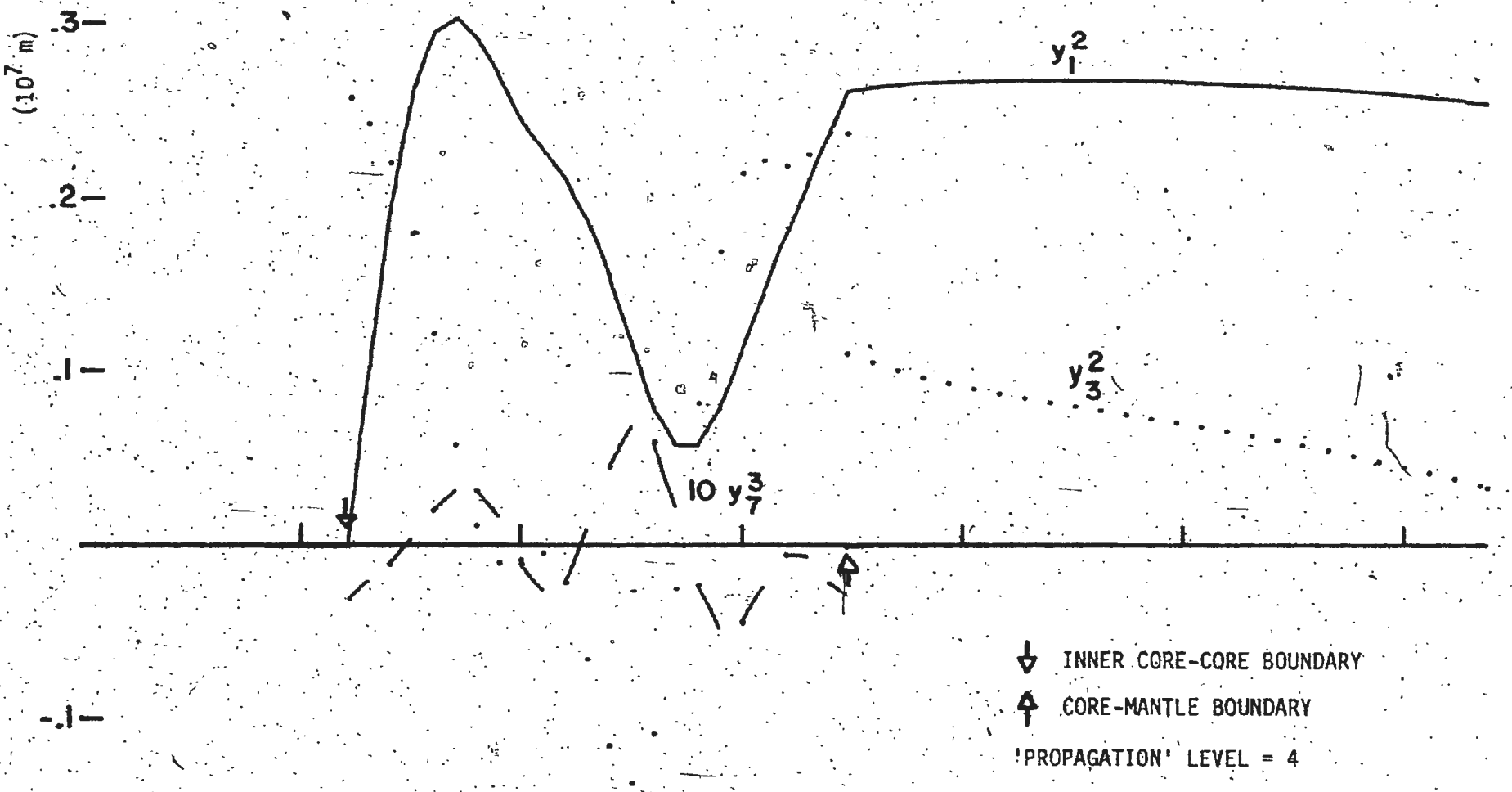

Fig. 17. Displacements at period of 11 hours; normalized to an inducing potential of 10^8 m^2/s^2 at 10^7 m.

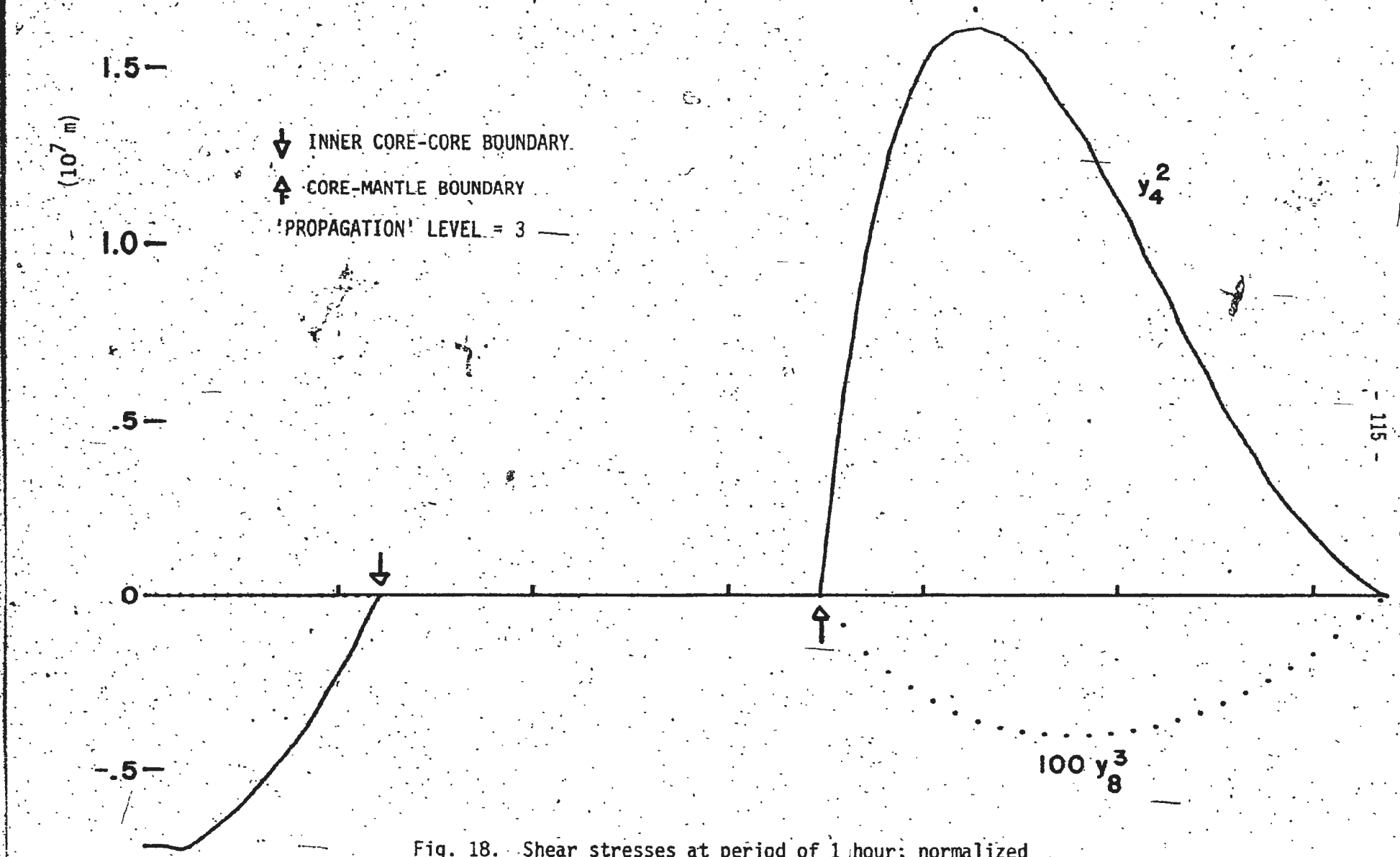

Fig. 18. Shear stresses at period of 1 hour; normalized to an inducing potential of 10^8 m^2/s^2 at 10^7 m.

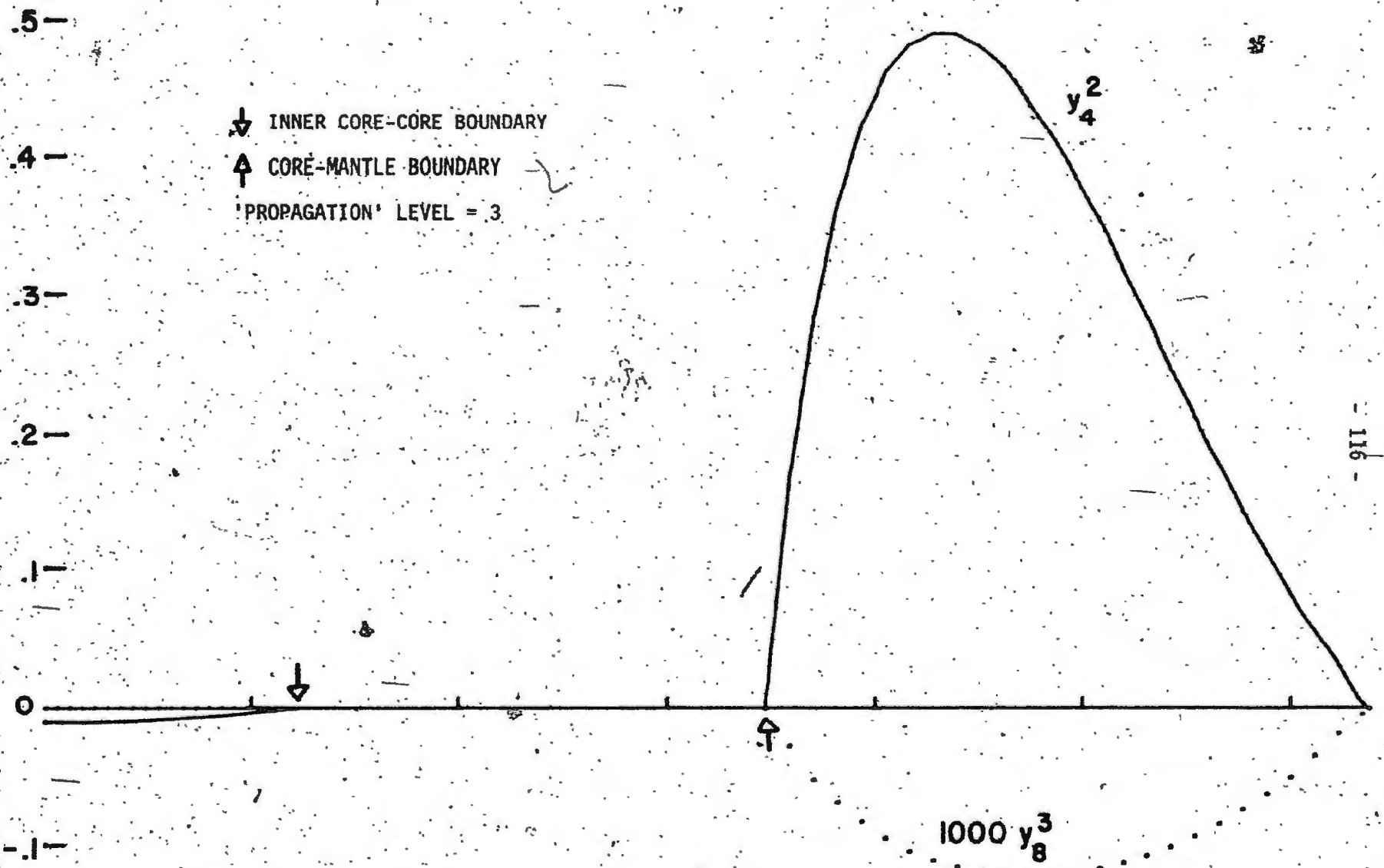

Fig. 19. Shear stresses at period of 5 hours; normalized to an inducing potential of 10^8 m^2/s^2 at 10^7 m.

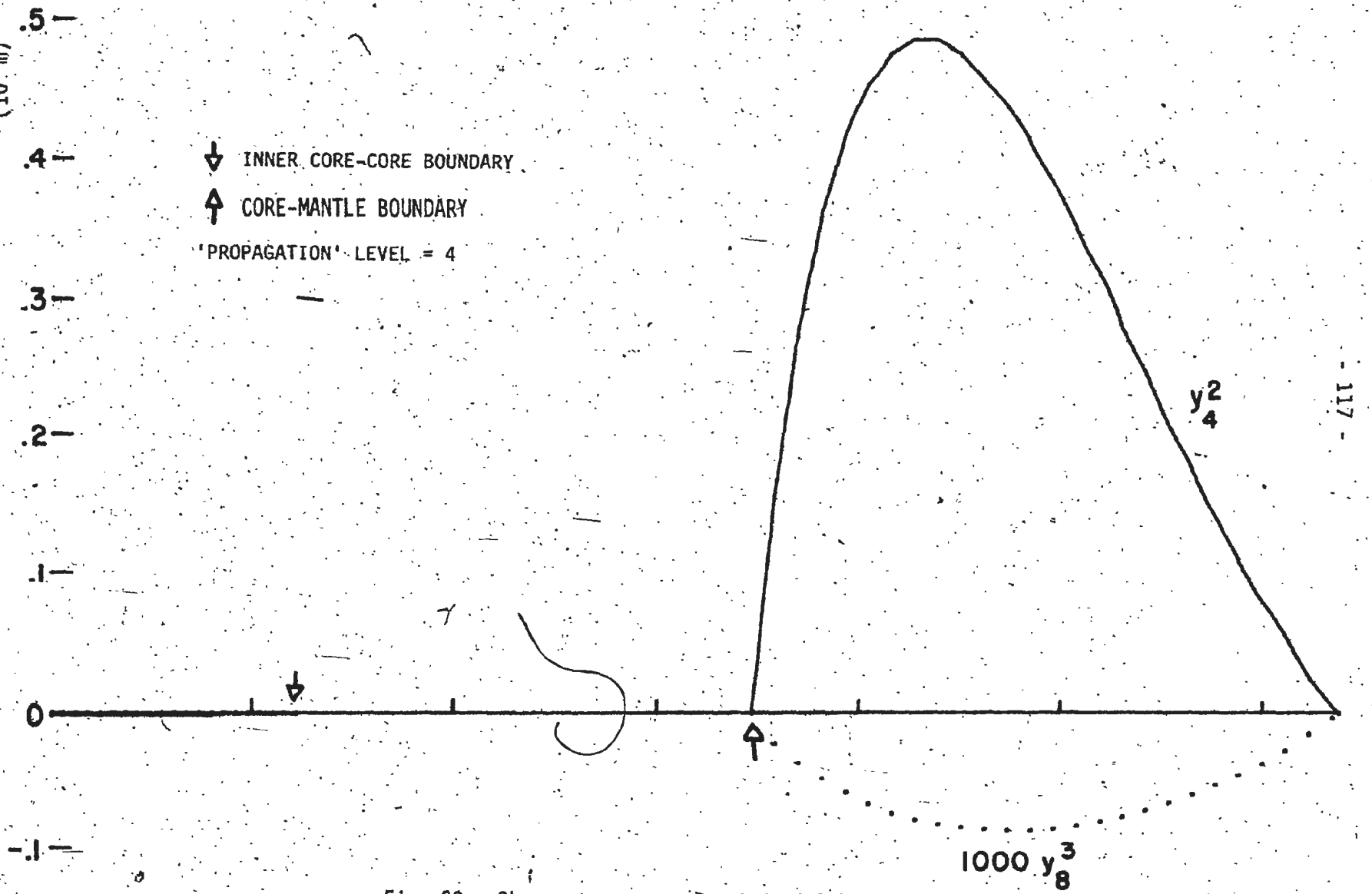

Fig. 20. Shear stresses at period of 7 hours; normalized to an inducing potential of 10^8 m^2/s^2 at 10^7 m.

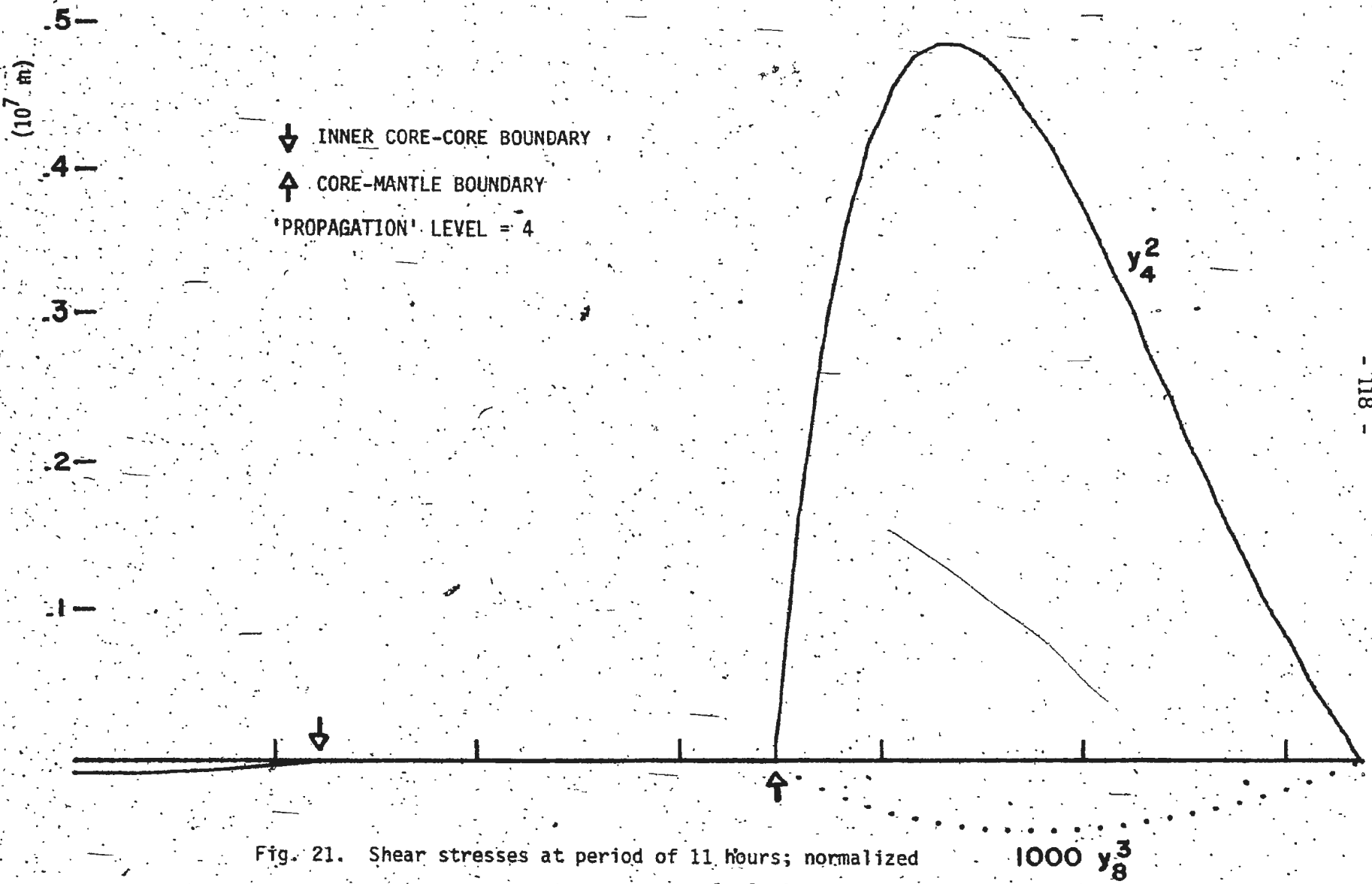

Fig. 21. Shear stresses at period of 11 hours; normalized to an inducing potential of 10^8 m^2/s^2 at 10^7 m.

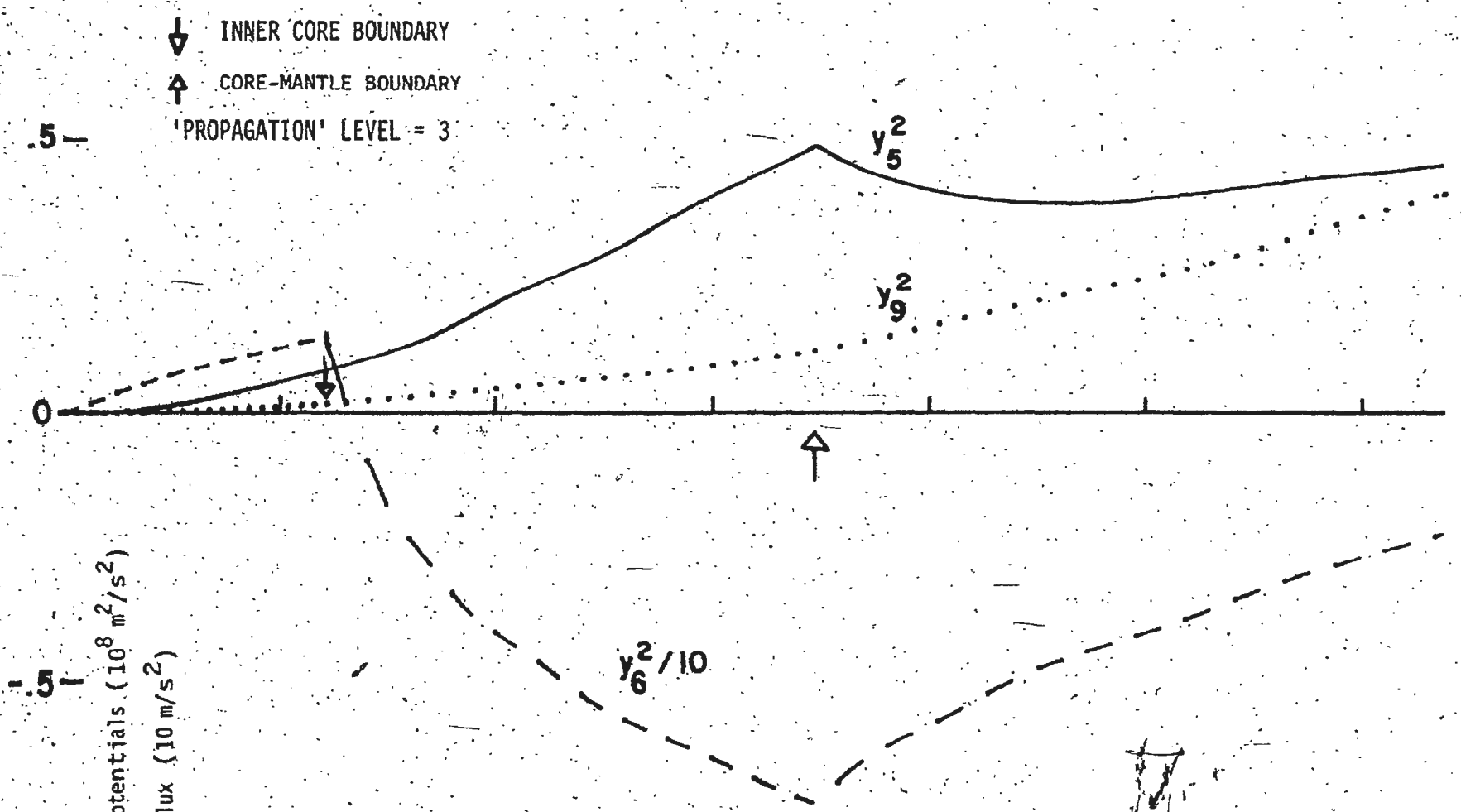

Fig. 22. Potentials and gravitational flux at period of 1 hour, normalized to an inducing potential of 10^8 m^2/s^2 at 10^7 m.

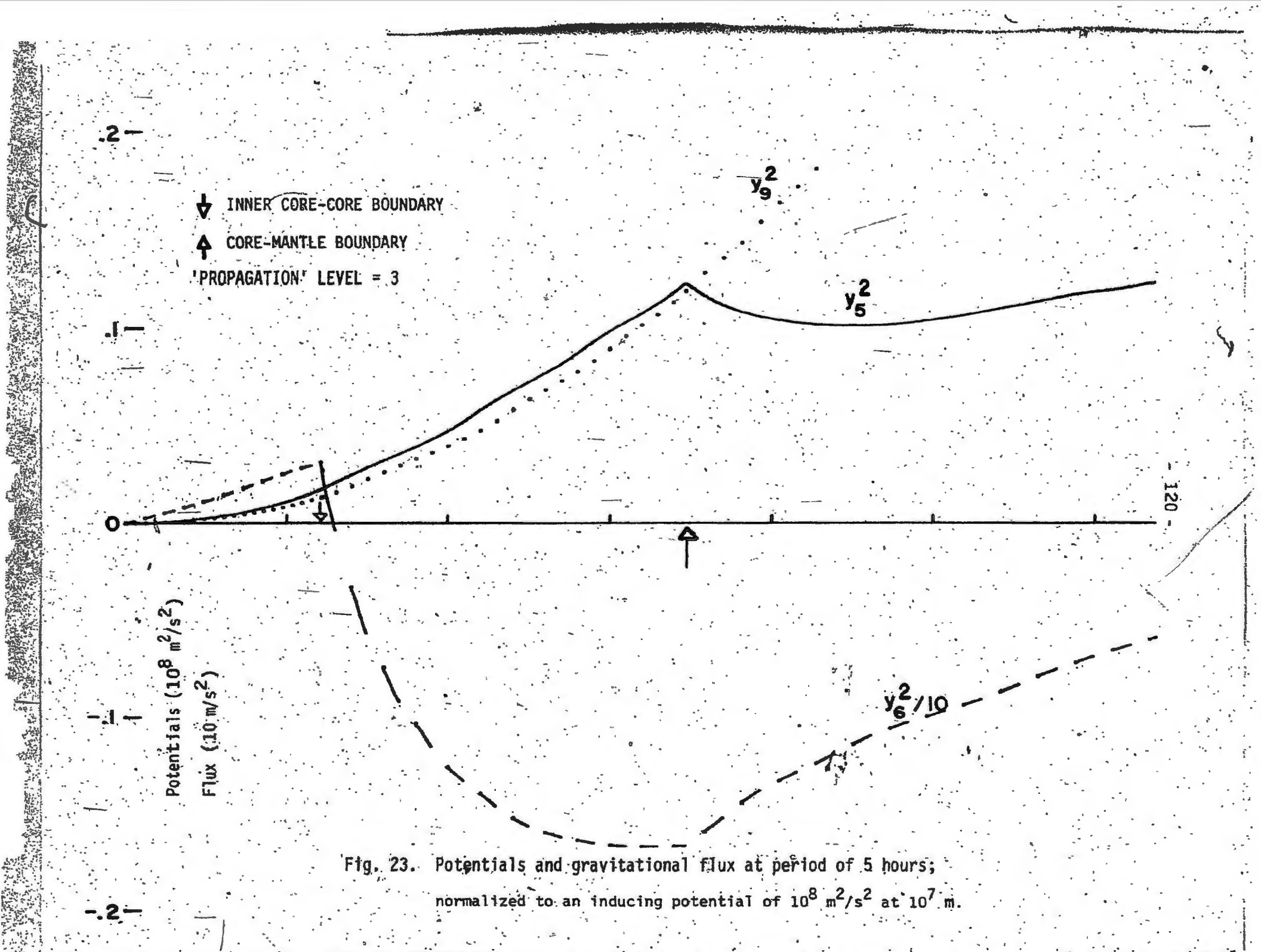

Fig. 23. Potentials and gravitational flux at period of 5 hours; normalized to an inducing potential of 10^8 m^2/s^2 at 10^7 m.

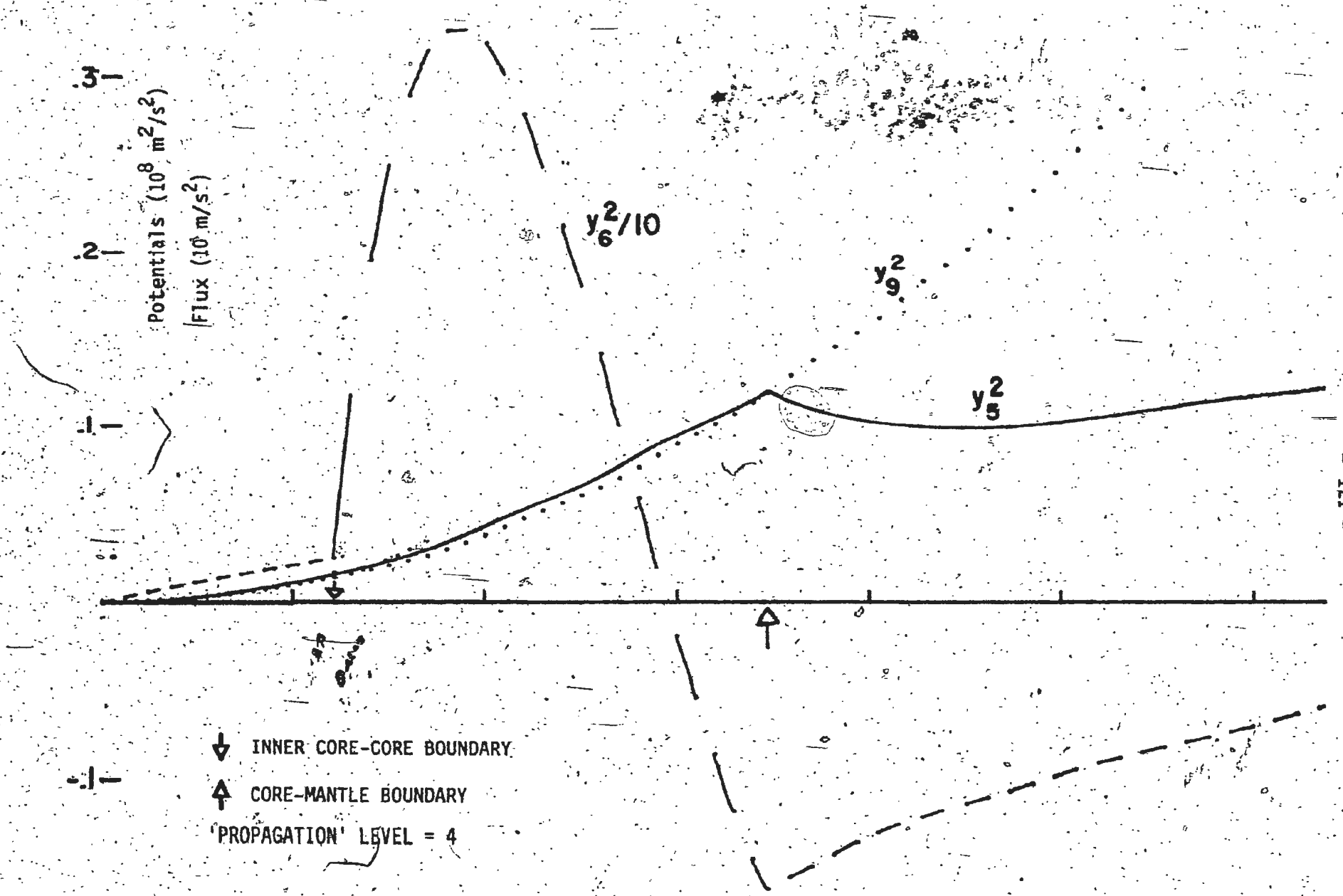

Fig. 24. Potentials and gravitational flux at period of 7 hours; normalized to an inducing potential of 10^8 m^2/s^2 at 10^7 m.

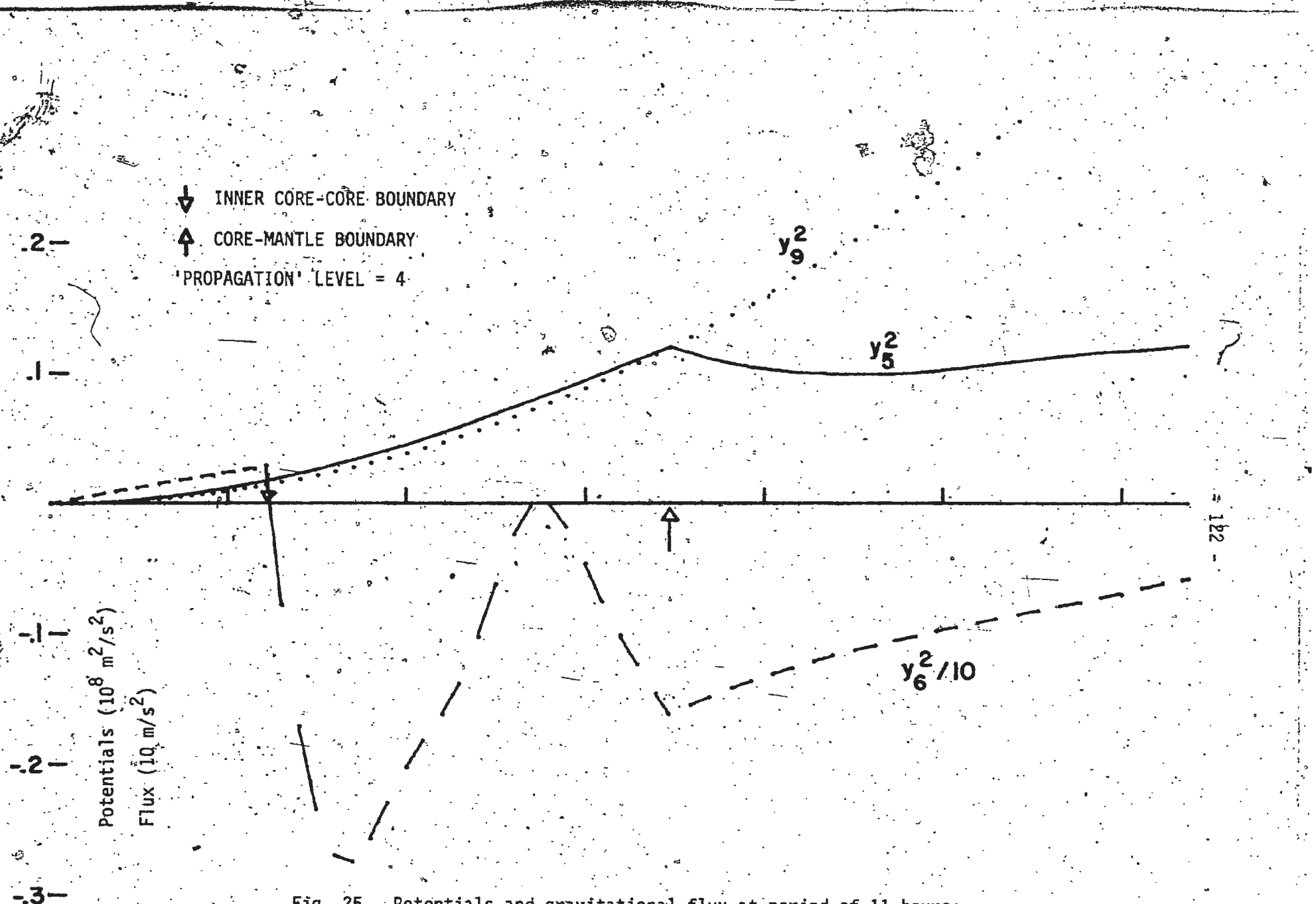

Fig. 25. Potentials and gravitational flux at period of 11 hours; normalized to an inducing potential of 10^8 m^2/s^2 at 10^7 m.

the free surface and the solid-fluid interfaces effectively control the solutions within the mantle and the inner core. The response at the surface (except at periods very near an undertone period) is not critically affected by the increasing inaccuracy of the solution throughout the fluid core as longer periods are considered, even when large propagation steps are used in the fluid core (Appendix G).

The surface response of the Earth to a tidal potential is usually represented by Love numbers and the stability of the solution in the mantle implies that the Love numbers obtained from a calculation may be more reliable than would be indicated by the behaviour of the solutions within the fluid region. The Love numbers were calculated with both 'propagation truncation' levels and the resulting Love numbers agree to better than 0.1% up to a period of 12 hours although the solutions for the radial stress within the fluid region at this period are drastically different. These are compared in Table 2.

I have accepted this evidence as justification for retaining only the modes included in the 'propagation truncation' level 3 solutions for the initial calculation of Love numbers in the period range from 1 hour to 15 hours. These solutions contain the spheroidal responses of degrees 2 and 4 and the torsional responses of degrees 3 and 5 (all responses being of order 2 so that the degree 0 spheroidal and the degree 1 torsional solutions are identically zero). These Love numbers are tabulated (Table 3) and are plotted (Figure 26).

The results show evidence of the fundamental spheroidal oscillation and of undertones, the 'blips' in the variation of the Love numbers.

TABLE 2

COMPARISON OF THE LOVE NUMBERS OBTAINED WITH 'PROPAGATION TRUNCATION' LEVELS OF 3 AND 4

Period (hours)	LEVEL = 3			LEVEL = 4		
	h	k	ℓ	h	k	ℓ
1.00	2.4260	1.1573	.1229	2.4260	1.1573	.1229
3.00	.6572	.3221	.0853	.6572	.3221	.0853
5.00	.6246	.3067	.0843	.6246	.3067	.0843
7.00	.6192	.3035	.0839	.6192	.3035	.0839
9.00	.6144	.3018	.0840	.6144	.3018	.0840
10.00	.6120	.3012	.0842	.6121	.3012	.0842
11.00	.6139	.3014	.0839	.6139	.3014	.0839
12.00	.6132	.3011	.0840	.6130	.3011	.0840

'Elimination truncation' level = 14 for both cases above.

TABLE 3

VARIATION OF THE LOVE NUMBERS (n = 2, m = 2) WITH PERIOD

('Propagation truncation' level = 3 and

'Elimination truncation' level = 14)

PERIOD			LOVE NUMBERS		
h	m	min	h	k	ℓ
1	00	60	2.4260	1.1573	.1229
1	20	80	1.0264	.4268	.1229
1	40	100	.8163	.3974	.0904
2	00	120	.7362	.3595	.0879
2	20	140	.6958	.3404	.0866
2	40	160	.6722	.3292	.0858
3	00	180	.6572	.3221	.0853
3	20	200	.6470	.3172	.0850
3	40	220	.6397	.3138	.0848
4	00	240	.6343	.3113	.0846
4	20	260	.6303	.3094	.0845
4	40	280	.6271	.3079	.0844
5	00	300	.6246	.3067	.0843
5	20	320	.6226	.3058	.0843
5	40	340	.6208	.3050	.0842
6	00	360	.6192	.3043	.0842
6	20	380	.6175	.3037	.0843
6	40	400	.6083	.3021	.0851
7	00	420	.6192	.3035	.0839
7	20	440	.6180	.3031	.0839
7	40	460	.6166	.3027	.0840
8	00	480	.6159	.3025	.0840
8	20	500	.6154	.3023	.0840
8	40	520	.6148	.3020	.0840

TABLE 3, continued

PERIOD			LOVE NUMBERS		
h	m	min	h	k	ℓ
9	00	540	.6144	.3018	.0840
9	20	560	.6140	.3017	.0840
9	40	580	.6134	.3015	.0841
10	00	600	.6120	.3012	.0842
10	20	620	.6182	.3023	.0836
10	40	640	.6145	.3015	.0838
11	00	660	.6139	.3014	.0839
11	20	680	.6136	.3013	.0839
11	40	700	.6132	.3012	.0839
12	00	720	.6132	.3011	.0840
12	20	740	.6129	.3010	.0840
12	40	760	.6123	.3009	.0840
13	00	780	.6143	.3013	.0839
13	20	800	.6125	.3009	.0840
13	40	820	.6126	.3008	.0840
14	00	840	.6125	.3008	.0840
14	20	860	.6116	.3006	.0841
14	50	880	.6121	.3007	.0840
15	00	900	.6117	.3006	.0841

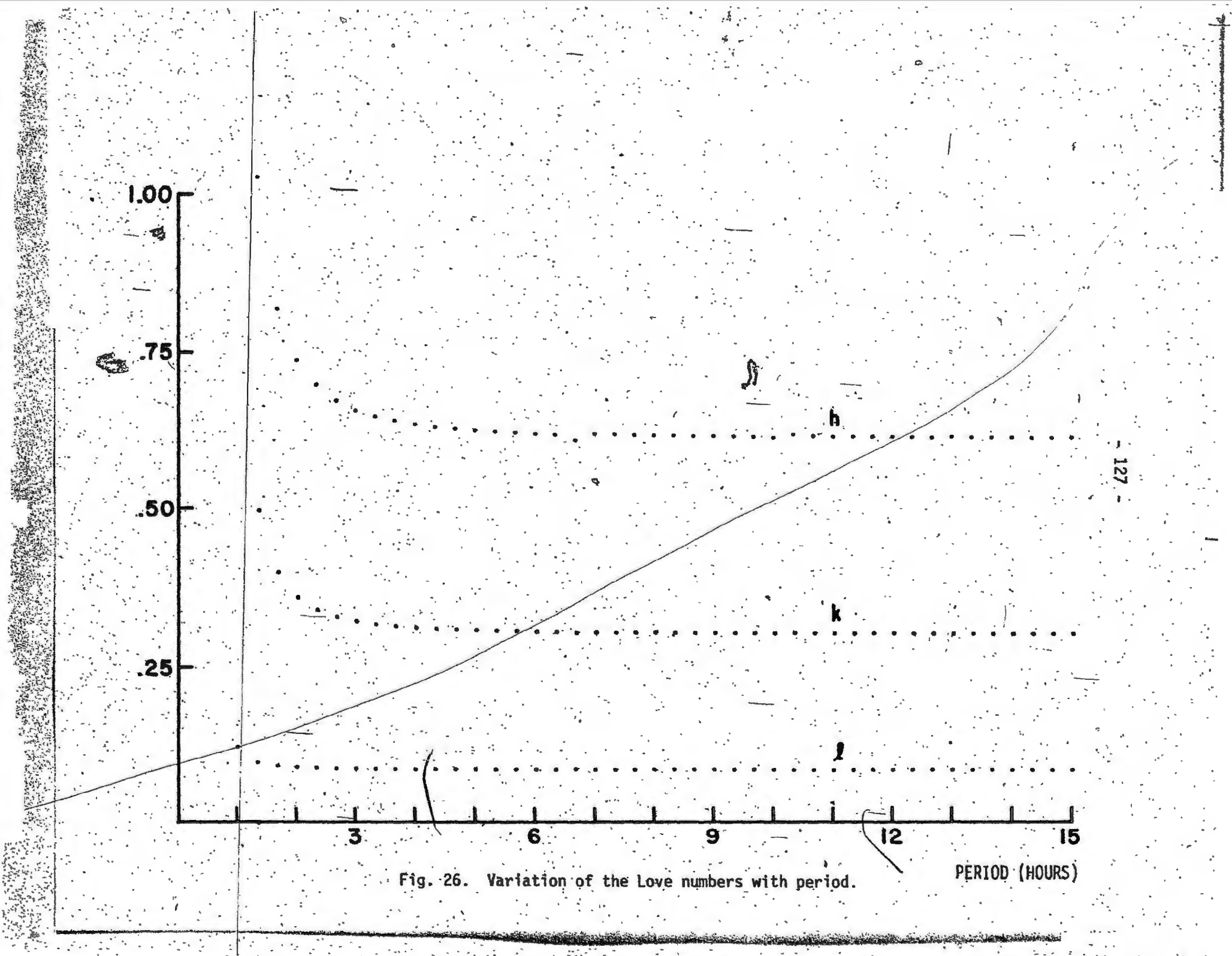

Fig. 26. Variation of the Love numbers with period.

By calculating the Love numbers at a finer period spacing and by examining the determinant obtained when the boundary conditions at the surface are applied, the first two undertones are found to have periods of $6^h43^m.51$ and $10^h14^m.10$ (or $403^m.51$ and $614^m.10$). These are compared with the results of Pekeris & Accad (1972), Smylie (1974) and Crossley (1975b) in the following table:

TABLE 4

UNDERTONE PERIODS FOR SUB-ADIABATIC FLUID CORES (HR)

	1st undertone	2nd undertone	3rd undertone
Pekeris & Accad	7.3515	11.6735	16.0187
Smylie (1)	7.4524	12.4716	17.5474
Smylie (2)	6.7598	10.5285	13.8070
Crossley	6.593	9.886	12.357
Pedersen	6.7252	10.2350	

The Earth model used in this study was tabulated by Smylie (1974) and has been used by Smylie and by Crossley in the determinations tabled above. Pekeris & Accad had introduced the use of the sub-adiabatic fluid condition for the core but their model differs from that used in this study by the absence of a solid inner core. Smylie (1974) attributes the difference between his results (1), obtained by neglecting rotational effects, and the results of Pekeris & Accad as 'presumably because of the presence of the solid inner core in the Earth model used in this study'. The second of Smylie's calculations does take into account the Coriolis

self-coupling term and Crossley's determinations also include the torsional motions (y_7^3) and the torsional shear stress (y_8^3). The inclusion of the torsional mode in the solution is equivalent to carrying a 'propagation truncation' level of 2 (and an 'elimination truncation' level of 2 as well) throughout the Earth. My results have been obtained with the retention of a 'propagation truncation' level of 3 and an 'elimination truncation' level of 14 throughout the Earth. I have also retained the relatively minor modification of the centrifugal couplings in the full rotational effects (Appendix G).

The variation of the Love numbers for n = 2, m = 2 with period near the undertone periods is shown in Figure 27.

The only forced tide with a period significantly less than 12 hours for which observational data is available is the terdiurnal tide with a period of 8.279 hours (Melchior & Venedikov, 1968). The driving potential for this Earth tide is of degree and order 3 (n = 3, m = 3). I have calculated the response at this period for two Earth models, one with a sub-adiabatic fluid core (Smylie, 1974) and for an adiabatic, Adams-Williamson fluid core (Wang, 1971, except for a small modification for the Earth's crust). The resulting stresses, displacements and potentials are shown in Figures 28 and 29.

For this tide I obtain the following Love numbers:

	sub-adiabatic	adiabatic
h_3	0.2932	0.2921
k_3	0.0933	0.0935
ℓ_3	0.0143	0.0156

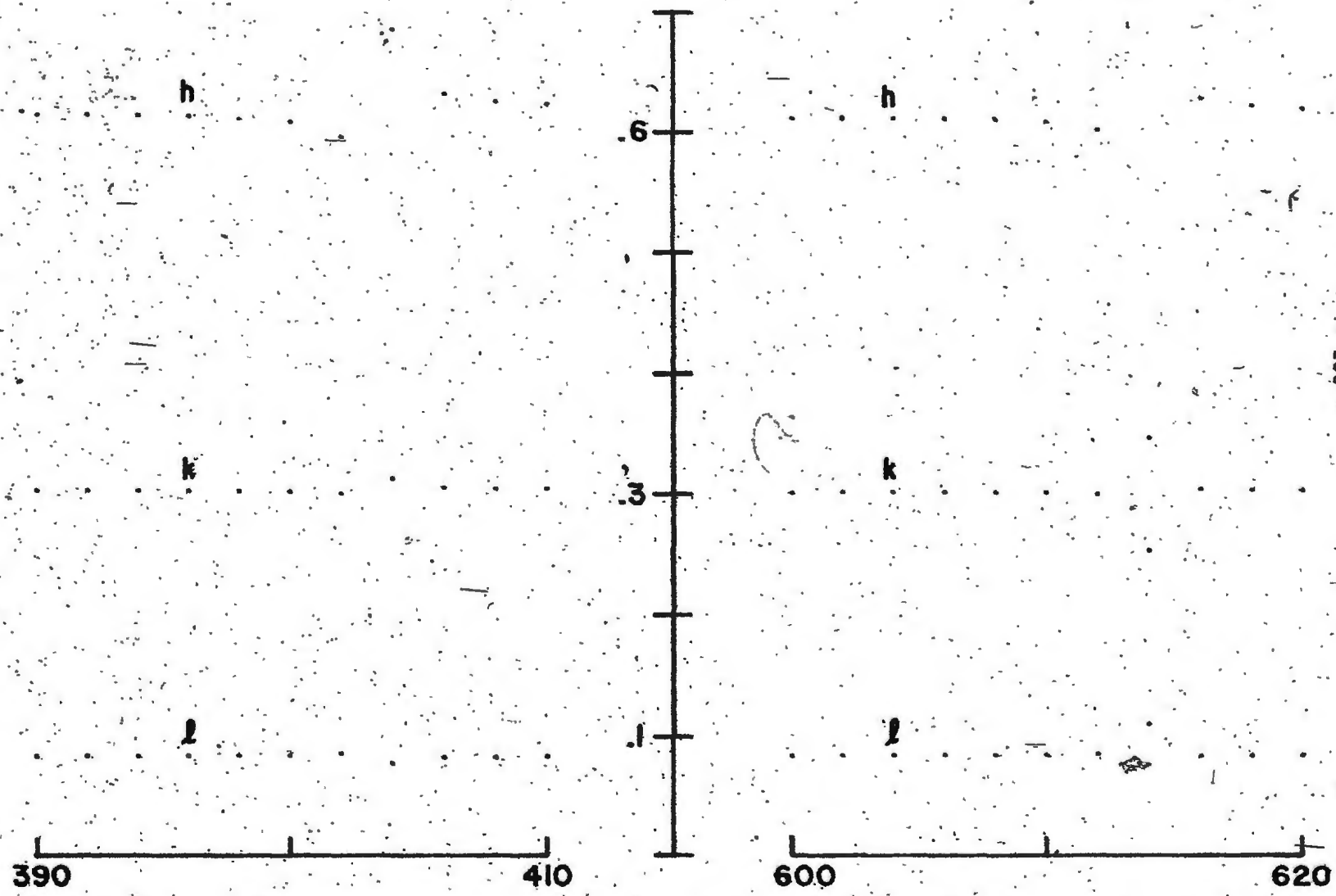

Fig. 27. Variation of the Love numbers near undertone periods.

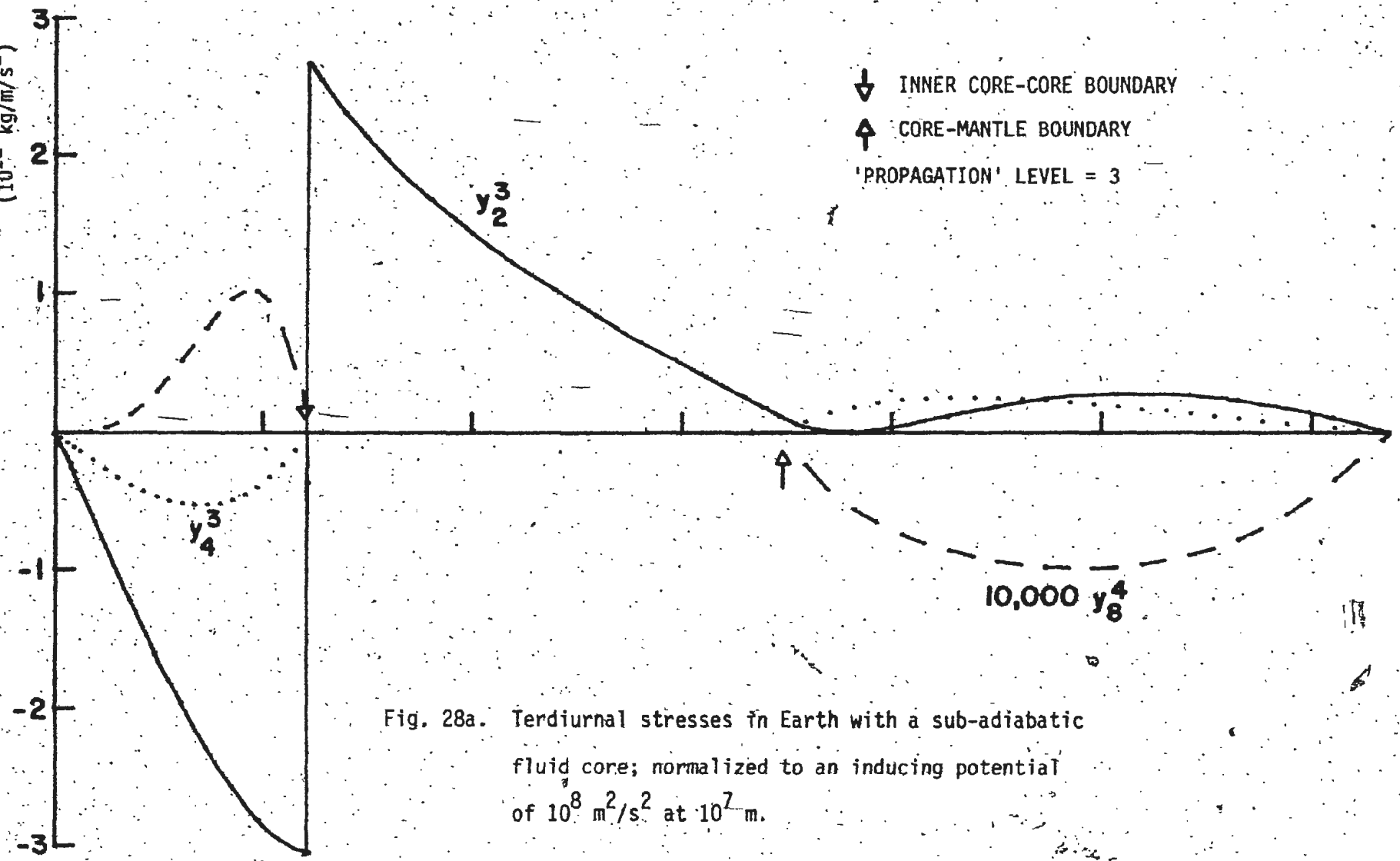

Fig. 28a. Terdiurnal stresses in Earth with a sub-adiabatic fluid core; normalized to an inducing potential of 10^8 m^2/s^2 at 10^7 m.

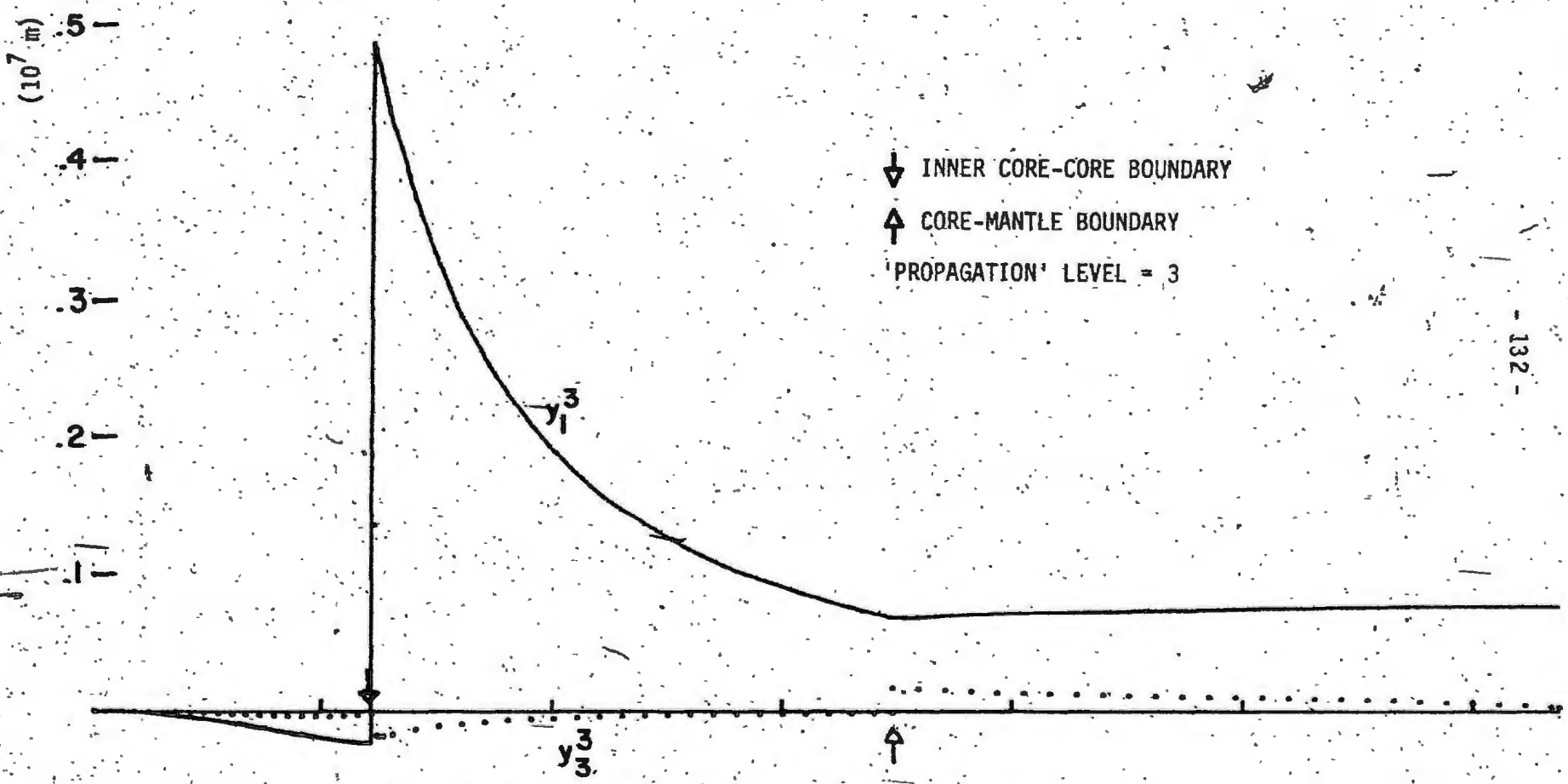

Fig. 28b. Spheroidal displacements for terdiurnal tide sub-adiabatic fluid core; normalized to an inducing potential of 10^8 m^2/s^2 at 10^7 m.

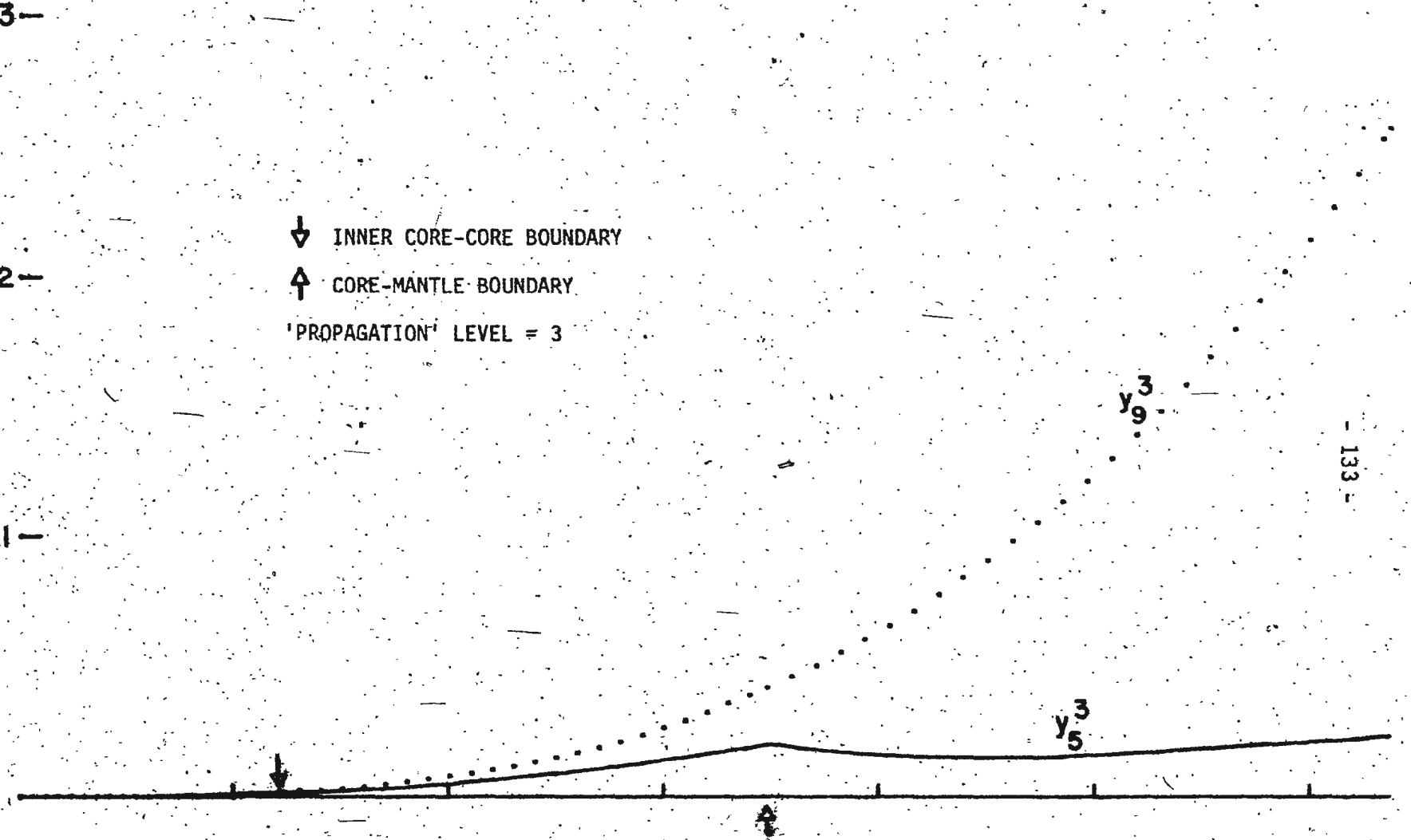

Fig. 28c. Potentials for terdiurnal tide sub-adiabatic fluid core; normalized to an inducing potential of $10^8\ m^2/s^2$ at 10^7 m.

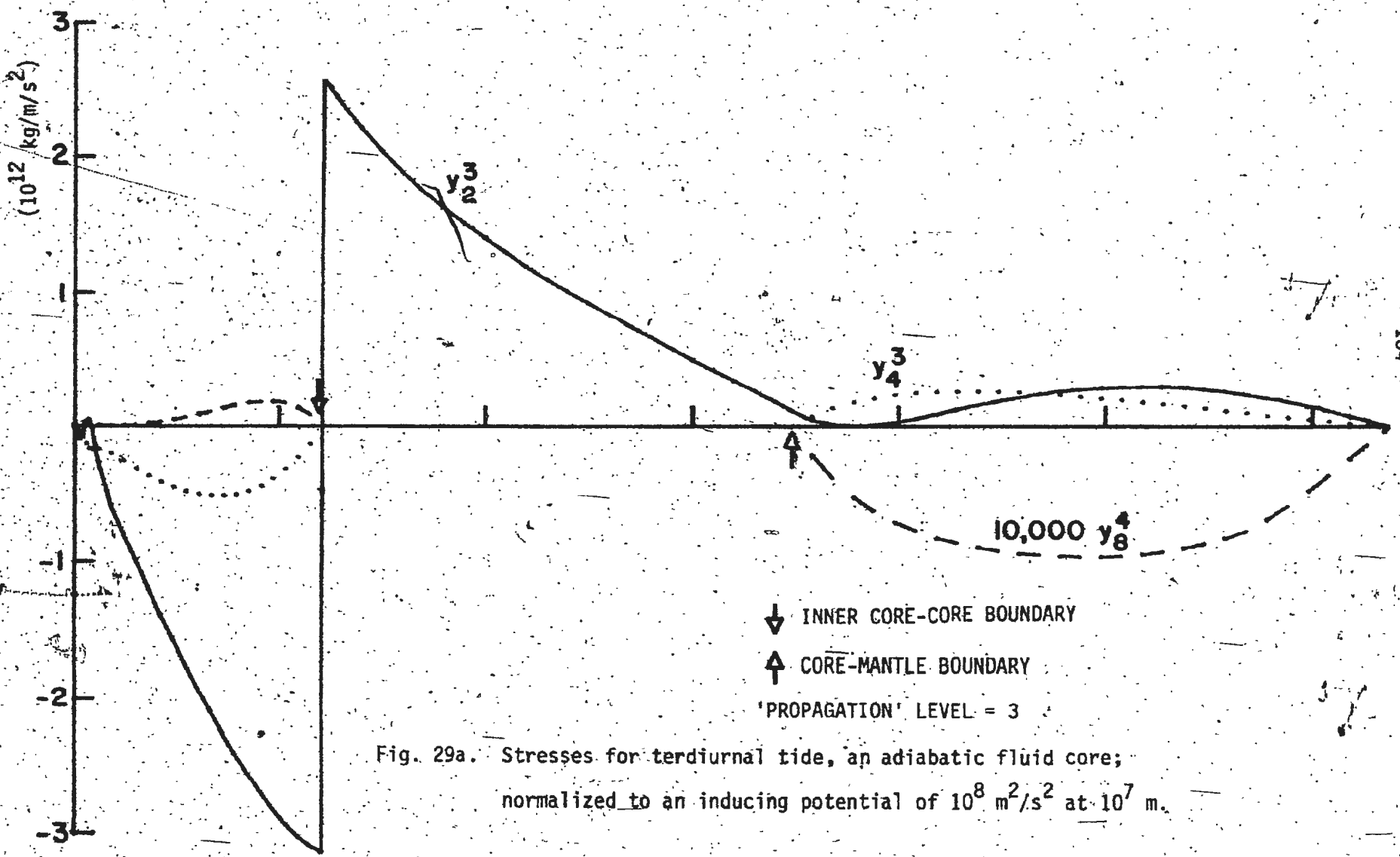

Fig. 29a. Stresses for terdiurnal tide, an adiabatic fluid core; normalized to an inducing potential of 10^8 m^2/s^2 at 10^7 m.

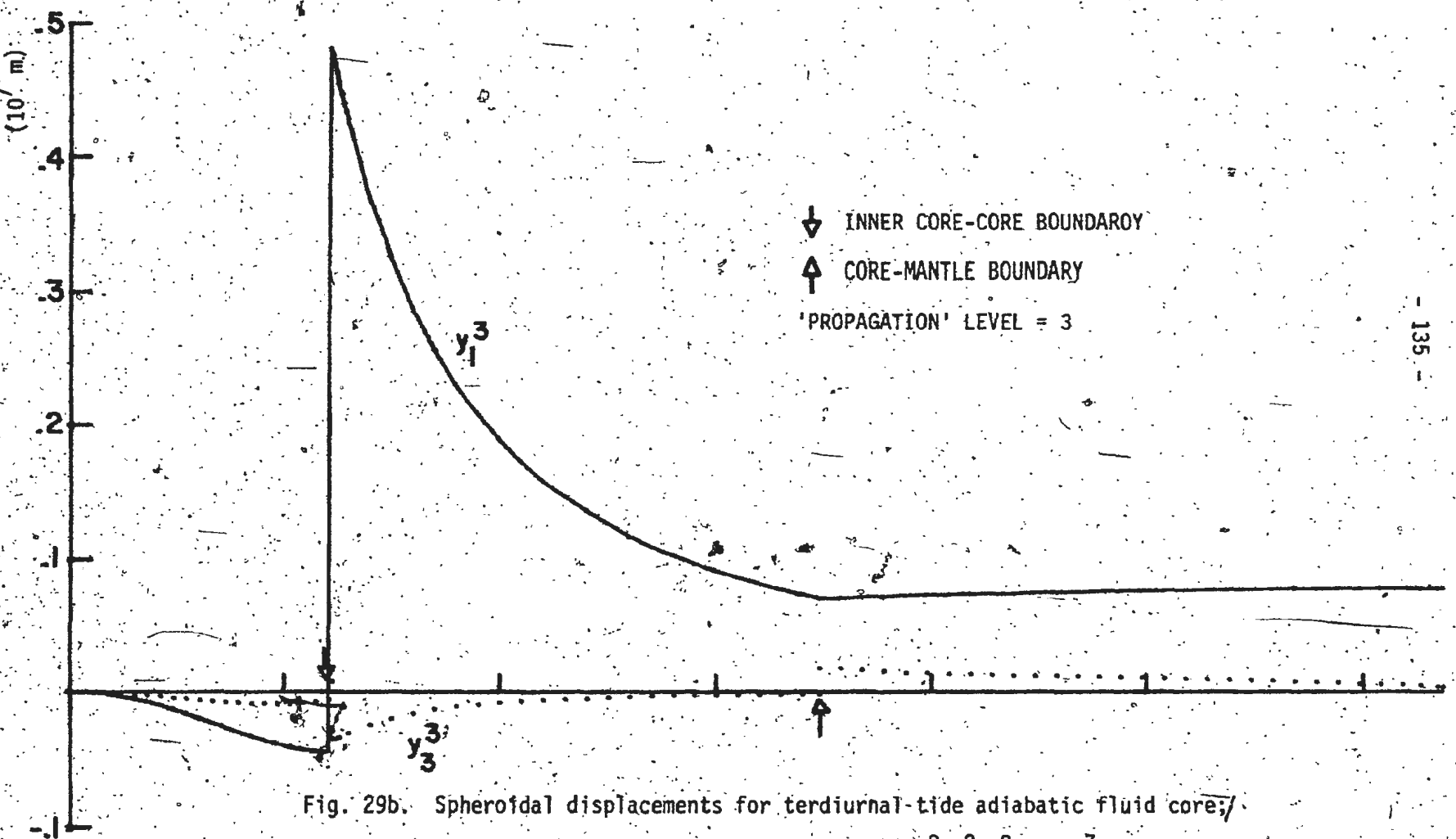

Fig. 29b. Spheroidal displacements for terdiurnal-tide adiabatic fluid core; normalized to an inducing potential of 10^8 m^2/s^2 at 10^7 m.

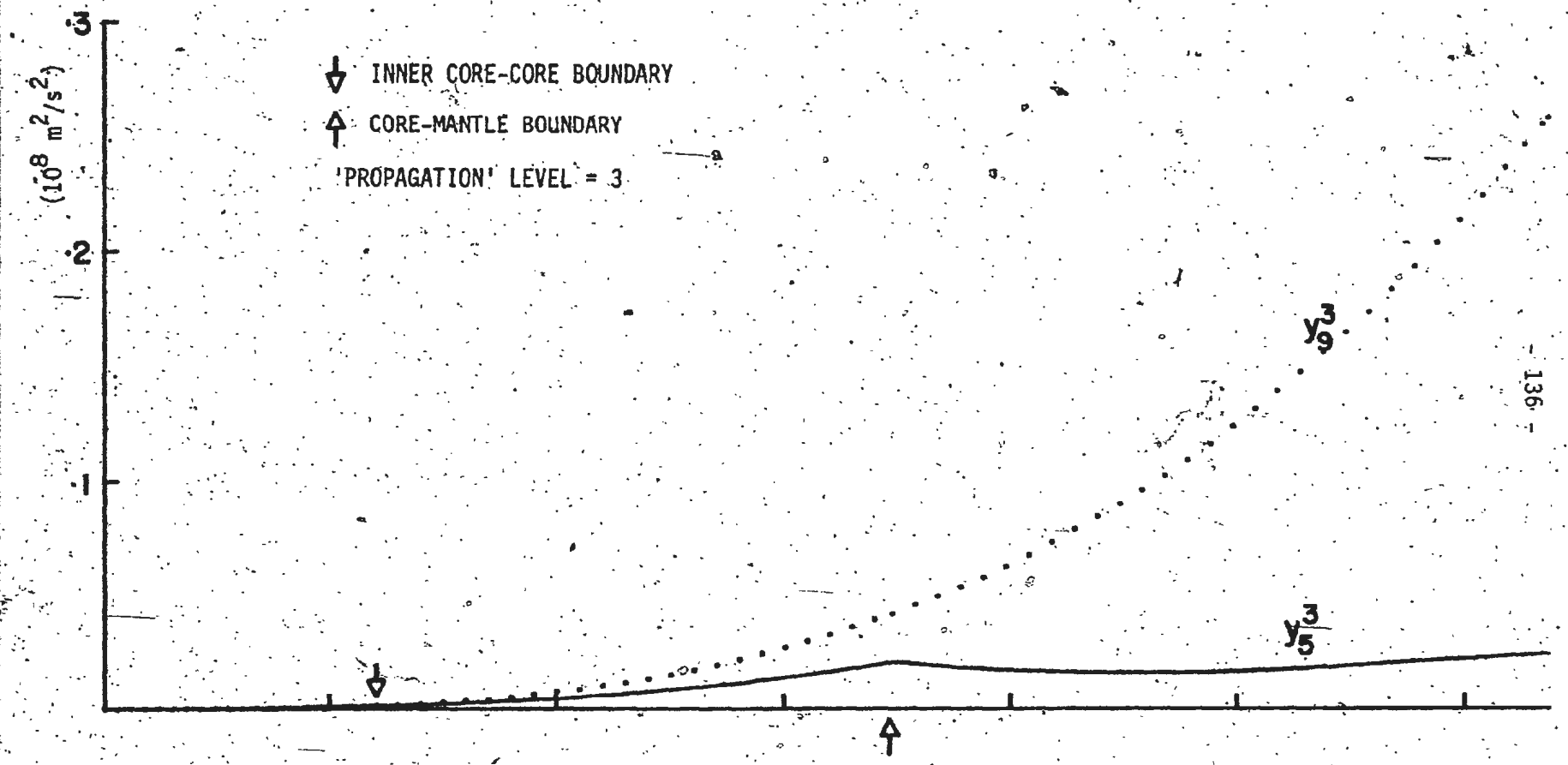

Fig. 29c. Terdiurnal tide adiabatic fluid core; normalized to an inducing potential of $10^8\ m^2/s^2$ at 10^7 m.

Love numbers have been previously obtained with theoretical calculations by Molodenskii & Kramer (1961), Takeuchi et al. (1962), Longman (1963, 1966) and Bodri (1974).

In the theoretically derived Love numbers obtained for the terdiurnal tide (tabled below) the other authors have used a static, not a dynamic, theory. Takeuchi et al. have modelled the fluid core as homogeneous whereas the other authors have adopted an adiabatic, Adams-Williamson density distribution. The two results quoted for Bodri are for two models of the mantle, B_1 and B_2, derived by Bullen & Haddon (1967).

TABLE 5

LOVE NUMBERS FOR THE TERDIURNAL TIDE

	h_3	k_3	ℓ_3
Molodenskii & Kramer	.294	.096	.013
Takeuchi et al.	.274	.083	.010
Longman	.290	.093	.014
Bodri (B_1)	.299	.097	.015
Bodri (B_2)	.298	.097	.015
Pedersen ($\beta = 0$)	.292	.094	.016
Pedersen ($\beta = -0.2$)	.293	.093	.014

Melchior & Venedikov (1968) report the observationally determined means (both a simple arithmetic mean and a weighted mean) for these Love numbers as

	Weighted Mean	Arithmetic Mean
h_3	.2220 ± .0376	.2704
k_3	.0572 ± .0261	.0964

Melchior & Venedikov state that the arithmetic mean may be the more reliable of the two means quoted above as the weighting scheme used did not take into account the possible systematic errors of each instrument; however it is clear that more observational data must be obtained for a more precise determination of these Love numbers.

CHAPTER 4

DISCUSSION AND CONCLUSIONS

The major advance of this study over the results of previous studies is the full inclusion of the direct effects of rotation. The indirect effect, the ellipticity of the Earth, has not been considered here but has been theoretically investigated by Smith (1974). Retention of the rotation in the development of the Earth's response leads to the excitation of spheroidal modes other than that corresponding to the degree of the harmonic forcing potential. When the density distribution in the fluid core is sub-adiabatic, undertones also exist and the undertone periods are modified greatly because of the Earth's rotation. Smylie (1974) has shown that retention of only the Coriolis self-coupling will lower all undertone periods for the degree 2, order 2 response below 36 hours and Crossley (1975b) has found indications that retaining all Coriolis couplings in the fluid will reduce all undertone periods below 12 hours. This is substantiated by the results of this thesis through the growing deterioration of the solutions obtained as the period approaches the semidiurnal in contrast to the agreement between the solutions obtained here and those of Pekeris & Accad (1972) at low periods. Except for the tidal periods very near an undertone, the Love numbers are for all practical purposes essentially insensitive to core stratification and the associated coupling. The variations in the Love numbers with period predicted in this thesis are below the present detection level (Lambeck et al., 1974).

The Love numbers obtained for the terdiurnal tide are in agreement with the results of previous calculations and with the admittedly poor observational data. As my results take the rotational effects into account, they are an improvement over the previous calculations. However the Love numbers are not very sensitive to the core model.

The final contribution of this study has been the indication of two undertone periods which will exist for an Earth with a fluid core where the density distribution is sub-adiabatic with the stability factor considered in this study. Although it is not known whether or not the fluid core is sub-adiabatic (throughout or in part) further study would delineate the spectra of undertone periods that could be expected for different sub-adiabatic fluid cores. Smylie is initiating at present an experimental search for these undertone periods and in the event that they are observed they will provide a significant constraint upon future Earth models. First, the existence of undertones would prove that at least a portion of the fluid core was sub-adiabatic and furthermore, since the location of the undertone periods is highly model dependent, would allow tighter constraints to be put upon the density profile; in order to uniquely determine the density distribution it would be necessary to know all the undertone periods, but even a partial knowledge would allow a more accurate representation of the structure of the fluid core.

REFERENCES

Alterman, Z., Jarosch, H. & Pekeris, C. L., 1959. Oscillations of the Earth, Proc. Roy Soc., A, 252, 80.

Arfken, G., 1970. Mathematical Methods for Physicists, 2nd edition, Academic Press, New York.

Backus, G., 1958. A class of self-sustaining dissipative spherical dynamos, Ann. Phys., 4, 381.

Bodri, B., 1974. Influence of viscosity on the phase of Earth tides, Phys. Earth Planet. Interiors, 9, 141.

Bullen, K. E. & Haddon, R. A. W., 1967. Earth models based on compressibility theory, Phys. Earth Planet. Interiors, 1, 1.

Crossley, D. J., 1975a. The free-oscillation equations at the centre of the Earth, Geophys. J. R. astr. Soc., 41, 153

Crossley, D. J., 1975b. Core undertones with rotation, Geophys. J. R. astr. Soc., 42, in press.

Crossley, D. J. & Gubbins, D., 1975. Static deformation of the Earth's liquid core, Geophys. Res. Letters, 2, 1.

Herglotz, G., 1905. Zeitschr. f. Math. u. Phys., Bd. 52.

Hoskins, L. M. 1920. The strain of a gravitating sphere of variable density and elasticity, Trans Am. math. Soc., 21, 1.

Jeffreys, H., 1926. The rigidity of the Earth's central core, Mon. Not. R. astr. Soc., Geophys. Suppl., 1, 371.

Jeffreys, H. & Vicente, R. O., 1957a. The theory of nutation and the variation of latitude, Mon. Not. R. astr. Soc., 117, 142.

Jeffreys, H. & Vicente, R. O., 1957b. The theory of nutation and the variation of latitude: the Roche model core, Mon. Not. R. astr. Soc., 117, 162.

Kakuta, C., 1970. The effect of a compressible core on Molodensky's theory of Earth tides, Publ. Astr. Soc. Japan, 22, 199.

Kelvin, Lord, 1863. Dynamical problems regarding elastic spheroidal shells and spheroids of incompressible liquids, Phil. Trans. R. Soc. London, A, 153, 583.

Lambeck, K., Cazenave, A. & Balmino, G., 1974. Solid Earth and ocean tides estimated from satellite orbit analyses, Rev. Geophys. Sp. Phys., 12, 421.

Landisman, M., Sato, Y. & Nafe, J., 1965. Free vibrations of the Earth and the properties of its deep interior regions. Part I: density, Geophys. J. R. astr. Soc., 9, 439.

Longman, I. M., 1963. A Green's function for determining the deformation of the Earth under surface mass loads, 2, J. Geophys. Res., 68, 485.

Longman, I. M., 1966. Computation of Love numbers and load deformation coefficients for a model Earth, Geophys. J. R. astr. Soc., 11, 133.

Love, A. E. H., 1909. The yielding of the Earth to disturbing forces, Proc. R. Soc. London, 82, 73.

Melchior, P. & Venedikov, A. P., 1968. Derivation of the wave M_3 ($8^h.279$) from the periodic tidal deformations of the Earth, Commun. Obs. Roy. Belgique, Ser. Geophys., 89, 363.

Molodenskii, M. S., 1961. The theory of nutation and diurnal Earth tides, Obs. Roy. Belgique, Ser. Geophys., 58, 25.

Molodenskii, M. S. & Kramer, M. V., 1961. Marées terrestres et nutation de la Terre, Yz. vo. Acc. des Sc. URSS.

Pedersen, G. P. H., 1967. The effect of the fluid core on Earth tides, M.Sc. thesis, University of Waterloo, Ontario, Canada.

Pekeris, C. L. & Accad, Y., 1972. Dynamics of the liquid core of the Earth, Phil. Trans. Roy. Soc., A, 273, 237.

Smith, M. L., 1974. The scalar equations of infinitesimal elastic-gravitational motion for a rotating, slightly elliptical Earth, Geophys. J. R. astr. Soc., 37, 491.

Smylie, D. E. & Mansinha, L., 1971. The elasticity theory of dislocations in real Earth models and changes in the rotation of the Earth, Geophys. J. R. astr. Soc., 23, 329.

Smylie, D. E., 1974. Dynamics of the outer core, Veroff. Zentralinst. Phys. Erde, Akad. Wiss, D. D. R., 30, 91.

Spain, B., 1960. Tensor Calculus, 3rd edition, Oliver and Boyd, London.

Takeuchi, H., 1950. On the Earth tides of the compressible Earth of variable density and elasticity, Trans. Am. Geophys. U., 31, 651.

Takeuchi, H., Sato, M. & Kobayashi, N., 1962. Statistical deformations and free oscillations of a model Earth, J. Geophys. Res., 67, 1141.

Wang, C.-Y., 1972. A simple Earth model, J. Geophys. Res., 77, 4318.

APPENDIX A

EXTRACTION OF THE COMPONENT EQUATIONS FOR THE SOLID REGIONS

1. Derivation of the Stress Force

In a curvilinear, orthogonal coordinate system (ξ , η , and ϕ) with scale factors h_ξ , h_η and h_ϕ the physical components of the strain tensor are

$$e_{\xi\xi} = \frac{1}{h_\xi}\left[\frac{\partial u_\xi}{\partial \xi} + \frac{u_\eta}{h_\eta}\frac{\partial h_\xi}{\partial \eta} + \frac{u_\phi}{h_\phi}\frac{\partial h_\xi}{\partial \phi}\right],$$

$$e_{\xi\eta} = e_{\eta\xi} = \frac{1}{2}\left[\frac{h_\xi}{h_\eta}\frac{\partial}{\partial \eta}\left(\frac{u_\xi}{h_\xi}\right) + \frac{h_\eta}{h_\xi}\frac{\partial}{\partial \xi}\left(\frac{u_\eta}{h_\eta}\right)\right]$$

with cyclic interchanges giving the other six coefficients (Spain, 1960, § 62).

For a spherically symmetric geometry the obvious choice is spherical polar coordinates r, θ and ϕ with scale factors 1, r and $r\sin\theta$. The strain tensor components are specifically (Love, 1909)

$$e_{rr} = \frac{\partial u_r}{\partial r}\ , \quad e_{\theta\theta} = \frac{1}{r}\left[\frac{\partial u_\theta}{\partial \theta} + u_r\right],$$

$$e_{\phi\phi} = \frac{1}{r\sin\theta}\left[\frac{\partial u_\phi}{\partial \phi} + \sin\theta\, u_r + \cos\theta\, u_\theta\right],$$

$$e_{r\theta} = e_{\theta r} = \frac{1}{2}\left[\frac{1}{r}\frac{\partial u_r}{\partial \theta} + \frac{\partial u_\theta}{\partial r} - \frac{u_\theta}{r}\right],$$

$$e_{r\phi} = e_{\phi r} = \frac{1}{2}\left[\frac{1}{r\sin\theta}\frac{\partial u_r}{\partial \phi} + \frac{\partial u_\phi}{\partial r} - \frac{u_\phi}{r}\right],$$

$$e_{\theta\phi} = e_{\phi\theta} = \frac{1}{2r}\left[\frac{1}{\sin\theta}\frac{\partial u_\theta}{\partial \phi} + \frac{\partial u_\phi}{\partial \theta} - \cot\theta\, u_\phi\right].$$

The stress and strain tensors for a Hookean body are related by

$$\tilde{\tau} = \lambda\Delta\,\tilde{I} + 2\mu\tilde{e} \quad .$$

The physical components of the body force equivalent, $\vec{f} = \vec{\nabla}\cdot\tilde{\tau}$, in orthogonal curvilinear coordinates, are therefore given by

$$f_\xi = \frac{1}{h_\xi h_\eta h_\phi}\left\{\frac{\partial}{\partial\xi}\left[h_\eta h_\phi \tau_{\xi\xi}\right] + \frac{1}{h_\xi}\frac{\partial}{\partial\eta}\left[h_\xi^2 h_\phi \tau_{\xi\eta}\right]\right.$$

$$\left. + \frac{1}{h_\xi}\frac{\partial}{\partial\phi}\left[h_\xi^2 h_\eta \tau_{\xi\phi}\right] - h_\phi \tau_{\eta\eta}\frac{\partial h_\eta}{\partial\xi} - h_\eta \tau_{\phi\phi}\frac{\partial h_\phi}{\partial\xi}\right\}$$

(with cyclic interchanges producing the other two components). For spherical polar coordinates this is

$$f_r = \frac{\partial}{\partial r}(\lambda\Delta) + \frac{1}{r^2}\frac{\partial}{\partial r}\left(r^2 2\mu e_{rr}\right) - \frac{2\mu}{r}\left[e_{\theta\theta} + e_{\phi\phi}\right]$$
$$+ \frac{1}{r\sin\theta}\left[\frac{\partial}{\partial\theta}\left(\sin\theta\, 2\mu e_{r\theta}\right) + \frac{\partial}{\partial\phi}\left(2\mu e_{r\phi}\right)\right],$$

$$f_\theta = \frac{1}{r}\frac{\partial}{\partial r}(\lambda\Delta) + \frac{1}{r\sin\theta}\frac{\partial}{\partial\theta}\left[\sin\theta\, 2\mu e_{\theta\theta}\right]$$
$$+ \frac{1}{r\sin\theta}\frac{\partial}{\partial\phi}\left[2\mu e_{\phi\theta}\right] + \frac{1}{r^3}\frac{\partial}{\partial r}\left[r^3 2\mu e_{r\theta}\right] - \frac{\cot\theta}{r}2\mu e_{\phi\phi},$$

$$f_\phi = \frac{1}{r\sin\theta}\frac{\partial}{\partial\phi}(\lambda\Delta) + \frac{1}{r\sin\theta}\frac{\partial}{\partial\phi}\left[2\mu e_{\phi\phi}\right]$$
$$+ \frac{1}{r^3}\frac{\partial}{\partial r}\left[r^3 2\mu e_{r\phi}\right] + \frac{1}{r\sin^2\theta}\frac{\partial}{\partial\theta}\left[\sin^2\theta\, 2\mu e_{\theta\phi}\right].$$

In terms of the spherical harmonic expansion chosen to represent the displacement field;

$$u_r = y_1 S$$

$$u_\theta = y_3 \frac{\partial S}{\partial \theta} + \frac{i y_7}{\sin\theta} \frac{\partial S}{\partial \phi}$$

$$u_\phi = \frac{y_3}{\sin\theta} \frac{\partial S}{\partial \phi} - i y_7 \frac{\partial S}{\partial \theta}$$

and with the consideration of spherical symmetry $(\lambda = \lambda(r), \mu = \mu(r))$ the radial component of the stress force is

$$f_r = \frac{\partial}{\partial r}[\lambda \Delta] + \frac{1}{r^2}\frac{d}{dr}\left[2\mu r^2 \frac{dy_1}{dr}\right] S$$

$$+ \mu \left[y_1 + r\frac{dy_3}{dr} - y_3 \right] \nabla^2 S$$

$$- 2\mu \left[\frac{2y_1}{r^2} S + y_3 \nabla^2 S \right]$$

$$= \frac{d}{dr}\left[(\lambda+2\mu)\frac{dy_1}{dr} + \frac{2\lambda y_1}{r} - \frac{n(n+1)y_3}{r} \right] S$$

$$+ \frac{2\mu}{r}\left[2\frac{dy_1}{dr} - \frac{2y_1}{r} + \frac{n(n+1)y_3}{r} \right] S$$

$$- \frac{n(n+1)}{r}\mu \left[\frac{dy_3}{dr} + \frac{y_1}{r} - \frac{y_3}{r} \right] S .$$

Similarly the meridional component simplifies to

$$f_\theta = \left\{ \frac{\lambda}{r}\left[\frac{dy_1}{dr} + \frac{2y_1}{r} - \frac{n(n+1)}{r}y_3\right] + \frac{2\mu}{r^2}y_1 \right.$$

$$- \frac{2\mu}{r^2}(n^2+n-1)y_3 + \frac{3\mu}{r}\left(\frac{dy_3}{dr} + \frac{y_4}{r} - \frac{y_3}{r}\right)$$

$$\left. + \frac{d}{dr}\left[\mu\left(\frac{dy_3}{dr} + \frac{y_4}{r} - \frac{y_3}{r}\right)\right]\right\} \frac{\partial S}{\partial \theta}$$

$$+ \left\{ \frac{d}{dr}\left[\mu\left(\frac{dy_4}{dr} - \frac{y_4}{r}\right)\right] + \frac{3\mu}{r}\left[\frac{dy_4}{dr} - \frac{y_4}{r}\right] \right.$$

$$\left. - \frac{(n^2+n-2)}{r^2}y_7 \right\} \frac{i}{\sin\theta}\frac{\partial S}{\partial \phi}$$

Finally the azimuthal component reduces to

$$f_\phi = \left\{ \frac{\lambda}{r}\left[\frac{dy_1}{dr} + \frac{2y_1}{r} - \frac{n(n+1)}{r}y_3\right] + \frac{2\mu}{r^2}y_1 \right.$$

$$- \frac{2\mu}{r^2}(n^2+n-1)y_3 + \frac{3\mu}{r}\left(\frac{dy_3}{dr} + \frac{y_4}{r} - \frac{y_3}{r}\right)$$

$$\left. + \frac{d}{dr}\left[\mu\left(\frac{dy_3}{dr} + \frac{y_4}{r} - \frac{y_3}{r}\right)\right]\right\} \frac{1}{\sin\theta}\frac{\partial S}{\partial \phi}$$

$$+ \left\{ \frac{d}{dr}\left[\mu\left(\frac{dy_4}{dr} - \frac{y_4}{r}\right)\right] + \frac{3\mu}{r}\left[\frac{dy_4}{dr} - \frac{y_4}{r}\right] \right.$$

$$\left. - \frac{(n^2+n-2)}{r^2}y_7 \right\} i \frac{\partial S}{\partial \theta}$$

2. Extraction of the Spherical Harmonic Components of the Displacement Equations

The full vector displacement equation is written on page 52 and the angular velocity vector $\vec{\Omega}$ is put into spherical polar form as

$$\vec{\Omega} = \Omega\hat{k} = \Omega\left[\cos\theta\,\hat{r} - \sin\theta\,\hat{\theta}\right].$$

Hence

$$\vec{\Omega}\times\dot{\vec{u}} =$$

$$\Omega\left[\dot{y}_3\cos\theta\,\vec{r}\times\vec{\nabla}S + i\dot{y}_7\, r\cos\theta\,\vec{\nabla}S + \dot{y}_1\sin\theta\, S\,\hat{\phi}\right.$$

$$\left. - \dot{y}_3\frac{\partial S}{\partial\phi}\hat{r} + i\dot{y}_7\sin\theta\,\frac{\partial S}{\partial\phi}\hat{r}\right]$$

and

$$\vec{\Omega}\times(\vec{\Omega}\times\vec{r}) = -\Omega^2 r\left[\sin^2\theta\,\hat{r} + \sin\theta\cos\theta\,\hat{\theta}\right]$$

from which

$$-\vec{u}\cdot\vec{\Omega}\times(\vec{\Omega}\times\vec{r})$$

$$= \Omega^2 r\left[y_1\sin^2\theta\, S + y_3\sin\theta\cos\theta\,\frac{\partial S}{\partial\theta} + iy_7\cos\theta\,\frac{\partial S}{\partial\phi}\right].$$

Due to the assumption of spherical symmetry and to Poisson's equation for the gravitational field

$$\vec{\nabla}(\vec{u}\cdot\vec{g}_0) = -\frac{d}{dr}\left[y_1 g_0\right]\hat{r}\,S - y_1 g_0\vec{\nabla}S$$

$$= -\left[g_0\frac{dy_1}{dr} + \left(4\pi G\rho_0 - \frac{2g_0}{r}\right)y_1\right]\hat{r}\,S - y_1 g_0\vec{\nabla}S\,.$$

Using the above expansions and forming the scalar product of the displacement equation with $\hat{r}S'$ where $S' = S_k^l(\theta,\phi)$:

$$\rho_0 \ddot{y}_1 S S' - 2\rho_0 \Omega \dot{y}_3 \frac{\partial S}{\partial \phi} S' + 2\rho_0 i\Omega \dot{y}_2 \sin\theta \frac{\partial S}{\partial \theta} S'$$

$$= \left[\frac{dy_2}{dr} + \frac{4\mu}{\lambda+2\mu} \frac{y_2}{r} - \frac{4\mu k}{r^2} y_1 + \frac{2\mu k}{r^2} n(n+1) y_3 \right.$$

$$- \frac{n(n+1)}{r} y_4 + \rho_0 \frac{dy_5}{dr} + \frac{n}{r}\rho_0 y_5 - \rho_0 g_0 \frac{dy_1}{dr} - 4\pi G \rho_0^2 y_1$$

$$\left. + 2\frac{\rho_0 g_0}{r} y_1 + \frac{\rho_0 g_0}{\lambda+2\mu} \left\{ y_2 + \frac{4\mu y_1}{r} - 2\mu \frac{n(n+1)}{r} y_3 \right\} \right] S S'$$

$$+ \rho_0 \Omega^2 \left[\frac{d}{dr}(r y_1) \sin^2\theta \, S S' + \frac{d}{dr}(r y_3) \sin\theta \cos\theta \frac{\partial S}{\partial \theta} S' \right.$$

$$\left. + i \frac{d}{dr}(r y_2) \cos\theta \frac{\partial S}{\partial \phi} S' \right]$$

$$- \frac{\rho_0 \Omega^2}{\lambda+2\mu} \left[r y_2 + 4\mu y_1 - 2\mu n(n+1) y_3 \right] \sin^2\theta \, S S' .$$

Application of the definitions and relationships previously stated reduces the RHS of this to

$$\left[\frac{dy_2}{dr} + \frac{4\mu}{\lambda+2\mu}\frac{y_2}{r} - \frac{4\mu k}{r^2}y_1 + \frac{2\mu k}{r^2}n(n+1)y_3 - \frac{n(n+1)}{r}y_4\right.$$

$$\left. + \rho_0 y_6 + \frac{n}{r}\rho_0 y_5 + \frac{4\rho_0 g_0}{r}y_1 - n(n+1)\frac{\rho_0 g_0}{r}y_3\right] S S'$$

$$+ \rho_0 \Omega^2 \left\{\left[n(n+1)y_3 - y_1\right]\sin^2\theta\, S S' + i\left[\frac{r y_6}{\mu} + 2y_5\right]\cos\theta \frac{\partial S}{\partial \phi} S'\right.$$

$$\left. + \left[\frac{r y_4}{\mu} - y_1 + 2y_3\right]\sin\theta\cos\theta \frac{\partial S}{\partial \theta} S'\right\}.$$

Integrating over the entire solid angle and using the orthogonality of the spherical harmonics then gives (1.20) where coupling coefficients A_1, A_2, A_3 and A_4 have been introduced and are defined as

$$A_1^{kn} \equiv \frac{2k+1}{4\pi}(-1)^m \int \sin^2\theta\, S_n^m S_k^\ell \sin\theta\, d\theta\, d\phi$$

$$A_2^{kn} \equiv \frac{2k+1}{4\pi}(-1)^m \int \sin\theta\cos\theta \frac{\partial S_n^m}{\partial \theta} S_k^\ell \sin\theta\, d\theta\, d\phi$$

$$A_3^{kn} \equiv \frac{2k+1}{4\pi}(-1)^m \int \sin\theta \frac{\partial S_n^m}{\partial \theta} S_k^\ell \sin\theta\, d\theta\, d\phi$$

$$A_4^{kn} \equiv \frac{2k+1}{4\pi}(-1)^m \int \cos\theta\, S_n^m S_k^\ell \sin\theta\, d\theta\, d\phi .$$

In Appendix C I have shown the degrees n which will couple to a prescribed degree k and calculated the numerical value of these coefficients.

Returning to the displacement equation and forming the scalar product with the vector $r\vec{\nabla}S'$:

$$\rho_0 \ddot{y}_3 r^2 \vec{\nabla}S \cdot \vec{\nabla}S' - i\rho_0 \ddot{y}_7 r \vec{\nabla}S' \cdot \vec{r}\times\vec{\nabla}S$$

$$+ 2\rho_0\Omega \left\{ \dot{y}_3 \cos\theta\, r\vec{\nabla}S' \cdot \vec{r}\times\vec{\nabla}S + i\dot{y}_7 r^2 \cos\theta\, \vec{\nabla}S \cdot \vec{\nabla}S' \right.$$

$$\left. + \dot{y}_1 r S \hat{\phi} \cdot \vec{\nabla}S' \right\}$$

$$= \left\{ \frac{dy_4}{dr} + \frac{3y_4}{r} + \frac{2\mu k}{r^2} y_1 + \frac{\lambda}{\lambda+2\mu}\frac{y_2}{r} \right.$$

$$+ \frac{2\mu}{r^2} y_3 - \frac{\rho_0 g_0}{r} y_1 - n(n+1)\frac{4\mu}{r^2}\left(\frac{\lambda+\mu}{\lambda+2\mu}\right) y_3$$

$$\left. + \rho_0 y_5 + \rho_0 y_9 \right\} r^2 \vec{\nabla}S \cdot \vec{\nabla}S'$$

$$- i \left\{ \frac{dy_8}{dr} + \frac{3y_8}{r} - (n^2+n-2)\frac{\mu y_7}{r^2} \right\} r\vec{\nabla}S' \cdot \vec{r}\times\vec{\nabla}S \ .$$

The product of spheroidal and torsional vectors vanish when integrated over the entire solid angle, i.e.

$$r \int \vec{\nabla} S' \cdot \vec{r} \times \vec{\nabla} S \sin\theta \, d\theta d\phi = 0$$

I also obtain

$$\int \vec{\nabla} f \cdot \vec{\nabla} S' \, dV = k(k+1) \int r^{-2} f S' \, dV$$

by use of the divergence theorem and for $f = f(\theta, \phi)$

$$\int \vec{\nabla} f \cdot \vec{\nabla} S' \sin\theta \, d\theta d\phi = \frac{k(k+1)}{r^2} \int f S' \sin\theta \, d\theta \, d\phi.$$

Finally the integral

$$r \int \cos\theta \, \vec{\nabla} S' \cdot \vec{r} \times \vec{\nabla} S \sin\theta \, d\theta d\phi$$

reduces to

$$-im \int S S' \sin\theta \, d\theta d\phi.$$

Incorporating these results produces (1.21).

The additional coupling coefficients introduced here are defined as

$$B_1^{kn} \equiv \frac{2k+1}{4\pi} (-1)^m r^2 \int \cos\theta \, \vec{\nabla} S \cdot \vec{\nabla} S' \sin\theta \, d\theta \, d\phi$$

$$B_2^{kn} \equiv \frac{2k+1}{4\pi} (-1)^m \int \sin\theta \cos\theta \, S \frac{\partial S'}{\partial \theta} \sin\theta \, d\theta \, d\phi$$

and the selection rules and numerical values are derived in Appendix C.

Finally the torsional component of the displacement equation is extracted by forming the scalar product with the vector $\vec{r} \times \vec{\nabla} S'$;

$$-i\rho_0 \ddot{y}_7\, r^2 \vec{\nabla}S\cdot\vec{\nabla}S' + \rho_0 \ddot{y}_3\, r\vec{\nabla}S\cdot\vec{r}\times\vec{\nabla}S'$$

$$+2\rho_0\Omega\left\{\dot{y}_3\cos\theta\, r^2\vec{\nabla}S\cdot\vec{\nabla}S' + i\dot{y}_7 r\cos\theta\,\vec{\nabla}S\cdot\vec{r}\times\vec{\nabla}S'\right.$$

$$\left. + \dot{y}_1 \sin\theta\, S\,\hat{\phi}\cdot\vec{r}\times\vec{\nabla}S'\right\}$$

$$= \left\{\frac{dy_4}{dr} + \frac{3y_4}{r} + \left(\frac{2\mu k}{r^2} - \frac{\rho_0 g_0}{r}\right)y_1 + \frac{\lambda}{\lambda+2\mu}\frac{y_2}{r}\right.$$

$$+ \frac{2\mu}{r^2}\left\{1 - n(n+1)\left(\frac{\lambda+\mu}{\lambda+2\mu}\right)\right\}y_3 + \rho_0 y_5 + \rho_0 y_9\Big\} r\vec{\nabla}S\cdot\vec{r}\times\vec{\nabla}S'$$

$$-i\left\{\frac{dy_8}{dr} + \frac{3y_8}{r} - (n^2+n-2)\frac{\mu}{r^2}y_7\right\} r^2\vec{\nabla}S\cdot\vec{\nabla}S'$$

$$+\rho_0\Omega^2 r\vec{\nabla}\left[r y_1 \sin^2\theta\, S + r y_3 \sin\theta\cos\theta\frac{\partial S}{\partial\theta} + i r y_7\cos\theta\frac{\partial S}{\partial\phi}\right]\cdot\vec{r}\times\vec{\nabla}S'$$

$$-\frac{\rho_0\Omega^2}{\lambda+2\mu}\left[r y_2 + 4\mu y_1 - 2\mu n(n+1)y_3\right]\sin\theta\cos\theta\, S\,\hat{\theta}\cdot\vec{r}\times\vec{\nabla}S'.$$

Again the orthogonality of the spheroidal and torsional vectors cause some coefficients to vanish and the torsional component is reduced to (1.22).

The coupling coefficient introduced here is defined as

$$B_4^{kn} \equiv \frac{2k+1}{4\pi} (-1)^m \int \sin\theta \, S \frac{\partial S'}{\partial \theta} \sin\theta \, d\theta \, d\phi .$$

In elastic free oscillation theory the periods are sufficiently short and the Earth's rotation can be neglected for all but the most precise calculations. Then the interdependence of the spheroidal and the torsional modes vanish. Hence a spheroidal (e.g. tidal) excitation would excite a purely spheroidal response. However the more complete treatment derived here shows that the torsional motions are indeed excited through the agency of rotation even when the driving mechanism is purely spheroidal.

APPENDIX B

EXTRACTION OF THE COMPONENT EQUATIONS FOR THE FLUID REGION

Within the fluid the displacement equation is given by (1.25),

$$\ddot{\vec{u}} + 2\vec{\Omega}\times\dot{\vec{u}} = -\rho\Delta\left[\vec{g}_0 - \vec{\Omega}\times(\vec{\Omega}\times\vec{r})\right] + \vec{\nabla}\left[\frac{\lambda\Delta}{\rho_0} + \psi + \Phi + \vec{u}\cdot\vec{g}_0 - \vec{u}\cdot\vec{\Omega}\times(\vec{\Omega}\times\vec{r})\right],$$

and is expanded by use of the spherical harmonic representation to

$$\ddot{y}_1\hat{r}S + \ddot{y}_3 r\vec{\nabla}S - i\ddot{y}_7\vec{r}\times\vec{\nabla}S$$

$$+ 2\vec{\Omega}\times\left[\dot{y}_1\hat{r}S + \dot{y}_3 r\vec{\nabla}S - i\dot{y}_7\vec{r}\times\vec{\nabla}S\right]$$

$$= \frac{d}{dr}\left[z + y_5 + y_9 - g_0 y_1\right]\hat{r}S$$

$$+ \left[z + y_5 + y_9 - g_0 y_1\right]\vec{\nabla}S$$

$$+ \Omega^2\vec{\nabla}\left[r y_1 \sin^2\theta\, S + r y_3 \sin\theta\cos\theta\frac{\partial S}{\partial\theta} + i r y_7\cos\theta\frac{\partial S}{\partial\phi}\right]$$

$$+ \frac{\beta z}{V^2} g_0 \hat{r}S - \frac{\beta\Omega^2 r}{V^2}\left\{\sin^2\theta\,\hat{r} + \sin\theta\cos\theta\,\hat{\theta}\right\}S .$$

In a manner similar to that used to extract the components of the corresponding equation in the elastic solid regions, the scalar product with $\hat{r}S'$ gives

$$\ddot{y}_1 S S' - 2\Omega \dot{y}_3 \frac{\partial S}{\partial \phi} S' + 2i\Omega \dot{y}_1 \sin\theta \frac{\partial S}{\partial \theta} S'$$

$$= \frac{d}{dr}\left[Z + y_5 + y_6 - g_0 y_1 \right] S S' + \Omega^2 \frac{d}{dr}(r y_1) \sin^2\theta S S'$$

$$+ \Omega^2 \frac{d}{dr}(r y_3) \sin\theta \cos\theta \frac{\partial S}{\partial \theta} S' + i\Omega^2 \frac{d}{dr}(r y_4) \cos\theta \frac{\partial S}{\partial \phi} S'$$

$$+ \frac{\beta g_0}{V^2} Z S S' - \frac{\beta \Omega^2 r}{V^2} Z \sin^2\theta S S' .$$

Integrating over the entire solid angle:

$$\ddot{y}_1^k - 2im\Omega \dot{y}_3^k + 2i\Omega A_3^{kn} \dot{y}_7^n$$

$$= \frac{d}{dr}\left[Z^k + y_5^k + y_6^k - g_0 y_1^k \right] + \Omega^2 A_1^{kn} \frac{d}{dr}(r y_1^n)$$

$$+ \Omega^2 A_2^{kn} \frac{d}{dr}(r y_3^n) - m\Omega^2 A_4^{kn} \frac{d}{dr}(r y_7^n)$$

$$+ \frac{\beta g_0}{V^2} Z^k - \frac{\beta \Omega^2 r}{V^2} A_1^{kn} Z^n$$

which simplifies to (1.28). The coupling coefficients used here have been defined in Appendix A.

Secondly, the product of the displacement equation with $r\vec{\nabla}S'$ obtains

$$\ddot{y}_3 r^2 \vec{\nabla}S\cdot\vec{\nabla}S' - i\ddot{y}_7 \vec{r}\times\vec{\nabla}S\cdot r\vec{\nabla}S' + 2\Omega\dot{y}_3\cos\theta\, r\vec{\nabla}S'\cdot\vec{r}\times\vec{\nabla}S$$

$$+ 2i\Omega\dot{y}_7\cos\theta\, r^2\vec{\nabla}S\cdot\vec{\nabla}S' + 2\Omega y_1 rS\,\hat{\phi}\cdot\vec{\nabla}S'$$

$$= \left[z + y_5 + y_9 - g_0 y_1\right] r\vec{\nabla}S\cdot\vec{\nabla}S'$$

$$+\Omega^2 r^2\vec{\nabla}\left[y_1\sin^2\theta S + y_3\sin\theta\cos\theta\frac{\partial S}{\partial\theta} + iy_7\cos\theta\frac{\partial S}{\partial\phi}\right]\cdot\vec{\nabla}S'$$

$$-\frac{\beta\Omega^2 r^2}{V^2} z\sin\theta\cos\theta S\,\hat{\theta}\cdot\vec{\nabla}S' .$$

The orthogonality of the spherical harmonics then reduces this to (1.29).

This and the following constraint on the torsional motion are both analytic - not differential - conditions. The torsional component of the motion is recovered by using $\vec{r}\times\vec{\nabla}S'$;

$$-i\ddot{y}_7 r^2\vec{\nabla}S\cdot\vec{\nabla}S' + \ddot{y}_3 r\vec{\nabla}S\cdot\vec{r}\times\vec{\nabla}S'$$

$$+2\Omega r^2\left[\dot{y}_3\cos\theta\,\vec{\nabla}S\cdot\vec{\nabla}S' + i\dot{y}_7\cos\theta\,\vec{\nabla}S\cdot\hat{r}\times\vec{\nabla}S' + \dot{y}_1\sin\theta S\,\hat{\phi}\cdot\hat{r}\times\vec{\nabla}S'\right]$$

$$= \left[z + y_5 + y_9 - g_0 y_1\right]\vec{\nabla}S\cdot\vec{r}\times\vec{\nabla}S'$$

$$+\Omega^2 r^2\vec{\nabla}\left[y_1\sin^2\theta S + y_3\sin\theta\cos\theta\frac{\partial S}{\partial\theta} + iy_7\cos\theta\frac{\partial S}{\partial\phi}\right]\cdot\hat{r}\times\vec{\nabla}S'$$

$$-\frac{\beta\Omega^2 r}{V^2} z\sin\theta\cos\theta S\,\hat{\theta}\cdot\vec{r}\times\vec{\nabla}S' .$$

This reduces to (1.30).

Using the analytic conditions on the transverse motions within the fluid, I solve for each of the y_3^n and the y_7^n (numerically) and then eliminate these variables from the differential equations which determine the other variables. Due to the retention of the centrifugal acceleration, I also have in the radial component small terms involving the derivatives of these displacements. In order to be able to eliminate these from that equation as well I employ the curl of the displacement equation (1.26). This is

$$\vec{\nabla} \times (\ddot{\vec{u}} + 2\vec{\Omega} \times \dot{\vec{u}})$$

$$= -\nabla(\beta\Delta) \times [\vec{g}_0 - \vec{\Omega} \times (\vec{\Omega} \times \vec{r})] .$$

As the hydrostatic condition led to

$$\vec{\nabla} \rho_0 \parallel \vec{g}_0 - \vec{\Omega} \times (\vec{\Omega} \times \vec{r})$$

and further to

$$\vec{\nabla} \lambda \parallel \vec{\nabla} \rho_0$$

this can be rephrased as

$$\vec{\nabla} \times [\ddot{\vec{u}} + 2\vec{\Omega} \times \dot{\vec{u}}]$$

$$= -\frac{1}{V^2} \vec{\nabla} \left[\beta \frac{\partial \Delta}{\rho_0}\right] \times [\vec{g}_0 - \vec{\Omega} \times (\vec{\Omega} \times \vec{r})] .$$

Again replacing the variables by their spherical harmonic representations obtains

$$
\begin{aligned}
&-\ddot{y}_1 \hat{r}\times\vec{\nabla}S \;+\; \frac{d}{dr}\left(r\ddot{y}_3\right)\hat{r}\times\vec{\nabla}S \\
&+ i\,\frac{d}{dr}\left(r\ddot{y}_1\right)\vec{\nabla}S \;+\; \frac{in(n+1)}{r}\,\ddot{y}_1\,\hat{r}S \\
&+ \frac{2\Omega}{r}\left\{-\frac{d}{dr}\left(r\dot{y}_1\right)\sin\theta\, S\,\hat{\theta} \;+\; \frac{\dot{y}_1}{\sin\theta\cdot\partial\theta}\left(\sin^2\theta S\right)\hat{r}\right. \\
&+ im\dot{y}_3\,\vec{r}\times\vec{\nabla}S \;-\; \frac{d}{dr}\left(r\dot{y}_3\right)\cos\theta\, r\vec{\nabla}S \;-\; \dot{y}_3\sin\theta\frac{\partial S}{\partial\theta}\hat{r} \\
&- n(n+1)\dot{y}_3\cos\theta\, S\hat{r} \;-\; i\dot{y}_1\,\vec{r}\times\vec{\nabla}\left(\sin\theta\frac{\partial S}{\partial\theta}\right) \\
&\left.+ m\dot{y}_1\hat{r}S \;+\; i\,\frac{d}{dr}\left(r\dot{y}_1\right)\cos\theta\,\vec{r}\times\vec{\nabla}S\right\} \\
&= -\frac{\rho}{V^2}\left[\, g_0 z\,\hat{r}\times\vec{\nabla}S \;+\Omega^2\left\{r\frac{dz}{dr}\sin\theta\cos\theta\, S\hat{\phi}\right.\right. \\
&\qquad \left.\left. - z\sin^2\theta\,\vec{r}\times\vec{\nabla}S \;-\; imz\cos\theta\,\vec{r}S\right\}\right].
\end{aligned}
$$

The radial component of this equation is simply a re-statement of the torsional component of the original displacement equation. I extract the component using $r\vec{\nabla}S'$ to get

$$\left[\frac{d}{dr}\left(r\ddot{y}_3\right) - \ddot{y}_1\right] \vec{r}\times\vec{\nabla}S\cdot\vec{\nabla}S' + i\frac{d}{dr}\left(r\ddot{y}_7\right) r\vec{\nabla}S\cdot\vec{\nabla}S'$$

$$-\frac{2\Omega}{r}\left\{\frac{d}{dr}(r\dot{y}_1)\sin\theta S\frac{\partial S'}{\partial\theta} - im\dot{y}_3\,\vec{r}\times\vec{\nabla}S\cdot\vec{\nabla}S'\right.$$

$$+\frac{d}{dr}(r\dot{y}_3)\cos\theta\, r^2\vec{\nabla}S\cdot\vec{\nabla}S' + i\dot{y}_7\vec{r}\times\vec{\nabla}\left(\sin\theta\frac{\partial S}{\partial\theta}\right)\cdot r\vec{\nabla}S'$$

$$\left.-i\frac{d}{dr}\left(r\dot{y}_7\right)\cos\theta\,\vec{r}\times\vec{\nabla}S\cdot r\vec{\nabla}S'\right\}$$

$$= -\beta\frac{\Omega^2 r}{V^2}\frac{dz}{dr}\cos\theta\, S\frac{\partial S'}{\partial\phi} - \beta\frac{g_0}{V^2}\,\mathcal{L}\,\vec{r}\times\vec{\nabla}S\cdot\vec{\nabla}S'$$

$$+\beta\frac{\Omega^2 r}{V^2}\,\mathcal{L}\sin^2\theta\,\vec{r}\times\vec{\nabla}S\cdot\vec{\nabla}S'$$

As

$$r\int \sin^2\theta\,\vec{r}\times\vec{\nabla}S\cdot\vec{\nabla}S'\sin\theta\,d\theta\,d\phi$$

$$= 2im\int\cos\theta\, SS'\sin\theta\,d\theta\,d\phi\,,$$

the orthogonality of the spherical harmonics leads to (1.31b).

Extraction of the torsional component now gives

$$\left[-\ddot{y}_1 + \frac{d}{dr}(r\ddot{y}_3)\right] r\vec{\nabla}S\cdot\vec{\nabla}S' + i\frac{d}{dr}(r\dot{y}_7)\vec{\nabla}S\cdot\vec{r}\times\vec{\nabla}S'$$

$$-2\Omega\frac{d}{dr}(r\dot{y}_1)\sin\theta\, S\,\hat{\theta}\cdot\hat{r}\times\vec{\nabla}S' + 2im\Omega\dot{y}_3 r\vec{\nabla}S\cdot\vec{\nabla}S'$$

$$-2\Omega\frac{d}{dr}(r\dot{y}_3)\cos\theta\,\vec{\nabla}S\cdot\vec{r}\times\vec{\nabla}S' - 2i\Omega\dot{y}_7 r\vec{\nabla}S'\cdot\vec{\nabla}\left(\sin\theta\frac{\partial S}{\partial\theta}\right)$$

$$+2i\Omega\frac{d}{dr}(r\dot{y}_7)\cos\theta\, r\vec{\nabla}S\cdot\vec{\nabla}S'$$

$$= -\frac{\beta\Omega^2 r}{v^2}\frac{dz}{dr}\sin\theta\cos\theta\, S\,\hat{\phi}\cdot\vec{r}\times\vec{\nabla}S'$$

$$-\frac{\beta g_0 z}{v^2} r\vec{\nabla}S\cdot\vec{\nabla}S' + \frac{\beta\Omega^2 r^2 z}{v^2}\sin^2\theta\,\vec{\nabla}S\cdot\vec{\nabla}S' .$$

A final application of the orthogonality of the spherical harmonics gives (1.31a), where

$$B_3^{kn} \equiv \frac{2k+1}{4\pi}(-1)^m\int\sin^2\theta\,\vec{\nabla}S\cdot\vec{\nabla}S'\sin\theta\,d\theta\,d\phi .$$

As stated in the main text (Ch. 1, section 6), this pair of equations defining the derivatives of the transverse motions, together with the pair of equations defining the components of the transverse motions, are used to solve for these motions in terms of the remaining variables

y_1, Z, $\frac{dZ}{dr}$, y_5 and y_9. These solutions are substituted back into the differential equations, and the latter are truncated consistently with the truncation choice in the elastic solid regions, leaving a set of differential equations in the variables y_1, Z, y_5, y_6 and y_9.

APPENDIX C

CALCULATION OF THE SELECTION RULES GOVERNING THE COUPLING COEFFICIENTS

In deriving the sets of differential equations which govern the response of the Earth to an external potential field (Appendices A and B) I have defined certain coefficients describing the rotational coupling of different modes. The coupling terms have coefficients subject to selection rules imposed by the orthogonality properties of spherical harmonics.

Defining the solid angle element as

$$d\Theta \equiv \sin\theta \, d\theta \, d\phi ,$$

the integrals are:

$$A_1^{kn} \equiv \frac{2k+1}{4\pi} (-1)^m \int \sin^2\theta \; S_n^m S_k^{\ell} \, d\Theta$$

$$= \frac{2k+1}{4\pi} (-1)^m \int \sin^2\theta \; S_n^m S_k^{-m} \, d\Theta$$

$$= \frac{2k+1}{2} (-1)^m \int (1-x^2) P_n^m(x) P_k^m(x) \, dx$$

where

$$x \equiv \cos\theta$$

By taking advantage of the recursion relationships between the Legendre polynomials (Arfken, 1970, p. 560) we have

$$A_1^{kn} = \frac{(-1)^m}{2(2n+1)} \int \left[P_{n+1}^{m+1} - P_{n-1}^{m+1} \right] dx \cdot$$

$$\left[(k-m)(k-m-1) P_{k-1}^{-(m+1)} - (k+m+1)(k+m+2) P_{k+1}^{-(m+1)} \right]$$

$$= -\left(\frac{k-m}{2k-1}\right)\left(\frac{k-m-1}{2k-3}\right) \delta_n^{k-2} + \frac{2(k^2+k+m^2-1)}{(2k-1)(2k+3)} \delta_n^k$$

$$-\left(\frac{k+m+1}{2k+3}\right)\left(\frac{k+m+2}{2k+5}\right) \delta_n^{k+2}$$

where

$$\delta_n^k = \begin{cases} 1 & n = k \\ 0 & n \neq k \end{cases}$$

is the Kronecker delta.

In a similar fashion we have

$$A_2^{kn} \equiv \frac{2k+1}{4\pi}(-1)^m \int \sin\theta \cos\theta \frac{\partial S_n^m}{\partial \theta} S_k^l \, d\Theta$$

$$= -\frac{2k+1}{2}(-1)^m \int x(1-x^2) \frac{dP_n^m}{dx} P_k^{-m} \, dx$$

$$= \frac{(-1)^m}{2(2n+1)} \int \left[n(n-m+1) P_{n+1}^m - (n+1)(n+m) P_{n-1}^m \right] \cdot$$

$$\left[(k+m+1) P_{k+1}^{-m} + (k-m) P_{k-1}^{-m} \right] dx$$

$$A_2^{kn} = (k-2)\left(\frac{k-m}{2k-1}\right)\left(\frac{k-m-1}{2k-3}\right)\delta_n^{k-2} - \frac{k^2+k-3m^2}{(2k-1)(2k+3)}\delta_n^k$$

$$- (k+3)\left(\frac{k+m+1}{2k+3}\right)\left(\frac{k+m+2}{2k+5}\right)\delta_n^{k+2} \quad ;$$

$$A_3^{kn} \equiv \frac{2k+1}{4\pi}(-1)^m \int \sin\theta \frac{\partial S_n^m}{\partial \theta} S_k^l \, d\Theta$$

$$= -\frac{2k+1}{2}(-1)^m \int (1-x^2)\frac{dP_n^m}{dx} P_k^{-m} \, dx$$

$$= \frac{2k+1}{2(2n+1)}(-1)^m \int \left[n(n-m+1)P_{n+1}^m - (n+1)(n+m)P_{n-1}^m\right] P_k^{-m} \, dx$$

$$= (k-1)\left(\frac{k-m}{2k-1}\right)\delta_n^{k-1} - (k+2)\left(\frac{k+m+1}{2k+3}\right)\delta_n^{k+1} \quad ;$$

$$A_4^{kn} \equiv \frac{2k+1}{4\pi}(-1)^m \int \cos\theta \, S_n^m S_k^l \, d\Theta$$

$$= \frac{2k+1}{2}(-1)^m \int x P_n^m P_k^{-m} \, dx$$

$$= \frac{(-1)^m}{2} \int P_n^m \left[(k+m+1)P_{k+1}^{-m} + (k-m)P_{k-1}^{-m}\right] dx$$

$$= \left(\frac{k-m}{2k-1}\right)\delta_n^{k-1} + \left(\frac{k+m+1}{2k+3}\right)\delta_n^{k+1} \quad ;$$

$$B_1^{kn} \equiv \frac{2k+1}{4\pi}(-1)^m \int \cos\theta\, \vec{\nabla} S_n^m \cdot \vec{\nabla} S_k^\ell \, d\Theta$$

$$= \frac{2k+1}{4\pi}(-1)^m \int \left[\vec{\nabla} S_n^m \cdot \vec{\nabla}(\cos\theta\, S_k^\ell) + \sin\theta\, S_k^\ell \frac{\partial S_n^m}{\partial \theta} \right] d\Theta$$

$$= n(n+1) A_4^{kn} + A_3^{kn}$$

$$= (k+1)(k-1)\left(\frac{k-m}{2k-1}\right)\delta_n^{k-1} + k(k+2)\left(\frac{k+m+1}{2k+3}\right)\delta_n^{k+1} \quad ;$$

$$B_2^{kn} \equiv \frac{2k+1}{4\pi}(-1)^m \int \sin\theta\cos\theta\, S_n^m \frac{\partial S_k^\ell}{\partial \theta} \, d\Theta$$

$$= -\frac{2k+1}{2}(-1)^m \int x\,(1-x^2) P_n^m \frac{dP_k^{-m}}{dx}\, dx$$

$$= \frac{(-1)^m}{2(2m+1)} \int \left[(n+m) P_{n-1}^m + (n-m+1) P_{n+1}^m \right] x$$

$$\left[k(k+m+1) P_{k+1}^{-m} - (k+1)(k-m) P_{k-1}^{-m} \right] dx$$

$$= -(k+1)\left(\frac{k-m}{2k-1}\right)\left(\frac{k-m-1}{2k-3}\right)\delta_n^{k-2} - \frac{k^2+k-3m^2}{(2k-1)(2k+3)}\delta_n^k$$

$$+ \frac{k(k+m+1)}{(2k+3)}\left(\frac{k+m+2}{2k+5}\right)\delta_n^{k+2} \quad ;$$

$$B_3^{kn} \equiv \frac{2k+1}{4\pi}(-1)^m \int \sin^2\theta \, \vec{\nabla} S_n^m \cdot \vec{\nabla} S_k^l \, d\Theta$$

$$= \frac{2k+1}{4\pi}(-1)^m \int \left[\vec{\nabla}(\sin^2\theta \, S_n^m) \cdot \vec{\nabla} S_k^l - 2\sin\theta\cos\theta \, S_n^m \frac{\partial S_k^l}{\partial \theta} \right] d\Theta$$

$$= k(k+1) A_1^{kn} - 2 B_2^{kn}$$

$$= -(k+1)(k-2)\left(\frac{k-m}{2k-1}\right)\left(\frac{k-m-1}{2k-3}\right)\delta_n^{k-2} + 2\frac{k(k+1)(k^2+k+m^2)-3m^2}{(2k-1)(2k+3)}\delta_n^k$$

$$- k(k+3)\left(\frac{k+m+1}{2k+3}\right)\left(\frac{k+m+2}{2k+5}\right)\delta_n^{k+2} \; ;$$

$$B_4^{kn} \equiv \frac{2k+1}{4\pi}(-1)^m \int \sin\theta \, S_n^m \frac{\partial S_k^l}{\partial \theta} \, d\Theta$$

$$= -\frac{2k+1}{2}(-1)^m \int (1-x^2) P_n^m \frac{dP_k^{-m}}{dx} \, dx$$

$$= \frac{(-1)^m}{2} \int P_n^m \left[k(k+m+1) P_{k+1}^{-m} - (k+1)(k-m) P_{k-1}^{-m} \right] dx$$

$$= \frac{k(k+m+1)}{2k+3}\delta_n^{k+1} - \frac{(k+1)(k-m)}{2k-1}\delta_n^{k-1} \; .$$

These coefficients then show that in the differential equations for the components of the stress force there are contributions from other modes than that under consideration. Inspection of these terms indicate that a Coriolis coupling will cause excitation of a spheroidal motion by torsional motions of neighbouring degrees and vice versa. Centrifugal coupling causes excitation of spheroidal terms by spheroidal motions either two degrees higher or lower. Due to the axial symmetry of the Earth model considered and to the nature of the rotational couplings, all modes excited have the same order (azimuthal number, m) as the mode which is tidally excited. These couplings have been indicated schematically in Figure 1 for the degree 2 excitation.

In Appendix F, I show that neglect of the torsional modes is a violation of the conservation of angular momentum.

APPENDIX D

BOUNDARY CONDITIONS AT THE CENTRE OF THE EARTH AND INITIALIZATION OF THE NUMERICAL SOLUTION

In this Appendix I derive the form of the solutions which are regular near the origin and specify the number of arbitrary constants required to fully determine the system. The technique developed by some authors for the core integration has been to take either a power series or an analytic solution appropriate to a static homogeneous solid as sufficient at some finite radius and integrate outwards from this value. To improve numerical accuracy, and because of the couplings between modes that I must consider, I incorporate a change of variable that permits a direct integration from the origin. I carry the second derivative throughout the inner core, and because the first derivatives vanish at the origin, the evaluation of the second derivatives at the origin must be done in a somewhat different fashion than that used elsewhere.

I perform these operations in two stages. First, I examine the power series solutions in the decoupled (static, non-rotating) case to determine the number of unknown coefficients required to determine the solution and specify the leading terms for each variable. This suggests the definition of new variables by removing the dominant power law behaviour and leaving a function which is more slowly varying. Secondly, these new variables are investigated for the full Earth model (dynamic, rotating) and the conditions necessary to initiate the integration are formulated.

In both sections I assume that the near-central region of the Earth is locally homogeneous. This assumption is physically acceptable and is used only to initiate the solution.

1. The Static, Non-Rotating Earth

In a static, non-rotating Earth the set of equations governing the displacements, stresses, potentials and the gravitational flux in each degree of the spherical harmonic expansion is completely decoupled from every other degree.

I develop the power series expansion for each mode and impose the conditions of regularity and conservation of linear momentum.

I shall first deal with the purely spherical expansion described by the degree zero harmonic. For this mode I have

$$y_3 = y_4 = y_7 = y_8 = y_9 = 0,$$

$$(\lambda+2\mu)\frac{dy_1}{dr} = -\frac{2\lambda}{r}y_1 + y_2,$$

$$\frac{dy_2}{dr} = -4\left[\frac{\rho_0 g_0}{r} - \frac{3\lambda+2\mu}{\lambda+2\mu}\frac{\mu}{r^2}\right]y_1 - \frac{4\mu}{\lambda+2\mu}\frac{y_2}{r} - \rho_0 y_6,$$

$$\frac{dy_5}{dr} = y_6 + 4\pi G\rho_0 y_1,$$

$$\frac{dy_6}{dr} = -\frac{2y_6}{r}.$$

The solution for the gravitational flux term is

$$y_6 = y_6(0)/r^2$$

and regularity as $r \to 0$ indicates that y_6 vanishes (as it does throughout the entire Earth).

I now choose to express the radial displacement in a power series

$$y_1 = \sum_{p=1}^{\infty} \alpha_{p-1} r^p$$

then

$$y_2 = (\lambda+2\mu) \Sigma\, p\, \alpha_{p-1} r^{p-1} + 2\lambda \Sigma\, \alpha_{p-1} r^{p-1}$$

and the differential equation for y_2 becomes

$$(\lambda+2\mu) \Sigma\, (p-1)(p+2)\, \alpha_{p-1} r^{p-2} = -4\rho_0 \Gamma \Sigma\, \alpha_{p-1} r^p$$

where

$$\Gamma \equiv \lim_{r \to 0} \left[\frac{g_0(r)}{r} \right] = \frac{4\pi G \rho_0(0)}{3} .$$

Thus α_0 is arbitrary and α_1 must vanish, and subsequent terms are given by the recursion relation

$$\alpha_{p+1} = -\frac{4\rho_0 \Gamma}{\lambda+2\mu} \frac{\alpha_{p-1}}{(p+2)(p-1)} \qquad p \geq 1,$$

$$= -\frac{4\Gamma}{v_p^2} \frac{\alpha_{p-1}}{(p+2)(p-1)} .$$

Thus I have the power series near the origin for the degree zero mode:

$$y_1 = \alpha_0 r + \alpha_2 r^3 + \cdots$$

$$y_2 = (3\lambda+2\mu)\alpha_0 + (5\lambda+6\mu)\alpha_2 r^2 + \cdots$$

$$y_5 = \gamma_0 + 3\Pi\left[\frac{\alpha_0 r^2}{2} + \frac{\alpha_2 r^4}{4} + \cdots\right]$$

which contains only two arbitrary constants.

For the other spherical harmonic modes I choose the induced potential and the spheroidal displacement components (the torsional are completely decoupled in the non-rotating case) as

$$y_1 = \sum_{p=1}^{\infty} \alpha_{p+1} r^p$$

$$y_3 = \sum_{p=1}^{\infty} \zeta_{p+1} r^p$$

$$y_5 + y_9 = \sum_{p=0}^{\infty} \gamma'_p r^p$$

with

$$y_9 = c_k r^k .$$

The other variables are then given by the power series expansions

$$y_2 = \sum_{p=1}^{\infty} [p(\lambda+2\mu) + 2\lambda]\, \alpha_{p+1}\, r^{p-1} - k(k+1)\lambda \sum_{p=1}^{\infty} \zeta_{p+1}\, r^{p-1} ,$$

$$y_4 = \mu \sum_{p=1}^{\infty} [(p-1)\zeta_{p+1} + \alpha_{p+1}]\, r^{p-1} ,$$

$$y_6 + \frac{dy_8}{dr} = \sum_{p=1}^{\infty} [(p-1)\gamma'_{p-1}\, r^{p-2} - 3\Gamma \alpha_{p+1}\, r^p] .$$

Using the differential equations for these variables and equating the coefficients of individual powers of r, I obtain

$$[(p+2)(p-1)(\lambda+2\mu) - k(k+1)\mu]\, \alpha_{p+1} + \rho_0 (p-1)\, \gamma'_{p-1} - k(k+1)[(p-1)(\lambda+\mu) - 2\mu]\, \zeta_{p+1} = \rho_0 \Gamma [k(k+1)\zeta_{p-1} - \alpha_{p-1}] ,$$

$$[p(\lambda+\mu) + 2(\lambda+2\mu)]\, \alpha_{p+1} + \rho_0 \gamma'_{p-1} + [p(p+1)\mu - k(k+1)(\lambda+2\mu)]\, \zeta_{p+1} = \rho_0 \Gamma \alpha_{p-1} ,$$

$$[p(p-1) - k(k+1)]\, \gamma'_{p-1} = 3\Gamma (p\alpha_{p-1} - k(k+1)\zeta_{p-1}) .$$

Thus knowledge of the coefficients α_{p-1} and ς_{p-1} in principle determines α_{p+1}, ς_{p+1} and γ'_{p-1}, and sequentially generates the entire power series expansion for each of the variables. Specifically, the coefficients are determined by the equation

$$A \begin{bmatrix} \alpha_{p+1} \\ \varsigma_{p+1} \\ \gamma'_{p-1} \end{bmatrix} = B \begin{bmatrix} \alpha_{p-1} \\ \varsigma_{p-1} \end{bmatrix}$$

where

$$A \equiv \begin{bmatrix} (p+2)(p-1)(\lambda+2\mu) - k(k+1)\mu & k(k+1)[2\mu - (p-1)(\lambda+\mu)] & e_0(p-1) \\ p(\lambda+\mu) + 2(\lambda+2\mu) & p(p+1)\mu - k(k+1)(\lambda+2\mu) & e_0 \\ 0 & 0 & e_0(p+k)(p-k-1) \end{bmatrix},$$

$$B \equiv e_0 \Gamma \begin{bmatrix} -1 & k(k+1) \\ 1 & 0 \\ 3p & -3k(k+1) \end{bmatrix}.$$

Hence we have

$$\begin{bmatrix} \alpha_{p+1} \\ \varsigma_{p+1} \\ \gamma'_{p-1} \end{bmatrix} = A^{-1} B \begin{bmatrix} \alpha_{p-1} \\ \varsigma_{p-1} \end{bmatrix}$$

providing that A is non-singular; $\det A \neq 0$. The alternative statement is equally important. The leading terms in the power series expansion must be obtainable from the condition that A is singular. I expand the determinant to find

$$\det A = e_0 \mu (\lambda+2\mu)(p+k)^2 (p-k-1)^2 (p-k+1)(p+k+2).$$

As p and k are non-negative integers, the condition that A is singular is

$$p = k \pm 1 .$$

Taking first the initial terms in the power series for the displacements (p=k-1), the set of equations reduces to

$$(k+1)[(k-2)(\lambda+2\mu)-k\mu][\alpha_k - k\zeta_k] = 0$$

$$[(k+1)(\lambda+2\mu)-(k-1)\mu][\alpha_k - k\zeta_k] = 0$$

and the identity

$$0 = 0.$$

The degeneracy is obvious and has the solution

$$\zeta_k = \frac{\alpha_k}{k} .$$

For p=k+1, the third equation in the set shows that γ_k' is indeterminate and reinforces the above condition. The other two equations both simplify to

$$[(k+3)(\lambda+2\mu)-(k+1)\mu]\alpha_{k+2} + \rho_0 \gamma_k'$$

$$+(k+1)[(k+2)\mu - k(\lambda+2\mu)]\zeta_{k+2} = \rho_0 \Gamma \alpha_k ,$$

which indicates that one of the α_{k+2} or ζ_{k+2} is arbitrary. I therefore choose the set of arbitrary variables α_k , γ_k' , and $\beta_k \equiv \alpha_{k+2}$ which will then completely determine the solution in a homogeneous solid core.

The leading terms for these solutions for the degree k response are:

$$y_1 = \alpha_k r^{k-1} + \beta_k r^{k+1} + \cdots$$

$$y_2 = 2\mu(k-1)\alpha_k r^{k-2} + \cdots$$

$$y_3 = \frac{\alpha_k}{k} r^{k-1} + \cdots$$

$$y_4 = 2\mu\left(\frac{k-1}{k}\right)\alpha_k r^{k-1} + \cdots$$

$$y_5 = \gamma_k r^k + \cdots$$

$$y_6 = (k\gamma_k - 3\Gamma\alpha_k) r^{k-1} + \cdots$$

$$y_9 = \zeta_k r^k$$

where

$$\gamma_k \equiv \gamma_k' - c_k \quad .$$

The decoupled torsional modes present a much simpler problem. These are governed by the pair of equations

$$\frac{dy_7}{dr} = \frac{y_8}{r} + \frac{y_8}{\mu}$$

$$\frac{dy_8}{dr} = (k+2)(k-1)\frac{\mu y_7}{r^2} - \frac{3y_8}{r} \quad .$$

Again we assume a regular power series solution

$$y_7 \equiv \sum_{p=1}^{\infty} \nu_p r^p$$

thus

$$y_8 = \mu \sum_{p=1}^{\infty} (p-1)\nu_p r^{p-1}$$

which then leads to the condition

$$\mu \sum_{p=1}^{\infty} (p-k)(p+k+1)\,\nu_p\, r^{p-2} = 0$$

therefore

$$(p-k)\,\nu_p = 0 .$$

The only arbitrary term (and the only non-vanishing term) is then ν_k. The torsional quantities are then given very simply by

$$y_1 = \nu_k r^k$$

$$y_2 = \mu(k-1)\,\nu_k r^{k-1} .$$

These results for a static, non-rotating, homogeneous, solid Earth core are those that will apply as $r \to 0$ in the Earth model under consideration and are in agreement with Crossley (1975a). I shall now include the dynamic and rotational effects in order to properly initialize the solutions.

2. The Dynamic, Rotating Earth

I now rewrite the full equations and include the dynamic and the rotational effects in terms of the set of variables x_i^n as described in Chapter 2 (eq. 2.5). Again I shall assume that at or near the centre of the Earth the inner core is locally homogeneous: $\dot{\rho}_0(0) = \dot{\lambda}(0) = \dot{\mu}(0) = 0$, where the dot denotes differentiation with respect to radius (no possibility of confusion exists as the time derivative $\frac{\partial}{\partial t}$ has been replaced by $i\sigma$ under the assumption of sinusoidal time variation).

For the degree zero mode I now have

$$\overline{(\lambda+2\mu)}\,\dot{x}_1^0 = \frac{1}{r}\left[x_2^0 - (3\lambda+2\mu)x_1^0\right],$$

$$\dot{x}_2^0 = -4\left[\rho_0 g_0 - \frac{2\mu}{r}\right]x_1^0 - \frac{4\mu}{\lambda+2\mu}\frac{x_2^0}{r}$$

$$-\rho_0\sigma^2 r x_1^0 - 2\rho_0\sigma\Omega r A_3^{01} x_1^1 + \rho_0\Omega^2 r A_1^{00} x_1^0$$

$$+\rho_0\Omega^2 r\left[A_1^{02} + A_2^{02}\right]x_1^2 - \rho_0\Omega^2 r\left[6A_1^{02} + 2A_2^{02}\right]x_3^2$$

$$-\frac{\rho_0\Omega^2 r}{\mu}A_2^{02}x_4^2,$$

$$\dot{x}_5^0 = 4\pi G\rho_0 r x_1^0 .$$

Regularity at the origin again produces the condition

$$x_2^0(0) = (3\lambda+2\mu)x_1^0(0)$$

and therefore

$$\dot{x}_1^0(0) = \dot{x}_2^0(0) = \dot{x}_3^0(0) = 0.$$

Under the assumption of local homogeneity, I differentiate these relations to find

$$(5\lambda + 6\mu)\,\ddot{x}_1^0(0) = \ddot{x}_2^0(0)$$

$$\ddot{x}_5^0(0) = 3\Gamma\, x_1^0(0)$$

where

$$\Gamma \equiv \lim_{r\to 0}\left[\frac{g_0(r)}{r}\right] = \frac{4\pi G\,\rho_0(0)}{3}\,.$$

By using the relationships between $\dot{x}_n^1(0)$ developed in the preceding section, I also obtain

$$\ddot{x}_2^0(0) = -4\mu\,\ddot{x}_1^0(0) - \rho_0(4\Gamma+\sigma^2)\,x_1^0(0)$$
$$+\rho_0\Omega^2\left\{A_1^{0,0}\,x_1^0(0) - (2A_1^{0,2}+A_2^{0,2})\,x_1^2(0)\right\}$$
$$-2\rho_0\sigma\Omega A_3^{0,1}\,x_1^1(0)\,.$$

The second degree spheroidal mode, because it couples down to the degree zero mode, must be treated separately.

I shall first list the differential equations that govern this mode.

$$(\lambda+2\mu)\,\dot{x}_1^2 = \frac{1}{r}\left[x_2^2 + 6\lambda x_3^2 - (3\lambda+2\mu)\,x_1^2\right],$$

$$\dot{x}_3^2 = \frac{1}{r}\left[\frac{x_4^2}{\mu} - x_1^2\right],$$

$$\dot{x}_3^2 = -4\left[\rho_0 g_0 - \frac{\mu\xi}{r}\right]x_1^2 - \frac{4\mu}{\lambda+2\mu}\frac{x_3^2}{r} - 6\left[\rho_0 g_0 - \frac{2\mu\xi}{r}\right]x_3^2$$
$$+ 6\frac{x_3^2}{r} - \rho_0 r x_4^2 - 2\rho_0 r x_1^2 - \rho_0 \Omega^2 r x_1^2$$
$$+ 2\rho_0\Omega^2\left[m r x_3^2 - r A_3^{2,1} x_1^1 - r^3 A_3^{2,3} x_1^3\right]$$
$$+ \rho_0\Omega^2\left\{r(A_1^{2,0} + A_2^{2,0})x_1^0 + r(A_1^{2,2} + A_2^{2,2})x_1^2 + r(A_1^{2,4} + A_2^{2,4})x_1^4\right.$$
$$- r(6A_1^{0,2} + 2A_2^{2,2})x_3^2 - r^3(20A_1^{2,4} + 2A_2^{2,4})x_3^4$$
$$- \frac{r}{\mu}A_2^{2,2}x_4^2 - \frac{r^3}{\mu}A_2^{2,4}x_4^4$$
$$\left. + m r A_4^{2,1}\left(x_1^1 + \frac{x_0^1}{\mu}\right) + m r^3 A_4^{2,3}\left(x_1^3 + \frac{x_0^3}{\mu}\right)\right\},$$

$$\dot{x}_4^2 = \left[\rho_0 g_0 - 2\frac{\mu\xi}{r}\right]x_1^2 - \frac{\lambda}{\lambda+2\mu}\frac{x_3^2}{r} - \frac{2\mu}{r}x_3^2 - \rho_0 r x_3^2$$
$$+ 2\frac{\mu}{r}\left(\frac{\lambda+\mu}{\lambda+2\mu}\right)x_3^2 - 3\frac{x_4^2}{r} - \rho_0 r x_3^2 - \rho_0 r x_4^2$$
$$+ \frac{\rho_0\Omega^2}{3}\left\{m r x_1^2 + m r x_3^2 - r B_1^{2,1} x_1^1 - r^3 B_1^{2,3} x_1^3\right\}$$
$$- \rho_0\Omega^2\left\{A_1^{2,0} r x_1^0 + r A_1^{2,2} x_1^2 + r^3 A_1^{2,4} x_1^4 + r A_2^{2,2} x_3^2\right.$$
$$\left. + A_2^{2,4} r^3 x_3^4 - m r A_4^{2,1} x_1^1 - m r^3 A_4^{2,3} x_1^3\right\}$$
$$+ \frac{\rho_0\Omega^2}{6(\lambda+2\mu)}\left\{4\mu B_2^{2,0} r x_1^0 + 4\mu r B_2^{2,2} x_1^2 + 4\mu r^3 B_2^{2,4} x_1^4\right.$$
$$+ r B_2^{2,0} x_2^0 + r B_2^{2,2} x_2^2 + r^3 B_2^{2,4} x_2^4$$
$$\left. - 12\mu r B_2^{2,2} x_3^2 - 40\mu r^3 B_2^{2,4} x_3^4\right\},$$

$$\dot{x}_5^2 = \frac{1}{r}\left[x_6^2 - 2x_5^2 - 4\pi G\rho_0 x_1^2\right],$$

$$\dot{x}_6^2 = \frac{1}{r}\left[-4\pi G\rho_0 6x_3^2 + 6x_5^2 - 3x_6^2\right],$$

$$\dot{x}_9^2 = 0.$$

Regularity at the origin produces the same relations between the variables that were obtained in the previous section:

$$x_2^2(0) = 2\mu x_1^2(0), \quad x_3^2(0) = \frac{1}{2}x_1^2(0),$$

$$x_4^2(0) = \mu x_1^2(0),$$

$$x_6^2(0) = 2x_5^2(0) = 3\Gamma x_1^2(0).$$

By returning these conditions to the above equations I find

$$\dot{x}_1^2(0) = 0.$$

By proceeding in the same manner as previously applied to the degree zero case, differentiating the above set of equations and then taking the limit as $r \to 0$, I find (after some rearranging)

$$(5\lambda + 6\mu)\ddot{x}_1^2(0) - \ddot{x}_2^2(0) - 6\lambda\ddot{x}_3^2(0) = 0,$$

$$\mu\ddot{x}_1^2(0) + 2\mu\ddot{x}_3^2(0) - \ddot{x}_4^2(0) = 0,$$

$$\ddot{x}_9^2(0) = 0,$$

$$\ddot{x}_2^2(0) + \mu \ddot{x}_1^2(0)$$
$$= \rho_0 [2\Gamma - \sigma^2 + m\sigma\Omega - \Omega^2(2A_1^{2,2} + A_3^{2,2})] x_1^2(0)$$
$$-2\rho_0 x_5^2(0) - 2\rho_0 x_4^2(0) + 2\rho_0\Omega[m\Omega A_4^{2,1} - \sigma A_3^{2,1}] x_1^1(0)$$
$$+ \rho_0\Omega^2(A_1^{2,0} + A_2^{2,0}) x_1^0(0),$$

$$4\ddot{x}_5^2(0) - \ddot{x}_6^2(0) - 3\Gamma\ddot{x}_1^2(0) = 0,$$

$$6\ddot{x}_5^2(0) - 5\ddot{x}_6^2(0) - 18\Gamma\ddot{x}_3^2(0) = 0.$$

Note that there are only six equations produced here from the seven first-order differential equations. The degeneracy of two of the derived equations is simply confirmation that one of the $\ddot{x}_1^2(0)$ is arbitrary, as in the previous section, and again I choose

$$\beta_2 = \frac{1}{2}\ddot{x}_1^2(0).$$

These conditions on the degree two mode have had to be treated separately as they couple to the degree zero mode and the degree zero mode had been reduced from the variables y_1^0 to the x_1^0 in a distinct fashion from that used for the remaining modes. For all other degree responses, the set of equations can be dealt with systematically in the above manner and give each of the second derivatives at the origin in terms of the chosen set of arbitrary constants. These are

$$(k+1)[k\lambda + (k-2)\mu]\ddot{x}_6^k(0)$$

$$= 2[(k+3)\lambda + (k+5)\mu]\beta_k + 2\rho_0 x_5^k(0) - 2\rho_0 x_9^k(0)$$

$$-2\rho_0\left[\Gamma - \frac{\pi^2}{k} + \frac{2m\sigma\Omega}{k^2} - \Omega^2(A_1^{kk} + \frac{A_2^{kk}}{k})\right]x_1^k(0)$$

$$-2\rho_0\Omega[m\Omega A_4^{kk-1} - \frac{2\sigma A_3^{kk-1}}{k}]x_7^{k-1}(0) - \frac{2\rho_0\Omega^2}{\mu}\frac{A_1^{kk-2}}{k}\ddot{x}_4^{k-2}(0),$$

$$\ddot{x}_3^k(0) = 2[2\lambda + (k+1)(\lambda+2\mu)]\beta_k - k(k+1)\lambda\ddot{x}_3^k(0),$$

$$\ddot{x}_4^k(0) = 2\mu\beta_k + k\mu\ddot{x}_8^k(0),$$

$$(4k+6)\ddot{x}_5^k = 3\Gamma[2(k+3)\beta_k - k(k+1)\ddot{x}_3^k(0)],$$

$$(4k+6)\ddot{x}_6^k = k(k+1)3\Gamma[2\beta_k - (k+2)\ddot{x}_3^k(0)].$$

Again one of the seven equations obtained was redundant, indicating that one of the $\ddot{x}_1^k(0)$ was arbitrary; my choice was again

$$\beta_k = \tfrac{1}{2}\ddot{x}_1^k(0).$$

For the torsional components, the differential equations for the degree one response are:

$$\dot{x}_7^1 = \frac{x_8^1}{r\mu},$$

$$\dot{x}_8^1 = -\rho_0\sigma^2 r x_7^1 - \frac{3x_8^1}{r} + m\rho_0\sigma\Omega r x_7^1$$

$$-\rho_0\Omega\sigma r[B_4^{1,0}x_1^0 + B_4^{1,2}x_1^2 + B_1^{1,2}x_3^2]$$

$$= \frac{m\rho_0\Omega^2 r A_4^{1,2}}{\lambda+2\mu}[x_2^2 + 4\mu x_1^2 - 12\mu x_3^2].$$

Regularity again leads to $x_8^1(0) = 0$ and hence

$$\dot{x}_1^1(0) = \dot{x}_8^1(0) = 0 .$$

It follows that

$$2\mu\, \ddot{x}_1^1(0) - \ddot{x}_8^1(0) = 0$$

$$5\mu\, \ddot{x}_1^1(0) = -\rho_0 \sigma^2 x_1^1(0) + m\rho_0 \sigma\Omega\, x_1^1(0)$$

$$-\rho_0 \sigma\Omega \left[B_4^{1,0}\, x_1^0(0) + \left[B_4^{1,2} + \tfrac{1}{2} B_1^{1,2} \right] x_1^2(0) \right] .$$

For the higher order torsional modes the second derivatives are given in terms of the arbitrary constants by the relations

$$(k+1)\mu\, \ddot{x}_1^k(0) - \ddot{x}_8^k(0) = 0 ,$$

$$(2k+3)\mu\, \ddot{x}_1^k(0)$$

$$= -\rho_0 \Omega \left[\tfrac{1}{2} m\Omega (k+2) A_4^{k,k-1} + \sigma B_4^{k,k-1} \right] \ddot{x}_1^{k-1}(0)$$

$$+ \rho_0 \Omega \left[\tfrac{1}{2} m\Omega k(k-1) A_4^{k,k-1} - \sigma B_1^{k,k-1} \right] \ddot{x}_3^{k-1}(0)$$

$$- \rho_0 \sigma \left[k(k+1)\sigma - 2m\Omega \right] x_1^k(0)$$

$$+ 2(2k+3)\rho_0 \sigma\Omega B_4^{k,k+1}\, x_1^{k+1}(0) .$$

Generally the set of the first derivatives of the x_i^k are used in the propagation through the inner core in the manner described in Chapter 2; however for the first iteration of the procedure certain of the coefficients (proportional to $\frac{1}{r}$) are not regular so that it has been necessary to show that the first derivatives of all quantities vanish at the origin and hence to calculate the second derivatives directly.

APPENDIX E

ANALYTIC SOLUTIONS FOR AN EARTH OF UNIFORM DENSITY

I propose in this section certain simplifications which will allow the formulation of an analytic solution with which I can compare the numerical solution. I shall approximate the inner core of the Earth as a homogeneous solid (i.e. $\beta = 1$), consider only the spheroidal components of the motion and neglect all centrifugal couplings.

Eliminating the quantities y_2, y_4 and y_5 leaves three second-order differential equations in y_1, y_3 and $y_5' = y_5 + y_9$.

$$\frac{d}{dr}\left[(\lambda+2\mu)\left(\frac{dy_1}{dr} + \frac{2y_1}{r} - \frac{k(k+1)}{r}y_3\right)\right]$$
$$+ \frac{k(k+1)}{r}\mu\left[\frac{dy_3}{dr} + \frac{y_3}{r} - \frac{y_1}{r}\right]$$

(E.1)

$$= -\rho_0\left[\sigma^2 + \frac{4g_0}{r} - 4\pi G\rho_0\right]y_1 - \rho_0\frac{dy_5'}{dr}$$
$$+ \rho_0\left[\frac{k(k+1)}{r}g_0 + 2m\Omega\sigma\right]y_3 \,,$$

$$\frac{d^2y_5'}{dr^2} + \frac{2}{r}\frac{dy_5'}{dr} - \frac{k(k+1)}{r^2}y_5'$$

(E.2)

$$= 4\pi G\rho_0\left[\frac{dy_1}{dr} + \frac{2y_1}{r} - \frac{k(k+1)}{r}y_3\right],$$

$$\frac{d}{dr}\left[\mu\left(\frac{dy_2}{dr} + \frac{y_3}{r} - \frac{y_2}{r}\right)\right] + \mu\left(\frac{dy_3}{dr} + \frac{y_3}{r} - \frac{y_2}{r}\right)$$

(E.3) $$+ \frac{\lambda+2\mu}{r}\left[\frac{dy_1}{dr} + \frac{2y_1}{r} - \frac{k(k+1)}{r}y_3\right]$$

$$= \rho_0 g_0 y_1 - \rho_0 y_5' - \rho_0 \sigma^2 y_3 + \frac{2m\rho_0\sigma\Omega}{k(k+1)}(y_1 + y_3) .$$

Reintroducing the dilatation

(E.4) $$\Delta \equiv \frac{dy_1}{dr} + \frac{2y_1}{r} - \frac{k(k+1)}{r}y_3$$

and the variable

(E.5) $$\chi \equiv \frac{dy_3}{dr} + \frac{y_3}{r} - \frac{y_2}{r}$$

which is the curl of the spheroidal component of the motion (or more generally is the torsional component of the curl of the motion), these can be rewritten as:

$$\frac{d}{dr}[(\lambda+2\mu)\Delta] + \frac{k(k+1)}{r}\mu\chi$$

(E.6) $$= -\rho_0[\Gamma + \sigma^2]y_1 + \rho_0[k(k+1)\Gamma + 2m\sigma\Omega]y_3$$

$$- \rho_0 \frac{dy_5'}{dr} ,$$

(E.7) $$\frac{d^2y_5'}{dr^2} + \frac{2}{r}\frac{dy_5'}{dr} - \frac{k(k+1)}{r^2}y_5' = 3\Gamma\Delta ,$$

(E.8) $$\frac{d}{dr}[\mu\chi] + \frac{\mu\chi}{r} + \frac{\lambda+2\mu}{r}\Delta = \rho_0\Gamma y_1 - \rho_0\sigma^2 y_3 - \frac{\rho_0 y_5'}{r} + \frac{2m\rho_0\sigma\Omega}{k(k+1)}(y_1+y_3)$$

where again

$$\Gamma \equiv \frac{g_0}{r} = \frac{4\pi G\rho_0}{3}$$

since the inner core is presumed homogeneous.

By differentiating (E.6) and (E.8) and eliminating y_5' a pair of coupled second-order differential equations in χ and Δ are obtained:

$$\frac{d^2}{dr^2}[(\lambda+2\mu)\Delta] + \frac{2}{r}\frac{d}{dr}[(\lambda+2\mu)\Delta] - \frac{k(k+1)}{r^2}[(\lambda+2\mu)\Delta]$$
$$= -\rho_0[4\Gamma+\sigma^2]\Delta + \rho_0[k(k+1)\Gamma + 2m\sigma\Omega]\chi ,$$

$$\frac{d^2}{dr^2}[\mu\chi] + \frac{2}{r}\frac{d}{dr}[\mu\chi] - \frac{k(k+1)}{r^2}[\mu\chi]$$
$$= \rho_0\left[-\sigma^2 + \frac{2m\sigma\Omega}{k(k+1)}\right]\chi + \rho_0\left[\Gamma + \frac{2m\sigma\Omega}{k(k+1)}\right]\Delta .$$

Definition of the second-order differential operator

$$D_k \equiv \frac{d^2}{dr^2} + \frac{2}{r}\frac{d}{dr} - \frac{k(k+1)}{r^2}$$

allows these to be simplified to

(E.9) $$(D_k + \alpha_1)\Delta = \alpha_2 \chi$$

(E.10) $$(D_k + \beta_2)\chi = \beta_1 \Delta$$

where the coefficients

$$\alpha_1 \equiv \frac{\rho_0[4\Gamma+\sigma^2]}{\lambda+2\mu} = \frac{4\Gamma+\sigma^2}{V_p^2},$$

$$\alpha_2 \equiv \frac{\rho_0[k(k+1)\Gamma + 2m\sigma\Omega]}{\lambda+2\mu},$$

$$\beta_1 \equiv \frac{\rho_0[\Gamma + 2m\sigma\Omega/k(k+1)]}{\mu} = \frac{\Gamma + \frac{2m\sigma\Omega}{k(k+1)}}{V_s^2}$$

$$\beta_2 \equiv \frac{\rho_0[\sigma^2 - 2m\sigma\Omega/k(k+1)]}{\mu}.$$

A simple operation will now give a fourth-order differential equation in either of the unknowns

$$(D_k+\beta_2)(D_k+\alpha_1)\Delta = (D_k+\beta_2)\alpha_2\chi = \alpha_2\beta_1\Delta$$

i.e.

$$[D_k^2 + (\alpha_1+\beta_2)D_k + (\alpha_1\beta_2 - \alpha_2\beta_1)]\Delta = 0.$$

This can be written in the form

(E.11) $$[D_k + \xi_1^2][D_k - \xi_2^2]\Delta = 0$$

where

$$k_1^2 = \frac{\sqrt{(\alpha_1-\beta_2)^2 + 4\alpha_2\beta_1} + \alpha_1 + \beta_2}{2} > 0$$

$$k_2^2 = \frac{\sqrt{(\alpha_1-\beta_2)^2 + 4\alpha_2\beta_1} - \alpha_1 - \beta_2}{2} .$$

The eigenfunctions of these operators are spherical Bessel and modified spherical Bessel functions of degree k (Arfken, 1970, p. 521).

$$(D_k + k_1^2)\Delta = 0$$

admits

$$\Delta = A j_k(k_1 r) + C \eta_k(k_1 r)$$

and

$$(D_k - k_2^2)\Delta = 0$$

admits

$$\Delta = B i_k(k_2 r) + D k_k(k_2 r).$$

Regularity at the origin restricts the solution to

$$\Delta = A j_k(k_1 r) + B i_k(k_2 r) .$$

Hence (E.9) gives

$$\chi = \frac{\alpha_1 - k_1^2}{\alpha_2} A j_k(k_1 r) + \frac{\alpha_1 + k_2^2}{\alpha_2} B i_k(k_2 r)$$

and (E.7)

$$D_k y_5' = 3\Gamma\Delta$$

has the solution

$$y_5' = -\frac{3\Gamma}{k_1^2} A j_k(k_1 r) + \frac{3\Gamma}{k_2^2} B i_k(k_2 r) + E r^k .$$

The displacements y_1 and y_3 satisfy the differential equations

$$\frac{dy_1}{dr} + \frac{2y_1}{r} - \frac{k(k+1)}{r} y_3 = A j_k(k_1 r) + B i_k(k_2 r),$$

$$\frac{dy_3}{dr} + \frac{y_3}{r} - \frac{y_1}{r} = \frac{\alpha_1 - k_1^2}{\alpha_2} A j_k(k_1 r) + \frac{\alpha_1 + k_2^2}{\alpha_2} B i_k(k_2 r).$$

These can be manipulated to produce two decoupled second-order differential equations

$$D_k[r y_1] = A\left[\frac{1}{r}\frac{d}{dr}(r^2 j_k) + k(k+1)\left(\frac{\alpha_1 - k_1^2}{\alpha_2}\right) j_k\right] + B\left[\frac{1}{r}\frac{d}{dr}(r^2 i_k) + k(k+1)\left(\frac{\alpha_1 + k_2^2}{\alpha_2}\right) i_k\right],$$

$$D_k[r y_3] = A\left[j_k + \frac{\alpha_1 - k_1^2}{\alpha_2}\frac{1}{r^2}\frac{d}{dr}(r^2 j_k)\right] + B\left[i_k + \frac{\alpha_1 + k_2^2}{\alpha_2}\frac{1}{r^2}\frac{d}{dr}(r^2 i_k)\right].$$

The solutions of these are

$$y_1 = Cr^{k-1} - \frac{A}{k_1^2}\left[\frac{dj_k}{dr} + k(k+1)\frac{\alpha_1 - k_1^2}{\alpha_2}\frac{j_k}{r}\right] + \frac{B}{k_2^2}\left[\frac{di_k}{dr} + k(k+1)\frac{\alpha_1 + k_2^2}{\alpha_2}\frac{i_k}{r}\right],$$

$$y_3 = \frac{Cr^{k-1}}{k} - \frac{A}{k_1^2}\left[\frac{\alpha_1 - k_1^2}{\alpha_2}\frac{dj_k}{dr} + \left(1 + \frac{\alpha_1 - k_1^2}{\alpha_2}\right)\frac{j_k}{r}\right] + \frac{B}{k_2^2}\left[\frac{\alpha_1 + k_2^2}{\alpha_2}\frac{di_k}{dr} + \left(1 + \frac{\alpha_1 + k_2^2}{\alpha_2}\right)\frac{i_k}{r}\right].$$

Substitution into (E.3) yields

$$E = \left[\Gamma - \frac{q^2}{k} + \frac{2m\sigma\Omega}{k^2}\right] C$$

which again shows that three arbitrary constants are required to specify the solution.

Since the shear stress must vanish at the top of the inner core, one of the coefficients can be solved for leaving two coefficients undetermined.

Considering the model with a homogeneous fluid outer core overlying the inner core and in the absence of any rotational effects other

than the Coriolis self-coupling, an analytical solution may be obtained if the fluid density is identical to the inner-core density. In this case g_0 is linear,

$$\Gamma = \frac{g_0}{r} = \frac{4\pi G \rho_0}{3}$$

and the stability factor is

$$\beta = 1 .$$

The set of equations reduces to

$$v^2 \frac{1}{\rho}\frac{d\Delta}{dr} = -\left\{4\Gamma + \sigma^2\right\} y_1 - y_6' + \left\{k(k+1)\Gamma + 2m\sigma\Omega\right\} y_3 ,$$

$$\frac{dy_1}{dr} = \Delta - \frac{2y_1}{r} + \frac{k(k+1)}{r} y_3 ,$$

(E.12)
$$\frac{dy_5'}{dr} = y_6' + 3\Gamma y_1 ,$$

$$\frac{dy_6'}{dr} = -\frac{k(k+1)3\Gamma}{r} y_3 + \frac{k(k+1)}{r^2} y_5' - \frac{2y_6'}{r} ,$$

(E.13)
$$k(k+1)\left[v^2\Delta + y_5' - 4\Gamma y_1\right] = 2m\sigma\Omega r(y_1 + y_3) - k(k+1)\sigma^2 r y_3 .$$

From these it is possible to derive the relationship

$$\left[k(k+1)\sigma^2 - 2m\sigma\Omega\right]\chi = \left[k(k+1)\Gamma + 2m\sigma\Omega\right]\Delta$$

(or this can be obtained directly as the torsional component of the curl of the displacement equation, Appendix B).

Elimination of the variables y_5' and y_6' leads to

$$v^2 D_k \Delta = -(4\Gamma+\sigma^2)\Delta + [k(k+1)\Gamma + 2m\sigma\Omega]\chi$$

or

$$D_k \Delta = \xi^2 \Delta$$

where

$$\xi^2 \equiv \frac{1}{v^2}\left[-4\Gamma - \sigma^2 + \frac{[k(k+1)\Gamma + 2m\sigma\Omega]^2}{[k(k+1)\sigma^2 - 2m\sigma\Omega]}\right].$$

For real ξ, the eigenfunctions are modified spherical Bessel functions and as y_5' satisfies

$$D_k y_5' = 3\Gamma\Delta$$

a total of 6 coefficients are allowed. Two of these are constrained by the analytic condition (E.13). Four coefficients remain and these are determined by the continuity of y_1, y_2, y_5' and y_6' at the interface between the solid inner core and the fluid outer core.

By also assuming that the mantle of the Earth is homogeneous and of the same density as the Earth's core it is possible to solve the set of differential equations analytically in this regime as well. Since the differential equations are identical to those relevant in the solid inner core the eigenfunctions are again Bessel functions with argument $\xi_1 r$ and modified Bessel functions with argument $\xi_2 r$ where ξ_1 and ξ_2 are defined by (E.11). It is possible to take values for the seismic velocities which represent mantle averages; however the restriction on the density (i.e. on gravity being a linear function of radius) cannot be relaxed.

The full solution for the dilatation will be a linear combination of these four Bessel functions and the other variables can then be derived from this.

The boundary conditions imposed on this set of solutions will uniquely determine these six coefficients and the two free coefficients introduced for the solutions in the inner core. These conditions are the continuity of y_1, y_2, y_4, y_5' and y_6' at the mantle-fluid interface (the condition that the shear stress vanishes is $y_4 = 0$), the vanishing of the radial and shear stress at the surface of the Earth and the requirement that the induced potential become harmonic at the surface. As the variable y_5' in this section includes the inducing potential, the last condition is stated as

$$R\, y_6'(R) + (k+1)\, y_5'(R) = (2k+1)\, \psi(R)$$

(eq. 1.33 in the main text) and to retain the same normalization as the main text

$$R\, y_6' + (k+1)\, y_5' = (2k+1) R^k .$$

For a model Earth with parameters

$\rho_o = 5.52$ kg/m^3

$v_p = 1.1 \times 10^4$ m/s, $v_s = 4.84 \times 10^3$ m/s } in the inner core

$v = 9.0 \times 10^3$ m/s in the fluid core

$v_p = 1.0 \times 10^4$ m/s, $v_s = 6.0 \times 10^3$ m/s } in the mantle

this gives a critical frequency $\sigma_c = 1.339 \times 10^{-3}$/s or $T_c = 1^h 18^m.22$ for a degree 2, order 0 inducing potential. (A critical period of $53^m.7$ corresponds to a fluid region with a uniform density of 11.71 gm/cm^3.)

For frequencies greater than this critical frequency the parameters k^2 in the fluid and k_2^2 in the solid regions become negative and the nature of the solutions changes.

For these frequencies it is more convenient to deal with a real parameter c (or c_2) than an imaginary parameter k (or k_2). In the inner core and the mantle this can be effected by the substitutions

$$j_\kappa(k_2 r) \longrightarrow j_\kappa(c_2 r)$$
$$k_\kappa(k_2 r) \longrightarrow \eta_\kappa(c_2 r)$$
$$k_2^2 \longrightarrow -c_2^2$$

Within the fluid the solutions are obtained by using the substitutions

$$j_\kappa(kr) \longrightarrow j_\kappa(cr)$$
$$k_\kappa(kr) \longrightarrow \eta_\kappa(cr)$$
$$k^2 \longrightarrow -c^2$$

For responses of other than the order m = 0 the critical condition $k = k_2 = 0$ becomes a quartic equation on σ^2 rather than a quadratic which then allows two frequency regions where the parameters k^2 and k_2^2 are negative and two frequency intervals where they are positive.

For a representative period of six hours and a degree 2, order 0 exciting potential, I have calculated the analytic solutions, and for purposes of testing my numerical programming I have also used the standard

numerical procedure of chapter 2 (after eliminating all rotational coupling) for the model under discussion in this chapter. The resulting values for the radial stress are shown in Figure E.1

Although this model is not realistic in respect to the constitution adopted for the Earth model and in the neglect of the rotational couplings (especially within the fluid region at low frequencies), it does allow a test of the computation scheme developed in the main text.

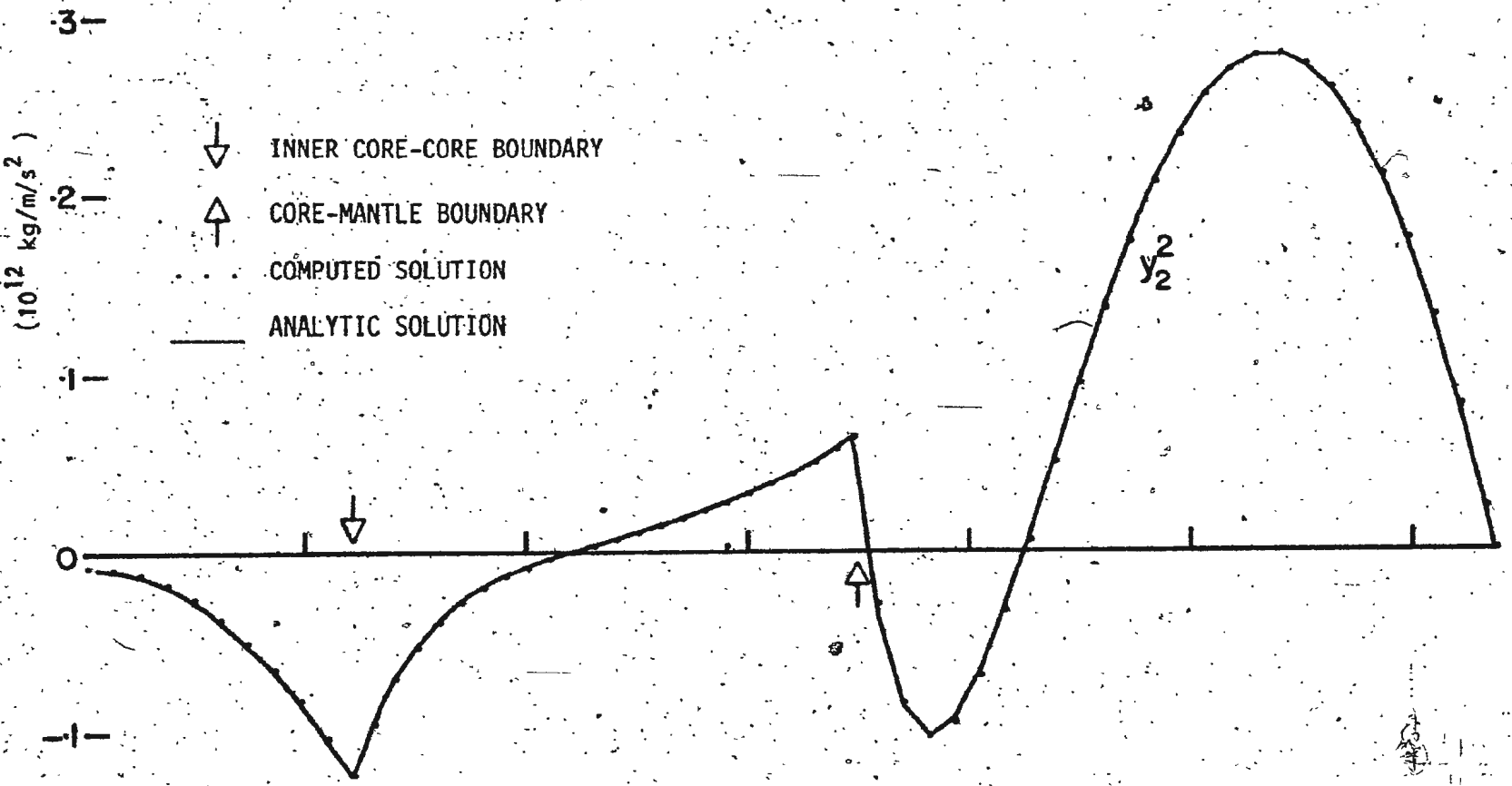

Fig. E.1. Comparison of the analytical and computed solutions for the radial stress in an Earth of uniform density; normalized to an inducing potential of 10^8 m^2/s^2 at 10^7 m.

APPENDIX F

CONSERVATION OF ANGULAR MOMENTUM AND THE TORSIONAL MODE

In Chapter 1 it was pointed out that omission of the torsional mode in the dynamic case is a physical inconsistency as it produces a violation of the conservation of angular momentum. This can be shown by considering a thin spherical shell of radius R with initial angular velocity $\vec{\Omega}$ which then suffers a deformation. Allowing the point initially at $\vec{r}$ to be displaced to $\vec{r}+\vec{u}$ (this is consistent to order u^2), the initial angular momentum of the shell is

$$\vec{L}_o = \int dm\, \vec{r}\times\vec{v} = \int dm\, \vec{r}\times(\vec{\Omega}\times\vec{r})$$

and the instantaneous angular momentum of the deformed shell is

$$\begin{aligned}\vec{L} &= \int dm\,(\vec{r}+\vec{u})\times[\vec{\Omega}\times(\vec{r}+\vec{u}) + \dot{\vec{u}}] \\ &= \vec{L}_o + \int dm\, \vec{r}\times(\vec{\Omega}\times\vec{u}) \\ &\quad + \int dm\, \vec{u}\times(\vec{\Omega}\times\vec{r}) + \int dm\, \vec{r}\times\dot{\vec{u}} \\ &\quad + O(u^2).\end{aligned}$$

Thus the change in the angular momentum due to the displacements is

$$\begin{aligned}\Delta\vec{L} = \int dm \Big\{ &2\vec{\Omega}(\vec{u}\cdot\vec{r}) - \vec{r}(\vec{u}\cdot\vec{\Omega}) \\ &- \vec{u}(\vec{r}\cdot\vec{\Omega}) + \vec{r}\times\dot{\vec{u}}\Big\}\end{aligned}$$

to order u.

Utilising the spherical harmonic expansion used before:

$$\vec{\Delta L} = R\Omega \int dm \left\{ \left(y_3 \sin\theta \frac{\partial S}{\partial \theta} + i y_7 \frac{\partial S}{\partial \phi} \right) \hat{r} \right.$$

$$- \left(2 \sin\theta y_1 S + y_3 \cos\theta \frac{\partial S}{\partial \theta} + i y_7 \cot\theta \frac{\partial S}{\partial \phi} \right) \hat{\theta}$$

$$\left. - \left(y_3 \cot\theta \frac{\partial S}{\partial \phi} - i y_7 \cos\theta \frac{\partial S}{\partial \theta} \right) \hat{\phi} \right\}$$

$$+ i\sigma R \int dm \left\{ \left(y_3 \frac{\partial S}{\partial \theta} + \frac{i y_7}{\sin\theta} \frac{\partial S}{\partial \phi} \right) \hat{\phi} \right.$$

$$\left. + \left(i y_7 \frac{\partial S}{\partial \theta} - \frac{y_3}{\sin\theta} \frac{\partial S}{\partial \phi} \right) \hat{\theta} \right\} .$$

Previous experience has shown that the different orders of spherical harmonics are decoupled from each other; hence I take the simplest for this illustration m = 0. In this case the change in the angular momentum is simply

$$\vec{\Delta L} = R\Omega \int dm \left\{ y_3 \sin\theta \frac{\partial S_r}{\partial \theta} \hat{r} \right.$$

$$\left. - \left(2 y_1 \sin\theta S + y_3 \cos\theta \frac{\partial S}{\partial \theta} \right) \hat{\theta} + i y_7 \cos\theta \frac{\partial S}{\partial \theta} \hat{\phi} \right\}$$

$$+ i\sigma R \int dm \left\{ y_3 \frac{\partial S}{\partial \theta} \hat{\phi} + i y_7 \frac{\partial S}{\partial \theta} \hat{\theta} \right\} .$$

Changing from the spherical polar unit vectors to Cartesian unit vectors,

$$\vec{\Delta L} = R\Omega \int dm \left\{ \left[y_3 \sin\theta \frac{\partial S}{\partial \theta} \right] \left[\hat{\imath} \sin\theta \cos\phi + \hat{\jmath} \sin\theta \sin\phi + \hat{k} \cos\theta \right] \right.$$

$$- \left[2 y_1 \sin\theta S + y_3 \cos\theta \frac{\partial S}{\partial \theta} \right] \left[\hat{\imath} \cos\theta \cos\phi + \hat{\jmath} \cos\theta \sin\phi - \hat{k} \sin\theta \right]$$

$$\left. + i y_1 \cos\theta \frac{\partial S}{\partial \theta} \left[-\hat{\imath} \sin\phi + \hat{\jmath} \cos\phi \right] \right\}$$

$$+ i\sigma R \int dm \left\{ \left[y_3 \frac{\partial S}{\partial \theta} \left[-\hat{\imath} \sin\phi + \hat{\jmath} \cos\phi \right] \right] \right.$$

$$\left. + i y_1 \frac{\partial S}{\partial \theta} \left[\hat{\imath} \cos\theta \cos\phi + \hat{\jmath} \cos\theta \sin\phi - \hat{k} \sin\theta \right] \right\}.$$

Integrating over the azimuth leaves only

$$\vec{\Delta L} = R\hat{k} \left\{ \Omega y_3 \int \sin\theta \cos\theta \frac{\partial S}{\partial \theta} dm \right.$$

$$+ 2\Omega y_1 \int \sin^2\theta S \, dm + \Omega y_3 \int \sin\theta \cos\theta \frac{\partial S}{\partial \theta} dm$$

$$\left. - \sigma y_1 \int \sin\theta \frac{\partial S}{\partial \theta} dm \right\}$$

$$= 2R\Omega \hat{k}\, y_3 \int \sin\theta \cos\theta \frac{\partial S}{\partial \theta}\, dm$$

$$+ 2R\Omega \hat{k}\, y_1 \int \sin^2\theta\, S\, dm$$

$$- R\sigma \hat{k}\, y_7 \int \sin\theta \frac{\partial S}{\partial \theta}\, dm$$

$$= MR\left[2\Omega A_2^{0,k} y_3^k - 2\Omega A_1^{0,k} y_1^k \right.$$

$$\left. - \sigma A_3^{0,k} y_7^k \right] \hat{k} .$$

Substituting the values of the coupling coefficients into the above statement and requiring that angular momentum be conserved leads to the condition

$$y_7^1 = \frac{2\Omega}{\sigma}\left[y_1^0 - \frac{1}{5} y_1^2 - \frac{3}{5} y_3^2 \right],$$

which is identical to the condition on the torsional motion stated in eqn. (1.30). Within the solid regions of the Earth there is a departure from the above condition since the shear stresses are able to distribute the angular momentum change to give a net of zero.

Obviously, neglect of the torsional motion is inconsistent with the conservation of angular momentum.

APPENDIX G

SYSTEMATIC REMOVAL OF ROTATIONAL EFFECTS

In this appendix I reduce the complexity of the program used in the main text to calculate, using these simplified versions of my program, results which have been obtained previously.

My approach is an improvement over these previous calculations because of the more complete treatment of the rotational effects. By systematically eliminating the coupling coefficients I can simplify my approach to duplicate the calculations performed by Smylie (1974) and Crossley (1975b). As Pekeris & Accad (1972) only did a complete investigation of models without a solid inner core, an attempt to confirm their results would necessitate a complete revamping of the procedure used at the geocentre.

The steps I take in this procedure are:

1) removal of all centrifugal terms for the standard case ('propagation truncation' level of 3 and 'elimination truncation' level of 14),

2) further removal of the Coriolis coupling terms which excite the fourth degree spheroidal and the fifth degree torsional response ('propagation truncation' level of 2 and 'elimination truncation' level of 14),

3) further removal of the higher degree response in the elimination procedure within the fluid region (the 'elimination truncation' level is reduced to 2; Crossley's investigation).

4) further removal of the torsional (degree 3) mode (Smylie's (2) investigation), and

5) removal of the Coriolis self-coupling term (Smylie's (1) solutions and similar to those of Pekeris & Accad except for the model).

To illustrate the variation in the solutions due to the retention of the various rotational terms, I display Tables of the Love numbers obtained for each of these simplifications (Tables G(1) to G(5)).

The undertone periods for each of the above simplifications are given in Table G(6). These are systematically higher than the periods reported for the undertones by Smylie and by Crossley, where an identical model is considered and the extent of the rotational coupling considered is identical to that of cases (3), (4) and (5). I shall return to this point after a discussion of the effect of the size of the propagation step upon the solution.

For all the previously discussed work, in the main text and in this appendix, the integrations have been carried out using a standard set of propagation step sizes; namely 80 iterations through the inner core (approximately 15 km each), 2270 steps through the fluid outer core (approximately 1 km each) and 1270 steps of about 2 km through the mantle and crust. As a confirmation of the accuracy of the obtained solutions the Love numbers have also been calculated by reducing the number of iterations in the inner core and the mantle to 20 and 284, respectively, while retaining the above step size in the fluid region (Table G(7)) and

TABLE G(1)

LOVE NUMBERS: CASE 1

Period (min)	h	k	l
60	2.4083	1.1487	.1219
80	1.0232	.4952	.0957
100	.8143	.3964	.0901
120	.7346	.3587	.0877
140	.6944	.3396	.0864
160	.6709	.3285	.0856
180	.6559	.3214	.0852
200	.6457	.3166	.0848
220	.6385	.3132	.0846
240	.6311	.3106	.0844
260	.6291	.3087	.0843
280	.6259	.3073	.0842
300	.6234	.3061	.0841
320	.6214	.3052	.0841
340	.6197	.3044	.0841
360	.6181	.3038	.0840
380	.6164	.3032	.0841
400	.6053	.3014	.0851
420	.6179	.3028	.0837
440	.6164	.3024	.0838
460	.6154	.3021	.0838
480	.6148	.3018	.0838
500	.6142	.3016	.0838
520	.6137	.3014	.0838
540	.6133	.3012	.0838
560	.6129	.3011	.0839
580	.6113	.3009	.0839
600	.6105	.3006	.0841

TABLE G(1), continued

Period (min)	h	k	l
620	.6151	.3011	.0836
640	.6131	.3008	.0837
660	.6125	.3007	.0838
680	.6124	.3007	.0838
700	.6121	.3006	.0838
720	.6121	.3005	.0838
740	.6116	.3004	.0838
760	.6115	.3004	.0838
780	.6121	.3004	.0838
800	.6113	.3003	.0838
820	.6116	.3003	.0838
840	.6112	.3003	.0838
860			
880	.6111	.3002	.0838
900	.6126	.3004	.0837

Case 1:

All centrifugal couplings have been neglected.

All Coriolis couplings have been retained.

'Propagation truncation' level = 3.

'Elimination truncation' level = 14.

TABLE G(2)

LOVE NUMBERS: CASE 2

Period (min)	h	k	l
60	2.4083	1.1487	.1219
80	1.0232	.4952	.0957
100	.8143	.3964	.0901
120	.7346	.3587	.0877
140	.6944	.3396	.0864
160	.6709	.3285	.0856
180	.6559	.3214	.0852
200	.6457	.3166	.0848
220	.6385	.3132	.0846
240	.6311	.3106	.0844
260	.6291	.3087	.0843
280	.6259	.3073	.0842
300	.6234	.3061	.0841
320	.6214	.3052	.0841
340	.6197	.3044	.0841
360	.6181	.3038	.0840
380	.6163	.3032	.0841
400	.6057	.3014	.0851
420	.6180	.3028	.0837
440	.6163	.3024	.0838
460	.6154	.3020	.0838
480	.6147	.3018	.0838
500	.6142	.3016	.0838
520	.6137	.3014	.0838
540	.6133	.3012	.0839
560	.6128	.3011	.0839
580	.6121	.3009	.0839
600	.6084	.3003	.0843

TABLE G(2), continued

Period (min)	h	k	l
620	.6141	.3010	.0837
640	.6130	.3008	.0838
660	.6126	.3007	.0838
680	.6123	.3006	.0838
700	.6121	.3006	.0838
720	.6119	.3005	.0838
740	.6116	.3004	.0838
760	.6544	.3058	.0793
780	.6119	.3004	.0838
800	.6116	.3003	.0838
820	.6114	.3003	.0838
840	.6112	.3002	.0838
860	.6101	.3000	.0839
880	.6118	.3003	.0838
900	.6114	.3002	.0838

Case 2:

All centrifugal couplings have been neglected. Coriolis couplings for the 'elimination' procedure retained for degrees ≤ 27; for the 'propagation' procedure retained for degrees 2 and 3.

TABLE G(3)

LOVE NUMBERS: CASE 3

Period (min)	h	k	l
60	2.4083	1.1487	.1219
80	1.0232	.4952	.0957
100	.8143	.3964	.0901
120	.7346	.3587	.0877
140	.6944	.3396	.0864
160	.6709	.3285	.0856
180	.6559	.3214	.0852
200	.6457	.3166	.0848
220	.6385	.3132	.0846
240	.6331	.3106	.0844
260	.6291	.3087	.0843
280	.6259	.3073	.0842
300	.6234	.3061	.0841
320	.6214	.3052	.0841
340	.6197	.3044	.0841
360	.6181	.3038	.0840
380	.6164	.3032	.0841
400	.6071	.3016	.0849
420	.6181	.3028	.0837
440	.6163	.3024	.0838
460	.6154	.3020	.0838
480	.6147	.3018	.0838
500	.6142	.3016	.0838
520	.6137	.3014	.0838
540	.6133	.3012	.0839
560	.6128	.3011	.0839
580	.6122	.3009	.0839
600	.6096	.3005	.0841

TABLE G(3), continued

Period (min)	h	k	l
620	.6143	.3011	.0836
640	.6130	.3008	.0837
660	.6126	.3007	.0838
680	.6123	.3006	.0838
700	.6121	.3006	.0838
720	.6119	.3005	.0838
740	.6117	.3003	.0838
760	.6107	.3003	.0839
780	.6120	.3004	.0838
800	.6117	.3004	.0838
820	.6115	.3003	.0838
840	.6113	.3003	.0838
860	.6110	.3002	.0839
880	.6137	.3006	.0836
900	.6116	.3003	.0838

Case 3:

Only the degree 2 and 3 responses, with Coriolis coupling between these, have been retained.

TABLE G(4)

LOVE NUMBERS: CASE 4

Period (min)	h	k	l
60	2.4078	1.1484	0.1219
80	1.0232	.4952	.0957
100	.8143	.3964	.0901
120	.7346	.3587	.0877
140	.6944	.3396	.0864
160	.6709	.3285	.0856
180	.6559	.3214	.0852
200	.6457	.3166	.0848
220	.6385	.3132	.0846
240	.6311	.3106	.0844
260	.6291	.3087	.0843
280	.6260	.3073	.0842
300	.6235	.3061	.0841
320	.6214	.3052	.0841
340	.6197	.3044	.0841
360	.6182	.3038	.0840
380	.6167	.3032	.0841
400	.6143	.3026	.0842
420	.6218	.3033	.0833
440	.6168	.3024	.0837
460	.6156	.3021	.0838
480	.6149	.3018	.0838
500	.6143	.3016	.0838
520	.6138	.3014	.0838
540	.6134	.3013	.0836
560	.6130	.3011	.0838
580	.6128	.3010	.0839
600	.6123	.3009	.0839

TABLE G(4), continued

Period (min)	h	k	l
620	.6116	.3007	.0839
640	.6092	.3003	.0842
660	.6146	.3010	.0836
680	.6130	.3007	.0837
700	.6125	.3006	.0838
720	.6122	.3005	.0838
740	.6120	.3005	.0838
760	.6118	.3004	.0838
780	.6117	.3004	.0838
800	.6115	.3003	.0838
820	.6114	.3003	.0838
840	.6111	.3003	.0838
860	.6091	.3000	.0841
880	.6118	.3003	.0838
900	.6115	.3002	.0838

Case 4:

Only the degree 2 response, with the Coriolis self-coupling term, has been retained.

TABLE G(5)

LOVE NUMBERS: CASE 5

Period (min)	h'	k	l
60	3.0827	1.4729	.1499
80	1.0984	.5322	.1015
100	.8511	.4147	.0935
120	.7592	.3710	.0902
140	.7131	.3490	.0884
160	.6861	.3361	.0873
180	.6688	.3278	.0866
200	.6569	.3222	.0860
220	.6484	.3181	.0857
240	.6421	.3151	.0854
260	.6372	.3128	.0852
280	.6334	.3110	.0850
300	.6304	.3096	.0849
320	.6279	.3084	.0848
340	.6259	.3075	.0847
360	.6241	.3066	.0847
380	.6226	.3060	.0846
400	.6212	.3054	.0846
420	.6197	.3048	.0846
440	.6174	.3042	.0847
460	.6342	.3061	.0828
480	.6205	.3041	.0841
500	.6190	.3037	.0842
520	.6181	.3034	.0842
540	.6175	.3032	.0842
560	.6169	.3029	.0842
580	.6165	.3028	.0842
600	.6161	.3026	.0842

TABLE G(5), continued

Period (min)	h	k	l
620	.6157	.3024	.0842
640	.6153	.3023	.0842
660	.6150	.3022	.0842
680	.6147	.3020	.0842
700	.6143	.3019	.0842
720	.6139	.3018	.0842
740	.6132	.3016	.0843
760	.6109	.3013	.0845
780	.6191	.3023	.0836
800	.6154	.3018	.0840
820	.6147	.3016	.0840
840	.6143	.3015	.0840
860	.6141	.3015	.0840
880	.6139	.3014	.0840
900	.6137	.3014	.0841

Case 5:

All rotational effects are neglected.

TABLE G(6)

UNDERTONE PERIODS (HOURS)

Description	1st Undertone	2nd Undertone	3rd Undertone
0)	6.725	10.235	
1)	6.714	10.145	
2)	6.716	10.085	12.664
3)	6.723	10.117	12.749
4)	6.896	10.808	14.390
5)	7.617	12.863	18.511

Description:

0) Results obtained by retaining 'propagation truncation' level of 3, 'elimination truncation' level of 14 and full rotation effects

1) Removal of all centrifugal couplings

2) Reduction for the propagation procedure to only degree 2 and 3 responses

3) Further reduction to only degree 2 and 3 responses for elimination procedure

4) Reduction to only degree 2 response

5) Further removal of all rotational (Coriolis self-coupling) from degree 2 response

TABLE G(7),

VARIATION OF THE LOVE NUMBERS WITH PERIOD:

STEP SIZE IN FLUID IDENTICAL TO THAT OF MAIN TEXT

LARGER STEP SIZES IN THE SOLID REGIONS

Period (min)	h	k	l
60	2.3971	1.1424	.1223
80	1.0215	.4940	.0959
100	.8132	.3956	.0903
120	.7338	.3580	.0878
140	.6936	.3390	.0865
160	.6702	.3279	.0857
180	.6553	.3208	.0852
200	.6451	.3160	.0849
220	.6379	.3126	.0847
240	.6326	.3101	.0845
260	.6285	.3082	.0844
280	.6254	.3068	.0843
300	.6229	.3056	.0842
320	.6208	.3047	.0842
340	.6191	.3039	.0841
360	.6175	.3032	.0841
380	.6158	.3026	.0842
400	.6067	.3010	.0850
420	.6175	.3023	.0838
440	.6163	.3019	.0838
460	.6149	.3016	.0839
480	.6142	.3013	.0839
500	.6136	.3011	.0839
520	.6132	.3009	.0839
540	.6127	.3007	.0839

TABLE G(7), continued

Period (min)	h	k	l
560	.6123	.3006	.0839
580	.6117	.3004	.0840
600	.6104	.3001	.0841
620	.6164	.3012	.0835
640	.6128	.3004	.0838
660	.6122	.3003	.0839
680	.6119	.3002	.0839
700	.6116	.3001	.0839
720	.6115	.3000	.0839
740	.6112	.3000	.0839
760	.6107	.2998	.0839
780	.6125	.3002	.0838
800	.6108	.2998	.0839
820	.6106	.2998	.0840
840	.6108	.2998	.0839
860	.6099	.2995	.0840
880	.6104	.2997	.0839
900	.6100	.2995	.0840

by then reducing the number of steps in the fluid to 1135 while continuing with the larger step size in the solid regions (Table G(8)).

By increasing the 'propagation truncation' level to 4 and repeating the first of these calculations for periods of 5, 7, 9, 10, 11 and 12 hours the only Love number that showed any change was the Love number h at a period of 12 hours which decreased from .6115 to .6113. This again indicates that the solution is numerically stable with regard to the 'propagation truncation' at a level of 3.

By comparing these results with those presented in Table 3 of the main text it is seen that the effect of the larger step size in the solid regions results in an (almost constant) reduction in all of the Love numbers at any given frequency. Also the increase of the step size through the fluid region has little effect at short periods but does cause a divergence of the Love numbers at longer periods.

As I have previously noted, the undertone periods obtained in this thesis for the simplified cases ("non-rotating", self-Coriolis and accounting for the first torsional mode) are systematically greater than those obtained by Smylie and by Crossley.

Smylie, Crossley and I are all using the same Earth model in our investigations, the model defined and tabulated by Smylie (1974) and given in the main text as Table 1. However a difference in computational procedure does exist. From the tabulated data Smylie and Crossley directly use a linear interpolation between these data points to obtain the density, gravity and seismic velocities used in each propagation step. My procedure has been to first apply a cubic interpolation formula to

TABLE G(8)

VARIATION OF THE LOVE NUMBERS WITH PERIOD:

LARGE STEP SIZES THROUGHOUT

Period (min)	h	k	l
60	2.3972	1.1424	.1223
80	1.0215	.4940	.0959
100	.8132	.3956	.0903
120	.7338	.3580	.0878
140	.6936	.3390	.0865
160	.6702	.3208	.0852
180	.6553	.3208	.0852
200	.6451	.3160	.0849
220	.6379	.3126	.0847
240	.6326	.3101	.0845
260	.6285	.3082	.0844
280	.6254	.3068	.0843
300	.6229	.3056	.0842
320	.6208	.3047	.0842
340	.6191	.3039	.0841
360	.6176	.3032	.0841
380	.6158	.3026	.0842
400	.6020	.3001	.0854
420	.6173	.3024	.0838
440	.6157	.3019	.0839
460	.6148	.3016	.0839
480	.6142	.3013	.0839
500	.6136	.3011	.0839
520	.6131	.3009	.0839
540	.6126	.3007	.0839
560	.6123	.3006	.0839
580	.6117	.3004	.0840

TABLE G(8), continued

Period (min)	h	k	l
600	.6102	.3001	.0841
620	.6167	.3012	.0835
640	.6130	.3004	.0838
660	.6123	.3003	.0839
680	.6119	.3002	.0839
700	.6116	.3001	.0839
720	.6116	.3001	.0839
740	.6113	.3000	.0839
760	.6107	.2998	.0839
780	.6112	.2999	.0839
800	.6109	.2998	.0839
820	.6086	.2997	.0842
840	.6106	.2997	.0839
860	.6104	.2996	.0839
880	.6102	.2996	.0839
900	.6099	.2995	.0840

generate a table with data specified at spacings of approximately 10 km throughout each region of the Earth and then a linear interpolation is used between these data points.

As the radial derivative of the density is monotonic decreasing, the density values obtained from a cubic interpolation technique will be systematically larger than those calculated by a linear interpolation and will be closer to the prescribed polytropic distribution.

I have investigated the effect this difference has on the period calculated for the first undertone of the "non-rotating" case. One series of calculations has been done with the standard (for this thesis) cubic interpolation of the data throughout the fluid region and a second series of calculations has been done with a simple linear interpolation within the fluid. In all other aspects the two programmes were identical. In both, the cubic interpolation was used within the solid regions, 80 iterations were used in the inner core, 2270 in the fluid, and 284 in the mantle. The variation of the Love numbers near the first undertone period is shown in Table G(9).

The use of the cubic interpolation yields a longer period for the first undertone than the linear interpolation, and as the cubic interpolation is more self-consistent with the assumption of a polytropic density distribution the period obtained is expected to be more reliable than that generated with the linear interpolation.

The actual shift in the undertone period is approximately 6 minutes or 0.1 hours, a relative shift of about 1% which is of the order of the difference between my results and those of Smylie and Crossley.

TABLE G(9)

COMPARISON OF THE LOVE NUMBERS (NEAR THE FIRST UNDERTONE) WHICH ARE OBTAINED USING DIFFERENT INTERPOLATION METHODS WITHIN THE FLUID CORE

	Period (min)	440	445	450	455	460
CUBIC	h	.6157	.6143	.6166	.5959	.6322
	k	.3031	.3029	.3024	.3033	.3050
	l	.0846	.0847	.0850	.0866	.0828
LINEAR	h	.6139	.6100	.5688	.6304	.6233
	k	.3028	.3022	.2965	.3049	.3039
	l	.0848	.0852	.0893	.0830	.0837

The maximum difference between the densities generated by the two interpolation techniques is only 0.009 gm/cm^3 (near the core-mantle boundary) and as the two methods must agree at the radii tabled in Table 1, the average density difference between the two methods is of the order of .003 gm/cm^3. For comparison, the difference between the adiabatic profile and the sub-adiabatic density profile is of the order of or less than .4 gm/cm^3. The difference in the interpolations then amounts to an increase in this departure by $\sim$ 1%.

APPENDIX H

THE EFFECT OF WOBBLE

Dr. Rochester has pointed out that the model used in this research is incomplete when wobble is present (e.g. the diurnal tides) and that the wobble can be taken into account by retaining the acceleration term $\dot{\vec{\Omega}} \times \vec{r}$. Denoting the amplitude of the wobble by α and the circular frequency by ω , the angular acceleration can be written

$$\dot{\vec{\Omega}} = \omega \alpha e^{i(\omega t - \phi)} [\sin\theta \hat{r} + \cos\theta \hat{\theta} + i\hat{\phi}] \times \vec{\Omega}$$

and the acceleration term becomes

$$\dot{\vec{\Omega}} \times \vec{r} = -r\Omega\omega\alpha e^{i(\omega t - \phi)} [-\hat{\theta} + i\cos\theta \hat{\phi}]$$

$$= -r\Omega\omega\alpha e^{i\omega t} [2i \vec{r} \times \vec{\nabla} S_1^{-1}].$$

The additional inertial force accompanying wobble will then cause the RHS of (1.22) to be supplemented by the term

$$-2r\rho_0\Omega\alpha \delta_m^{-1} \delta_n' \omega$$

and the RHS of (1.30) by

$$-r\Omega\omega\alpha \delta_m^{-1} \delta_n'$$

when $\omega = \sigma$.